Studies on the treatment of biorecalcitrants present in pulp & paper mill effluents using photoelectrocatalysis

A Thesis submitted in fulfilment of the requirement for the award of the degree of

DOCTOR OF PHILOSOPHY

By

HIMADRI RAJPUT

(Regd. No. 901514003)

School of Energy and Environment

Thapar Institute of Engineering and Technology

Patiala- 147004, India

March, 2019

DECLARATION

This is to declare that the research work which is being presented in this thesis entitled **"Studies on the treatment of biorecalcitrants present in pulp & paper mill effluents using photoelectrocatalysis"** in fulfilment of requirement of the degree of 'Doctor of Philosophy' in School of Energy and Environment, Thapar Institute of Engineering and Technology, Patiala, India, is an authentic record of my own research work carried out under the supervision of Dr. Amit Dhir (Associate Professor, School of Energy and Environment, TIET, Patiala, India) and Dr. Vikas Kumar Sangal (Associate Professor, Department of Chemical Engineering, MNIT, Jaipur, India). Documents, embodied in this thesis, from other researchers' works are duly listed in the reference section.

The matter presented in this thesis has not been submitted, in part or full, to any other institute in India or Abroad for the award of any degree.

Himadri Rajput

Himadri Rajput
(Regd. No. 901514003)

CERTIFICATE

This is to certify that the thesis entitled "**Studies on the treatment of biorecalcitrants present in pulp & paper mill effluents using photoelectrocatalysis**" which has been submitted by Ms. Himadri Rajput in the fulfilment of the requirements for the award of the degree of 'Doctor of Philosophy' in School of Energy and Environment, Thapar Institute of Engineering and Technology, Patiala, India, is a record of the candidate's own independent and original research work carried out by her under our supervision and guidance. The matter embodied in this thesis has not been submitted, in part or full, to any other institute for the award of any degree in other University or Institute.

Supervisors

Dr. Amit Dhir

Associate Professor & Head

School of Energy and Environment

TIET, Patiala, India

Dr. Vikas Kumar Sangal

Associate Professor

Department of Chemical Engineering

MNIT, Jaipur, India

ACKNOWLEDGEMENT

Firstly, I would like to express my sincere gratitude to my advisors ***Dr. Amit Dhir,*** *Associate Professor & Head, School of Energy and Environment, TIET, Patiala and* ***Dr. Vikas Kumar Sangal****, Associate Professor, Department of Chemical Engineering, MNIT, Jaipur, for the continuous support of my Ph.D study and related research, for their patience, motivation, and immense knowledge. Their guidance helped me in all the time of research and writing of this thesis. I could not have imagined having better advisors and mentors for my Ph.D study.*

I express my heartfelt gratitude to ***Dr. Prakash Gopalan****, Director, TIET, Patiala, for providing the opportunity to work in this esteemed organization. Without the precious support it would not be possible to conduct this research. I feel special gratitude towards* ***Dr. Rafat Siddique****, Dean, Research and Sponsored Projects, TIET, Patiala for his valuable guidance and support during my research work. I am very thankful to* ***Dr. N.Tejo Prakash****, the former Head of School of Energy and Environment, TIET for providing me access to the laboratory and research facilities.*

Beside my advisors, I would like to thank the rest of my thesis committee: ***Dr. Anita Rajor*** *and* ***Dr. J.P. Kushwaha****, for their insightful comments and encouragement, but also for their keen interest in me at every stage of my research work from various perspectives. I am highly thankful to* ***Dr. S.K. Pandey*** *and* ***Dr. Rachana Pandey*** *for increasing my morale and providing their never ending support.*

I am thankful to ***Mr. Suhail****,* ***Mr. Gurpreet Singh*** *and* ***Mr. Bharat*** *for their constant support and kind help throughout my research work. This research work would have not come to a successful completion without the help I received from SAI Labs, TIET, Patiala and MRC, MNIT, Jaipur.*

A very special gratitude goes out to ***Council of Scientific & Industrial Research (CSIR), Government of India****, for providing the funding for the work.*

I take this opportunity to thank my special lab-mates ***Dr. Palak, Ms. Jayishnu, Ms Priyanka Goyal, Mr. Vagish, Ms. Harleen, Mr. Pali, Dr. Sumit Jaiswal, Dr. Noorpreet Dhanjal*** *for the stimulating discussions, cheerful support, cooperation, and for all the fun that we have had together.*

I feel a deep sense of gratitude for ***Ms. Rupali Dhir*** *for her kind support, encouragement and blessings.*

*I am very grateful to my **Grandmother, Mother, Father, Sister, Brother and Brother-in-Law**, who have constantly provided the moral and emotional support in my life. I am very much indebted to my **grandfather, nani and father-in-law** for always showering their blessings from above. I am also grateful to my other family members and friends who have supported me along the way. A special thanks to the special one in my life, **Dr. Rahil Changotra**, for always supporting me. This could not be possible without your never ending encouragement and love.*

Above all, I owe it all to the Almighty God for granting me the wisdom, health and strength to undertake this research task and enabling me to its completion.

Himadri Rajput

Abstract

Huge consumption of fresh water and generation of huge quantity of effluent having high toxic potential towards environment is one of the most important environmental concerns associated with pulp and paper (P & P) industry. Advanced oxidation processes (AOPs) and electrochemical advanced oxidation processes (EAOPs) such as photocatalysis (PC) and electrochemical oxidation (EC) has proven their potential against the treatment of highly toxic and recalcitrant pollutants present in wastewater. However, these techniques possess few drawbacks which results in the restriction of their application. Photoelectrocatalysis (PEC), a combination of photocatalysis and electrochemical oxidation has shown its viability by overcoming the shortcomings observed in these two treatment techniques.

In the present study, efforts have been made to study the potential viability of PEC treatment process against the biorecalcitrant pollutants commonly found in P & P industrial effluent. For PEC treatment method, novel electrodes have also been synthesized at laboratory scale to overcome the issues associated with present electrodes. The synthesized electrodes have been evaluated for their possible application in the PEC treatment of highly stable contaminants. PEC treatment of pentachlorophenol (PCP) and 4-chloroguaiacol (4-CG) and P & P mill simulated effluent have been studied using prepared electrodes.

TiO_2 and GO/TiO_2 nanotube array electrodes have been synthesized on a titania plate by a simple in-situ anodization method. The physicochemical characteristics of synthesized TiO_2 and GO/TiO_2 electrodes has been determined by Field emission scanning electron microscopy (FE-SEM), X-ray diffraction (XRD), Raman Spectroscopy, Ultraviolet-vis diffuse reflectance spectroscopy (UV-vis DRS), Fourier Transform Infrared spectra (FTIR), Photoluminescence (PL) spectroscopy and X-ray photoelectron spectroscopy (XPS). Synthesized GO/TiO_2 nanotube electrode has been adjudged for its efficacy in the PEC degradation of PCP aqueous solution. Box-Behnken design (BBD) has been used to optimize the effect of graphene oxide (GO) loading (0.005-0.25 g/L), pH (3-8), applied current (20-60 mA) and degradation time (10-120 min) on the decomposition of PCP and energy consumption. At optimum conditions, 91% degradation and 85% mineralization of PCP has been achieved after 90 min under UV-A illumination with 0.015 g/L of GO concentration, 20.68 mA applied current and at pH 3.14 by consuming 0.00068 kWh energy. Effect of reactive species scavengers on the degradation of PCP has also been studied and presence of

hydroxyl radical has been determined. Based on the LC-MS analysis results possible intermediates has been identified and corresponding decomposition pathway of PCP has been proposed.

The other model compound (4-CG) has been then targeted using novel Cesium (Cs) doped TiO_2 nanotubes photoelectrode (Cs/TiO_2NTs). The electrode has been synthesized by simple electrochemical anodization method and characterized by several physicochemical techniques. In particular, the PC, EC and PEC activity of newly synthesized Cs/TiO_2NTs electrodes has been investigated using against the degradation of 4-CG. The effect of operating parameters like Cs concentration, electrolyte concentration, external current and pH on degradation efficacy has been examined. PEC oxidation using Cs/TiO_2NTs lead to 92% degradation of 4-CG in 6 h of solar light irradiation under optimized conditions (2.5 mM Cs, 160 mg L^{-1} Na_2SO_4, 0.03 A current and pH 3). A comparative assessment between PEC, PC and EC process manifested that PEC process has been most efficient when compared with other two processes and Cs/TiO_2NTs exhibited higher PEC activity than bare-TiO_2 electrodes in terms of degradation and mineralization of organic pollutant. The generation of $^{\bullet}OH$ radicals has been found to be highest in PEC when compared to EC and PC process. Possible intermediates/byproducts have been identified by GC-MS technique and a corresponding tentative degradation pathway has been proposed. Cytotoxicity study showed that PEC has potential to detoxify 4-CG. Hence, combination of TiO_2 electrodes decorated with Cs metal can act as a highly efficient photoelectrode for the degradation of hazardous pollutants.

An attempt has been made to synthesize Au/TiO_2NTs electrode for the effect degradation of 4-CG. Anodization technique has been adopted for the preparation gold loaded TiO_2 nanotubes electrode. The synthesized electrode has been characterized by FE-SEM and EDS, XRD, UV-vis DRS and Raman measurements. 4-CG degradation experiments have been performed and optimum process parameters have been determined (0.15 mM Au concentration, 0.08 g/L electrolyte concentration, 0.03 A external current and pH 3). The presence of generated $^{\bullet}OH$ radicals has been detected and their concentration with respect to treatment time has been determined. The intermediates formed during the degradation process have also been identified.

A novel Ag co-doped GO/TiO_2 nanotube photoelectrode has been synthesized by anodic oxidation method to assess its PEC, PC and PEC activity against the degradation of PCP. The nanotube electrode has been characterized by XPS, XRD, along with different spectroscopic and microscopic techniques, enabling to ensure the synthesis of planned photoeletrode material. The effect of applied current, pH, Na_2SO_4 concentration and Ag

loading on the removal of PCP has been studied which resulted in high degradation (87%) and mineralization (78%) efficacy after 25 min of short treatment time. Moreover, it exhibited enhanced activity when compared to TiO_2 and GO/TiO_2 nanotube electrodes. The contribution of different reactive species in PEC process has been studied by conducting experiments in the presence of scavengers and assessment of •OH in the degradation process has been performed. The photoelectrode exhibited good reusability properties. Degradation products have also been identified using LC-MS technique. This study demonstrates that the combination of semiconductor and graphene oxide decorated with Ag nanoparticles can act as a highly efficient photoelectrodes for removing biorecalcitrant compounds.

Finally, the PEC degradation potential of all the synthesized electrodes have been assessed for the treatment of simulated P & P mill effluent. The simulated effluent has been prepared by diluting the real effluent of P & P mill collected after the bleaching section of P & P mill with tap water. During the experiments, the conductivity and pH of the effluent has not been altered. All the experiments have been performed under the naturally available solar light. The prepared effluent has been characterized before and after treatment by measuring its chemical oxygen demand (COD), total organic carbon (TOC), total solids (TS), chloride, sulphate, nitrate, nitrite and phosphate concentrations. All the electrodes exhibited satisfactory performance in treating the simulated effluent however, the co-doped Ag-GO/TiO_2 nanotube electrode has been observed to be best among all the other synthesized electrodes.

All the synthesized nanotubes electrodes exhibited significant degradation efficiency towards the biorecalcitrant compounds and simulated P & P mill effluents. Cs/TiO_2 and Au TiO_2 nanotube electrodes exhibited considerable degradation of 4-CG while, GO/TiO_2 and Ag-GO/TiO_2 nanotube electrodes showed the significant degradation of PCP. The role of reactive species in the degradation process has been studied and observed that each reactive species has significant effect in regulating the PEC degradation. The simulated effluent was subjected to PEC treatment using all the synthesized electrodes and analyzed by measuring its COD, TOC, chloride, sulphate, nitrate, nitrite, phosphate and total solids concentration.

Dedicated to my beloved Family

List of Symbols/Abbreviations

P & P	Pulp and Paper
S.S	Suspended Solids
COD	Chemical Oxygen Demand
BOD	Biochemical Oxygen Demand
TDS	Total Dissolved Solids
WWTPs	Wastewater Treatment Plants
AOPs	Advanced Oxidation Processes
$^{\bullet}OH$	Hydroxyl radical
ROS	Reactive Oxygen Species
$O_2^{-\bullet}$	Superoxide radicals
H_2O_2	Hydrogen peroxide
O_3	Ozone
e^-/h^+	Election-hole
TiO_2	Titanium dioxide
PC	Photo-catalysis
EC	Electrocatalysis
PEC	Photoelectrocatalysis
UV	Ultraviolet
PCP	Pentachlorophenol
4-CG	4-Chloroguaiacol
TOC	Total Organic Carbon
ASP	Activated Sludge Process
CPCB	Central Pollution Control Board
VB	Valence Band
CB	Conduction Band

List of Tables

List of Figures

Contents

Chapter 1

Introduction

Increased generation of toxic compounds as a result of anthropogenic activities have caused a considerable damage to our environment. In recent times, problems related to environmental quality of water have been considered increasingly critical and persistent. Out of the total earth's surface, over two third parts is covered by water. With increasing population, pressure on the earth's water resources is also increasing. Due to intensive human activities, rivers, oceans and other inland water resources are under huge pressure and are also facing challenge of poor quality which indicates water pollution. Industrialization around the globe has further intensified the problem of environmental contamination.

Negative impact on water bodies is caused by human activities such as fertilizers used by farmers in the fields gets gradually washed into ground and surface water by rain, chemicals emitted in the atmosphere by industrial chimneys can fall back to the surface of earth with rain, ultimately polluting lakes, seas and rivers causing water pollution. There are many sources of water pollution like chemical waste, plastic waste, sewage, radioactive waste, nutrients etc. The common contaminants consists toxic compounds like heavy metals, dyes, chlorinated/non-chlorinated aromatic and aliphatic compounds, noxious gases such as NH_3, SOx, NOx, CO and pathogens like viruses, bacteria and fungi (Zhang et al., 2012). The existence of recalcitrant contaminants like phenols, hormones, pesticides, pharmaceuticals, dyes, surfactants, color in water and wastewater are one of the most critical and serious problems for humans as well as for the environment (Chong et al., 2010).

The remediation of contaminated water and wastewater is a major research field as its consumption at global level is fast due to high growth rate of population and rapid industrial expansion. One of the serious environmental concerns today is the impact related with the disposal of industrial effluent/wastewater and some other residues into surface and ground water reservoirs. A continuing consistent change in the water, soil and air composition has been observed due to the industrial revolution. In the developing world, a wide range of organic contaminants are responsible for the highest pollution exposures in the environment. The anthropogenic domestic, agricultural and industrial activities gives rise to these pollutants which have characteristics, like bioaccumulation, bio-concentration, and persistence in the atmosphere or longer half- lives (Zeghioud et al., 2016). Some considerably major sources of water pollution have been shown in Figure 1.1. Extensive research has being

carried out worldwide to develop techniques which can treat wastewater effectively at low cost.

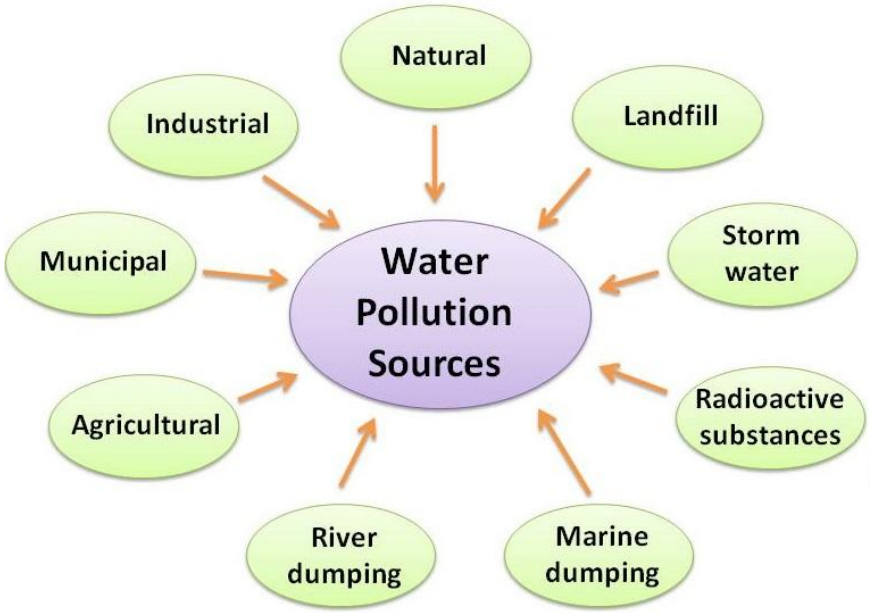

Fig. 1.1 Some major sources of water pollution (Novotny, 1994)

1.1 Pulp and Paper Industry and associated environmental concerns

The pulp and paper (P & P) industry in India is oldest and core industrial division and is considered one of the major pollution contributing industries worldwide (Sumathi & Hung, 2006). The manufacturing of paper is extremely capital intensive as well as water and energy intensive procedure which gives rise to significant amount of waste effluent, which is generally characterized by the presence of high colour, Chemical Oxygen Demand (COD), Biochemical Oxygen Demand (BOD), Total Dissolved Solids (TDS), tannins, resin acids and potentially toxic chlorinated compounds (Singh et al. 1996; Kumar et al., 2012; Haq et al. 2017). The production of 1 ton pulp contributes approximately 100 kg of colour imparting compounds and around 2 to 4 kg total organo-chlorines to the effluents coming out from industry (Dhir et al., 2012). The consistently rising demand of paper and its products with limited availability of natural wood based raw materials has compelled the consideration and utilization of alternative agro-residues based raw materials such as bagasse, wheat straw, sarkanda, rice straw, cotton stalks, jute, etc., availability of which are plentiful in an agriculture based country like India (Government of India, Report 1995; Kansal et al., 2008; Dhir et al., 2011).

Worldwide, the total P & P industries are 7745 and paper demand is 402 million per

annum. India has approximately 759 P & P industries with the approximate production of paper ranging up to 10.11 million tons, which is about 2.52% of total world production (Singh et al. 2016). P & P industry is extremely water intensive which consumes around 100-250 m^3 freshwater/ton paper and generates around 75-225 m^3wastewater/ton of paper production that possess characteristics like high COD, BOD and TDS values depending upon the type of raw materials utilized and the employed manufacturing process (Howe and Wagner, 1999; Pathak et al., 2012; Kamali and Khodaparast, 2015; Haq et al. 2017). In P & P industries, the steps including in paper production are pulping of raw material followed by bleaching, and paper making. The raw wastewater from pulping process commonly called as 'black liquor' is of very polluting potential and its dark brown or black color adversely affects aquatic ecosystem (Thompson et al., 2001). The high molecular weight lignin and its derivates are the primary contributors of dark colored appearance of black liquor. Black liquor is used in chemical recovery plants for the recovery of chemicals and energy from incineration of dissolved lignin and other organics. Few medium scale agro-based P & P industries have started the usage of non-conventional chemical recovery plants in order to incinerate black liquor, which is a major environment polluter. Lignin is highly recalcitrant in nature because of the existence of aryl ether bonds and non-hydrolysable C-C linkages (Minu et al., 2012). Generally, COD, BOD and TDS present in wastewater of P & P mill is contributed by alkali-lignin and degradation residues of polysaccharide (Lara et al., 2003). Several studies performed in the early 80's in the United States, Japan, Scandinavia and Canada demonstrated existence of chlorinated compounds such as lignosulfonic acids, phenols, hydrocarbons, and resin acids in P & P effluents (Kringstad and Lindstrom, 1984). The main challenge for P & P industries is to comply with strict environmental regulations (Kamali and Khodaparast, 2015). The environmental concerns of P & P industry are not only limited to the high consumption of fresh water resources, but also, huge volumes of generated wastewater, solid waste generation concerns including sludge generation from wastewater treatment plants (WWTPs) and harmful air emissions are some other problems for which effective disposal and treatment is essential. The effluent also gives rise to problems like scum formation, slime growth, color problems, thermal impacts and also imparts toxicity in the water causing serious harm to zooplankton and fishes (Pokhrel and Viraraghavan, 2004). The different type of wastewater generated during various stages of paper making process has been shown in Figure 1.2.

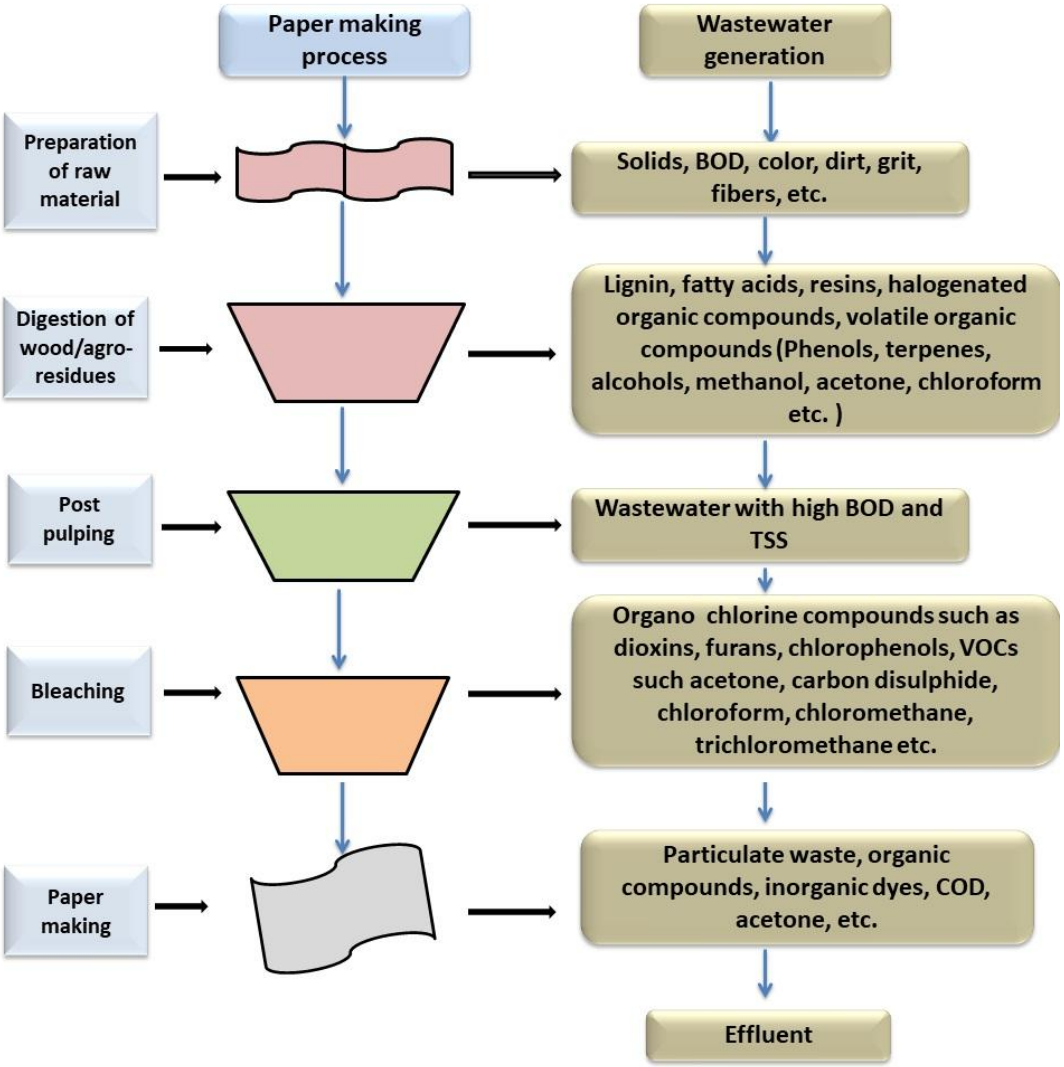

Fig. 1.2 Different type of wastewater generation during various stages of paper making (Hubbe et al., 2016)

The common treatment processes employed in P & P industries includes primary treatment by sedimentation/flotation, secondary treatment comprising activated sludge process (ASP) /anaerobic digestion processes and/or tertiary processes like membrane technology (Thomson et al., 2001). In most of the wastewater treatment plants, ASP are commonly used for the removal of organic contaminants; however, there are various problems with ASP process such as, generation of sludge with highly variable settling properties, sensitivity towards shock loading and incapability in removing non-biodegradable toxic pollutants. Conventional treatment technologies like precipitation, adsorption (Gautam et al., 2017; Zha et al., 2018), reverse osmosis and flocculation simply transfers organic contaminants from one phase to other phase or even concentrate them in one

phase, without degrading those (Chong et al., 2010). Therefore, many scientists have attempted the development of new techniques which can support or can replace some of the conventional treatments (Khansorthong and Hunsom, 2009). Among them, advanced oxidative processes (AOPs) have received attention as an effective and competent approach for the degradation of pollutants as an alternative to conventional treatment techniques (Mansilla et al., 1994; Rodriguez et al., 1998).

1.2 Pollutants present in pulp and paper mill effluent

Due to the consumption of significant amount of chemicals and solvents in paper manufacturing, larger quantities of effluents are generated containing organic and inorganic salts, biorecalcitrants and toxic pollutants. The list of pollutants generated by P & P mill has been listed in Table 1.1.

Table 1.1 List of pollutants present in P & P mill effluents (Ali and Sreekrishnan, 2001)

Type of pollutants	Example of pollutants
Organic pollutants and suspended solids	Organic acids, hemi-cellulose, starch, fugitive fibers etc.
Organochlorine compounds	Phenols, chlorinated derivatives of phenols, , chloroform, carbon tetrachloride, chlorinated benzenes, epoxy stearic acid and dichloromethane, guaiacols etc.
Chemicals	Chloroform, chloro-acetones, aldehydes, acetic acids etc.
Chlorophenolics	Trichlorophenol, pentachlorophenol etc.
Dioxins and Furans	Polychlorinated dibenzo-dioxins, Polychlorinated dibenzofurans etc.

The Central Pollution Control Board (CPCB) has taken several initiatives to control the pollution by P & P mill effluents in water bodies. Accordingly, wastewater discharge norms and standards have been brought out by CPCB for Indian P & P industries which are given in Table. 1.2.

Table 1.2 Wastewater discharge norms by Indian pulp and paper industry

Parameter	General standard	Discharge standards	
		Small scale industry	Large scale industry
Volume (m^3/ton)	-	Agro based :200 Waste Paper: 75	Writing and Printing: 200 Rayon grade/ News print: 150
pH	5.5-9.0	5.5 –9.0	7.0 - 8.5
BOD_5 at 200 °C mg/l	30 (Inland surface water) 350 (Public Sewer on land discharge) 100 (Land for irrigation) 100 (Marine / Coastal areas)	30 (inland discharge) 100 (on land discharge)	30
COD, mg/l	250 (inland surface water) - (Public Sewer on Land discharge) - (Land for irrigation) 250 (Marine / Coastal areas)	Not specified	250
SS, mg/l	100 (inland surface water) 600 (Public Sewer on land discharge) 200 (Land for irrigation)	100	50
Total Organic Chloride (TOCl), kg/t_{paper}	-	Not specified	2.0
Absorbable Organic Halides (AOX), kg/t_{paper}	-	2.0	1.0
Sodium Absorption Ration (SAR)	-	26	-
Color, PCU	being implemented	500	500

Source: CPCB, 2005

1.3 Advanced Oxidation Processes: an overview

In past, various physical, chemical and biological treatment methods have been explored for the degradation of organic contaminants present in wastewater. Conversion of organic pollutants into secondary pollutants has been observed when the conventional treatment technologies were employed (Saha et al., 2011). This leads to the development of energy effective and innovative treatment technology such as AOPs, which facilitates the oxidation of recalcitrant environmental pollutants by generating extremely reactive hydroxyl radical ($^{\bullet}OH$) species (Hoffmann et al., 1995). AOPs have been proven as a powerful and efficient treatment method for the decomposition and mineralization of highly stable, toxic and recalcitrant pollutants (Legrini et al., 1993; Sahoo et al., 2013). These techniques can be used for the remediation of polluted surface water, groundwater and wastewaters contaminated with stable and recalcitrant organic pollutants with low biodegradability. AOPs have been observed to be successfully employed for the remediation of landfill leachates (Amor et al., 2015); dyes and pigments (Wang et al., 2015); wastewater (Rodríguez-Chueca

et al., 2014); surface water and drinking water (Lanao et al., 2010); agri-food industries (Velegraki and Mantzavinos, 2015) and many more.

AOPs are a group of techniques in which generation of $^{\bullet}OH$ radicals (second highest powerful oxidant after fluorine) as a primary oxidant takes place. The relative oxidizing power of different oxidizing species has been shown in Table 1.3. $^{\bullet}OH$ radical gets generated by oxidizing agent like hydrogen peroxide (H_2O_2) and ozone (O_3), ultrasound, ultraviolet (UV) irradiation and homogeneous/ heterogeneous catalysts. $^{\bullet}OH$ radicals are non-selective and can rapidly react with a wide variety of pollutants (Changotra et al., 2018). They can degrade pollutants either by abstracting or adding an atom of hydrogen to the double bonds. When toxic and non-biodegradable pollutants are involved, use of alternate treatment technology like AOPs is needed. The pollutants gets eliminated by reactive oxygen species (ROS) including $^{\bullet}OH$ radicals, superoxide radicals ($O_2^{-\bullet}$) and H_2O_2 generated by different routes, which causes breakdown of contaminants into simpler molecules to facilitate biodegradation process (Xiong et al., 2016; Changotra et al., 2019). The classification of AOPs has been shown in Figure 1.3.

Table 1.3 Relative oxidizing powers of different oxidizing species (Carey, 1992)

S.No.	Oxidizing Species	Oxidation power
1	Positively charged hole on TiO_2 (TiO_2^{+})	2.35
2	Hydroxyl radical ($HO^{\bullet}$)	2.05
3	Atomic oxygen	1.78
4	Ozone (O_3)	1.52
5	Hydrogen peroxide (H_2O_2)	1.31
6	Permanganate	1.24
7	Hypochlorous acid (HClO)	1.10
8	Chlorie (Cl)	1.00

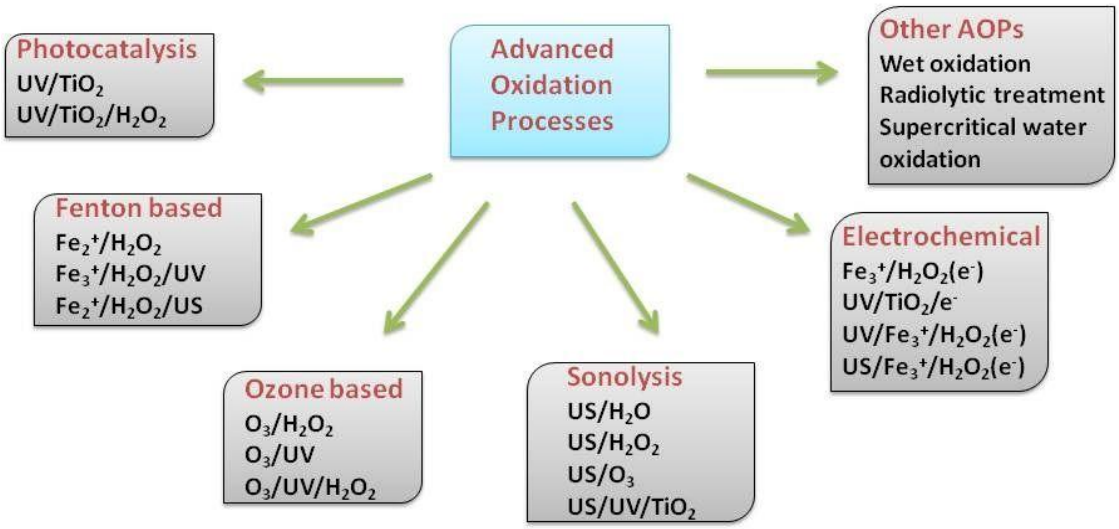

Fig. 1.3 Classifications of Advanced Oxidation Processes (Divyapriya et al., 2016)

The AOP technique is particularly useful in treating biologically toxic and recalcitrant materials like pesticides, volatile organic compounds, insecticides, aromatics and petroleum constituents (Brillas et al., 1998; Rezaei et al., 2013; Roshani et al., 2014; Mudhoo et al., 2018). Additionally, AOPs can be useful for treating secondary treated effluent from WWTPs which is commonly considered as tertiary treatment (Audenaert et al., 2011). After undergoing AOP treatment techniques, environmental pollutants gets mineralized and majorly gets converted into stable and non-toxic inorganic compounds like water, carbon dioxide and salts. The goal of using AOP techniques for wastewater purification is the overall reduction of toxicity and chemical pollutants to a degree where the wastewater after treatment may be reintroduced to ground and surface water reservoirs or, at least can be introduced into a conventional sewage treatment unit.

1.3.1 Photocatalysis (PC), Electrocatalysis (EC) and Photoelectrocatalysis (PEC)

To remediate the serious problems associated with environmental pollution, various efforts have been made, and several catalytic oxidation techniques are being developed and applied for environmental protection.

1.3.1.1 Mechanism of Photocatalysis

Among the AOP techniques, heterogeneous photocatalysis has proven its promising potential in pollutant removal (Daghrir et al., 2013). In this process, when semiconductor

photo-catalyst gets exposed to irradiations, redox reactions takes place on its surface after absorption of photons energy with equals to or higher than the band gap energy of semiconductor. This promotes the transfer of electrons (e^-) from valence band (VB) to conduction band (CB) resulting in formation of election-hole (e^-/h^+) pairs which further facilitates the formation of ROS mostly accountable for the degradation of pollutants (Akpan and Hameed, 2009). Figure 1.4 represents the photocatalytic mechanism of titanium dioxide (TiO_2) semiconductor.

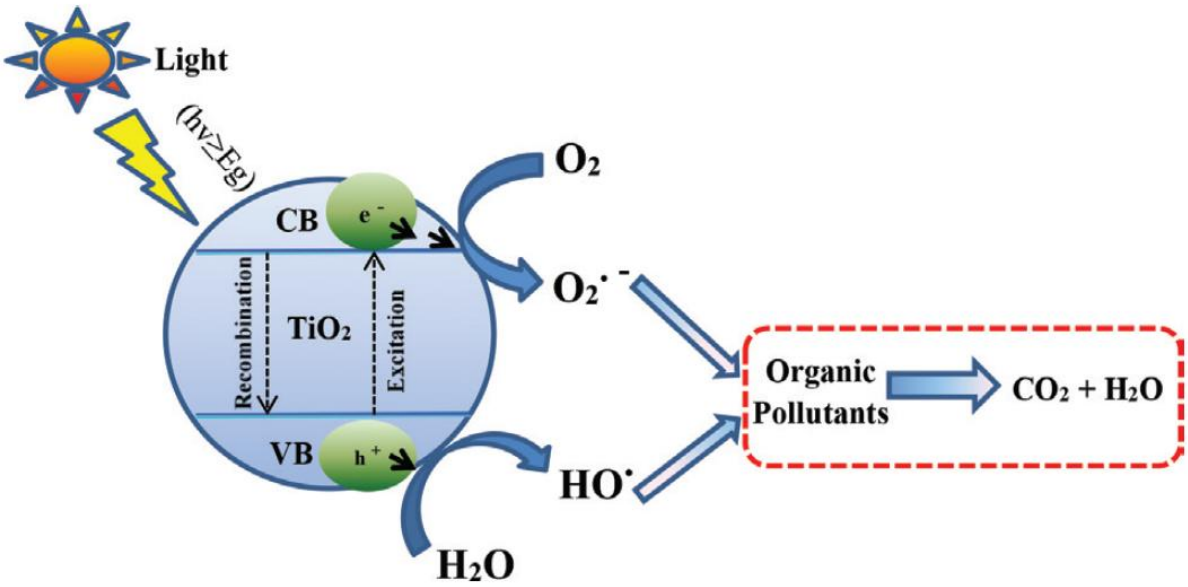

Fig. 1.4 Mechanism of photocatalysis (Samsudin et al., 2015)

Several semiconductor photocatalyst have been examined and reported like titanium dioxide (Pattanaik and Sahoo, 2014; Tryba et al., 2019), zinc oxide (Shen et al., 2008), iron oxide (Yamada et al., 2007), tungsten trioxide (Yu et al., 2008a), copper oxide (Bhatta et al., 1991) and cadmium sulfide (Di et al., 2009). Previous findings shows that TiO_2 is highly promising than the other semiconductor photocatalysts for applications in air purification, water decontamination (Pichat et al., 2000), antimicrobial (Chung et al., 2008), adsorption of contaminants (Dixit et al., 2017; Tanzifi et al., 2018), cleaning of cement slabs (Arora et al., 2018) and treatment of wastewater (Shahrezaei et al., 2012) due to its properties like low cost, non-corrosivity, high chemical resistance and antioxidant ability (Chen et al., 2011; Choi et al., 2009). PC has proven its applications in various environmental fields like removal of aqueous pollutants (Matthews, 1991), metal recovery, air purification, and materials synthesis such as self-cleaning glass surfaces (Pichat et al., 2000).

The series of reaction involved in the photocatalytic process are as follows:

$$OH^- + h_{vb}^+ \rightarrow {}^\bullet OH \quad (1.1)$$

$$O_2 + e_{cb}^- \rightarrow {}^\bullet O_2^- \quad (1.2)$$

$${}^\bullet O_2^- + H^+ \rightarrow {}^\bullet HO_2 \quad (1.3)$$

$$2{}^\bullet HO_2 \rightarrow O_2 + H_2O_2 \quad (1.4)$$

$$H_2O_2 + {}^\bullet O_2^- \rightarrow OH^- + O_2 \quad (1.5)$$

Doping of TiO_2 is performed in order to extend the spectral response into visible region and to ensure the effective separation of photo-generated (e^-/h^+) pairs (Zhao, 2004; Fujishima et al., 2008; Wu et al., 2015). The photocatalytic mechanism of un-doped TiO_2 (hv_1), metal-doped TiO_2 (hv_2), and non-metal doped TiO_2 (hv_3), has been shown in Figure 1.5. The photocatalytic activity of metal doped TiO_2 in visible region can be due to the production of new energy level in TiO_2 band gap by the metal nano-particle dispersion occurred in TiO_2 matrix. As explained in Figure 1.5, e^- can get excited from the defect state to TiO_2 conduction band by photon of energy equal or higher to hv_2. Furthermore, the advantage of TiO_2 metal doping is trapping of e^- which results in inhibited recombination rates of e^-/h^+ which ultimately results in elevated photo-catalytic activities. The three major TiO_2 modifications occur by non-metal doping are (i) narrowing of band gap, (ii) formation of impurity energy levels, and (iii) vacancies of oxygen.

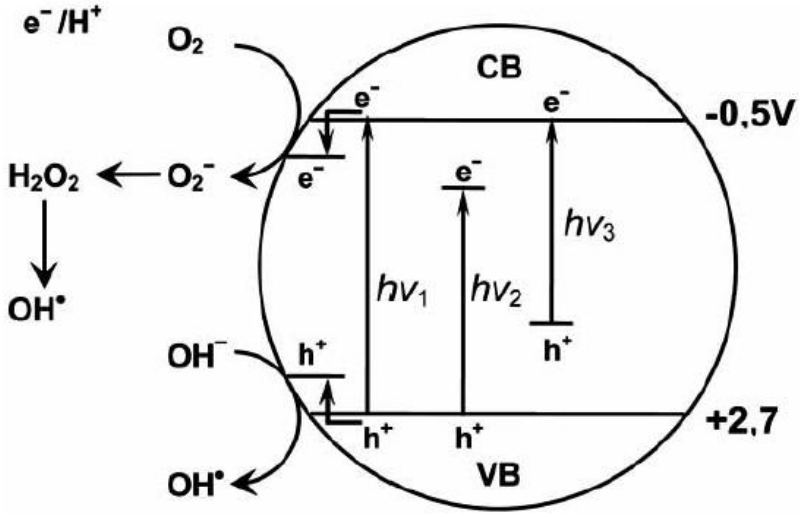

Fig. 1.5 Photocatalytic mechanism of un-doped TiO_2 (hv_1), metal doped TiO_2 (hv_2), and non metal doped TiO_2 (hv_3) (Zaleska, 2008)

1.3.1.2 Mechanism of Electrocatalysis

Recently electrochemical based AOPs i.e., electrochemical advanced oxidation processes (EAOPs), have came into picture (Fryda et al., 2003; Sirés and Brillas, 2012). The EAOPs possess various advantages for the remediation of environmental pollution concerns as the electrons are a clean reagent. Electrocatalytic oxidation is an eco-friendly technology capable in completely mineralizing non-biodegradable organic pollutants. The oxidation of contaminants occur at the surface of anode by the help of external current and the pollutants get transformed into simpler non-toxic end products. In the wastewater treatment by EC process, contaminants gets directly oxidized at the electrode surface or by electrochemically in-situ generated oxidizing agents. EC oxidation of contaminants can occur via two different oxidation routes (a) Direct oxidation and (b) Indirect oxidation, as represented in Figure 1.6. Direct anodic oxidation of contaminants at the surface of anode can occur as well as indirect oxidation can occur where mediator oxidative species (HClO, $H_2S_2O_8$ etc.) gets generated electrochemically which can degrade the pollutants. During electro-oxidation of polluted aqueous solutions, both the direct and indirect oxidation mechanisms can coexist (Chiang et al., 1995).

During direct anodic oxidation, contaminants get directly oxidized by getting diffused from bulk solution to the surface of anode followed by their oxidation via anodic electron transfer reactions. Direct electro-oxidation of contaminants can occur due to the physically adsorbed "active oxygen" (adsorbed $^{\bullet}OH$) or chemically adsorbed "active oxygen" (oxygen in the oxide lattice, $MO_{(x+1)}$) (Kaur et al., 2015). The treatment efficiency of direct electro-oxidation depends on several parameters such as: nature of used anode material, generation of $^{\bullet}OH$ radicals, O_2 evolution potential. Two steps are involved in the direct oxidation of pollutants:

- Contaminant's diffusion from bulk solution to the surface of anode
- Oxidation of contaminants at anode surface.

$$MO_X + H_2O \rightarrow MO_X(OH^{\bullet}) + H^+ + e^- \quad (1.6)$$

$$R + MO_X(OH^{\bullet}) \rightarrow CO_2 + H^+ + e^- + MO_X \quad (1.7)$$

$$R + MO_{X+1} \rightarrow RO + MO_X \quad (1.8)$$

$$MO_X(OH^{\bullet}) \rightarrow \frac{1}{2}O_2 + H^+ + e^- \quad (1.9)$$

During the indirect oxidation process, generation of strong oxidizing agents at anode surface occurs which degrades the pollutants present in the bulk solution. Chlorine is the common electro-generated oxidant generated by the oxidation of chloride at anode, however; its role in EC process is not clearly defined yet. Some other oxidizing agents generated during the indirect electrochemical oxidation process are ozone, hydrogen peroxide, peroxodisulfuric acid and the reactions involved are stated in Eq. 1.10 to Eq. 1.19 (Särkkä et al., 2015). All the in-situ generated oxidants are utilized immediately in the degradation reactions.

$$2Cl^- \rightarrow Cl_2 + 2e^- \quad (1.10)$$

$$Cl_2 + OH^- \rightarrow Cl^- + ClO_3^- + ClO^- \quad (1.11)$$

$$Cl_2 + H_2O \rightarrow HOCl + H^+ + Cl^- \quad (1.12)$$

$$HOCl \rightarrow H^+ + OCl^- \quad (1.13)$$

$$H_2O \rightarrow OH^\bullet + H^+ + e^- \quad (1.14)$$

$$2OH^\bullet \rightarrow H_2O_2 \quad (1.15)$$

$$O_2 + O^\bullet \rightarrow O_3 \quad (1.16)$$

$$O_2 + 2H^+ + 2e^- \rightarrow H_2O_2 \quad (1.17)$$

$$HCl + SO_3 \rightarrow ClSO_3H \quad (1.18)$$

$$ClSO_3H + H_2O_2 \rightarrow H_2S_2O_8 + 2HCl \quad (1.19)$$

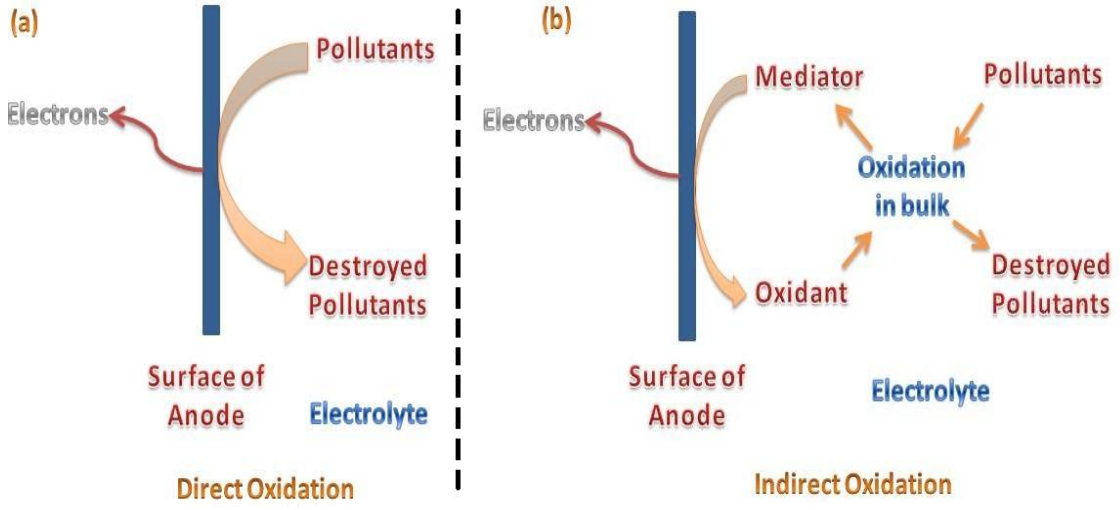

Fig. 1.6 Mechanism of (a) Direct and (b) Indirect electro-oxidation (Anglada et al., 2009)

1.3.1.3 Mechanism of Photoelectrocatalysis

Photoelectrocatalysis has been intensively studied as potential alternative method to degrade organic pollutants and also to eliminate toxicity from polluted waters, since they remove pollutants in short durations. The wide applications of TiO_2 is greatly inhibited by wide band gap (i.e ~3.2 eV), which need UV radiations for its activation, resulting in very poor efficiency towards solar irradiations utilization (Yin et al., 2003; Chong et al., 2010). In PEC processes, TiO_2 is extensively utilized as photo-anode material (Berger et al., 2012). When TiO_2 gets exposure to irradiations, generation of e^-/h^+ pairs takes place where, the h^+ get concentrated in the semiconductor while e^- gets relocated from TiO_2/solution interface to the substrate. Afterwards, electrons travel towards cathode by the external circuit of the cell, thereby giving rise to photocurrent (Gerischer, 1990). The major constraint of TiO_2 is its activation requirements through UV light, which limits its overall PEC performance. TiO_2 modification can improve the visible light absorption allowing the utilization of sunlight (Akpan and Hameed, 2010). The PEC mechanism has been shown in Figure 1.7.

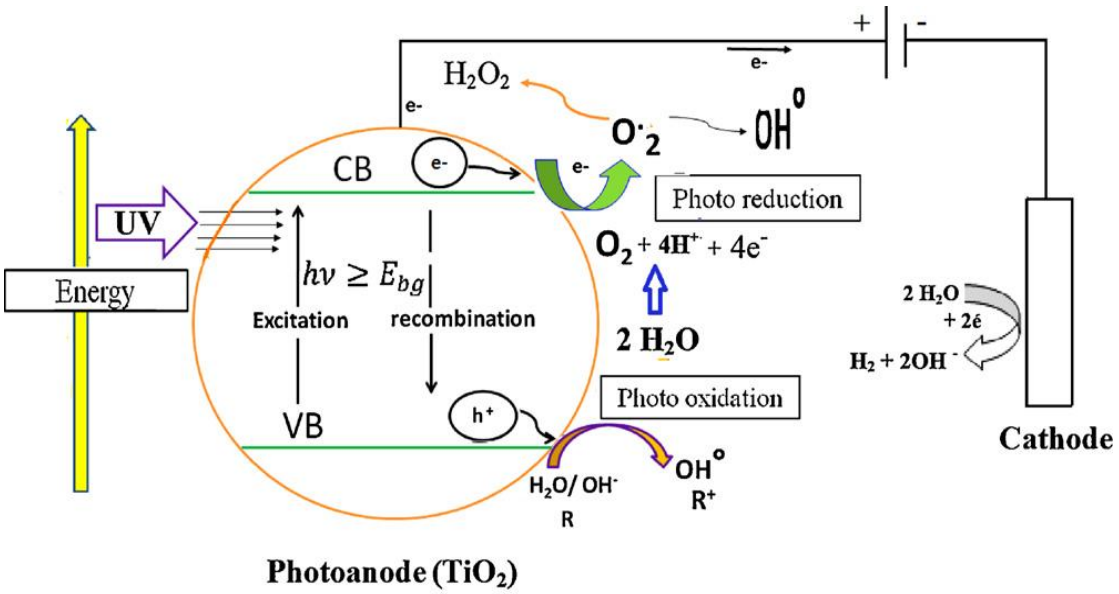

Fig. 1.7 Mechanism of Photoelectrocatalysis (Daghrir et al., 2012a)

The PEC treatment efficiency is dependent on various parameters such as electrode material, pH of the solution, type of electrolyte, conductivity and applied current. The electrochemical mediated oxidation of polluted water is dominantly influenced by the properties of used anode material such as stability, conductivity, high oxygen and hydrogen evolution over potential, and resistance towards anodic corrosion (Anglada et al., 2009).

The influence of current have significant impact on the electrochemical mediated

oxidation of wastewater as the generation of oxidants is directly influenced by the amount of current supplied. With increase in the electric current, the rate of generation of oxidant species also increases. However, after the current reaches a certain optimum limit, it hinders the degradation performance, as at values higher than the optimum limit various side reactions become prominent (Sirés et al., 2014).

The conductivity of wastewater to be treated is highly responsible in the overall energy consumption of the treatment process. It has been reported that electrochemical oxidation becomes more cost effective and convenient when aqueous solution requiring treatment already possess high salinity, as the energy consumption gets reduced with increasing conductivity of electrolyte (Anglada et al., 2009).

The pH of electrolyte influences the performance as the type of oxidant generated is highly dependent upon the pH of the solution. Electrochemical oxidation can perform well in both acidic and basic environment. Under acidic environment, direct anodic oxidation is dominant while under alkaline environment indirect electrochemical oxidation is dominant. However, acidic environment provides better degradation chances as at acidic pH, chlorine the strongest oxidation specie dominates followed by HOCl specie (Anglada et al., 2009; Särkkä et al., 2015). The plot of generation of chlorinated species with respect to pH has been shown in Figure 1.8.

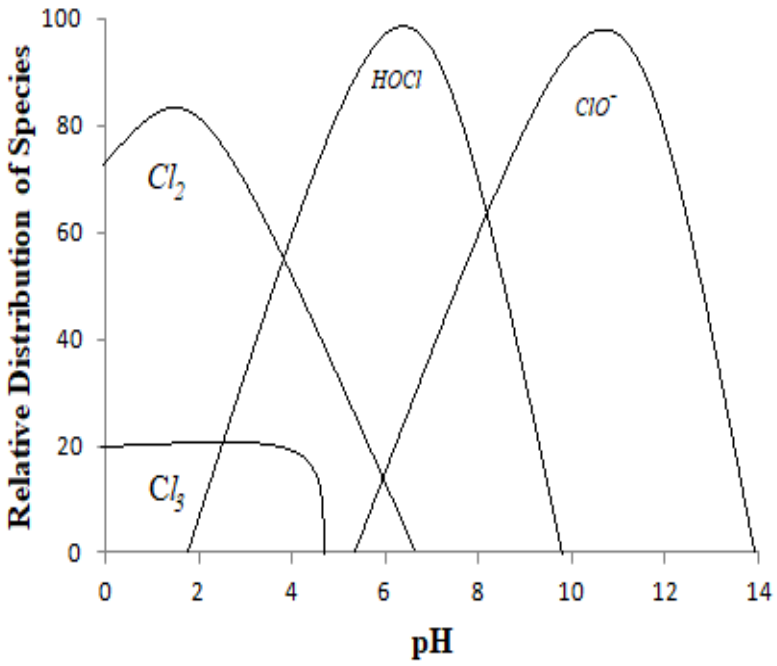

Fig 1.8 Generation of chlorinated species with respect to pH

1.4 Motivation and Aim of the proposed study

For treating phenolic wastewater, various treatment technologies including biological treatment (Fang et al., 2006), precipitation/coagulation (Golbaz et al., 2014), adsorption (Zagklis et al., 2015) and chemical oxidation (Santos et al., 2006) have been tested which possess drawbacks like generation of secondary pollutants, incomplete degradation and high consumption of energy. Hence, the proposed research work has been performed to investigate the PEC degradation of recalcitrant compounds i.e. Pentachlorophenol (PCP) and 4-chloroguaiacol (4-CG) commonly found in the effluent of P & P industry.

Efforts have been carried out to overcome the e^-/h^+ recombination limitation of PC technique by making use of external current as well as by adopting doping of TiO_2. PEC treatment technology was employed using novel laboratory synthesized electrodes to overcome certain limitations like catalyst separation, recombination of charged species and longer treatment time. The synthesized electrodes have been extensively characterized using various techniques to study their physicochemical properties. The treatment process has been carried out in batch mode and degradation of model compounds and simulated P & P mill effluent has been assessed. The role of $^{\bullet}OH$ radicals was studied and their quantitative analysis has been performed. The practical viability of the optimized processes was assessed by treating simulated effluent which was prepared by diluting the real effluent collected from bleaching section of P & P mill located in Punjab province of India. Moreover, the treatment cost associated with degradation studies of model compounds and simulated effluent has also been examined. The mineralization studies were performed through residual Total Organic Carbon (TOC) concentration and formed intermediates during the course of reaction were identified using Gas Chromatography-Mass Spectroscopy (GC-MS) and Liquid Chromatography-Mass Spectroscopy (LC-MS).

Chapter 2

Review of Literature

P & P industry is considered as a major environmental polluter worldwide. The recalcitrant compounds present in the effluent of P & P mills are hazardous and have long retention time in the environment as they cannot be biologically degraded. Hence, special attention is required in this area and this chapter deals with the literature analysis related to P & P industries concerning their impacts on environment and past studies conducted to treat the P & P industries wastewater using conventional treatment technologies/advanced treatment technologies.

2.1 Overview of pollution caused by P & P industry

All the aspects of environment i.e. air; water and land are severely polluted by the discharged pollutants from P & P industries. Each process involved in pulping consumes huge amounts of fresh water and discharges it in the form of black liquor. The most polluter process steps involved in the production of paper are raw material preparation and its washing, pulping and washing of pulp, screening and washing, bleaching of pulp, paper machine and coating procedures. Among these, wastewater generated by pulping process specifically, by the means of chemical pulping is of very high strength. Chlorine/chlorine dioxide is utilized for brightening of pulp in the bleaching process which generates most of the toxic compounds. For the preparation of pulp fibres, wide species of plants can be utilized like, bamboos, wood, canes, reeds, straws and grasses. The non-biodegradable compounds like carbohydrate, lignin and other extractives are the constituents of raw material which gets washed from the fibres during the paper making processes (washing, dewatering and screening).

During the paper making process, various toxic compounds are generated which depends on the type of pulping process adopted such as, unsaturated fatty acids, chlorinated resin acids, diterpene alcohols, resin acids, juvaniones, etc. The pollutants generated at different stages of paper making have been shown in Table 2.1. Majority of environmental problems are originated form chlorine based bleaching step involved in paper making. Effluents from bleaching segment consists huge concentration of recalcitrant compounds like chlorophenols, chloroguaiacols, chlorinated resin acids, adsorbable organic halogens (AOX), dioxins, dichlorodiphenyltrichloroethane (DDT), polychlorinated dibenzodioxines, furans,

and polychlorinated biphenyls (Ali and Sreekrishnan, 2001; Karrasch et al.,2006; Requejo et al., 2012).

Constantly and continuously studies by various scientific groups have been performed to find out the toxic effect of P & P mill effluent on various species of fishes. Several studies suggested the appearance of toxic effects upon exposure to P & P effluents on various species of fish like toxicity and mutagenicity, genotoxic effects, lethal effects, liver damage, mixed oxygenase activity and respiratory stress (Erisction and Larsson, 2000; Li et al., 2018). The effect on aquatic organism of P & P mill effluent discharged into Dong Nai River in Vietnam has been studied by Yen et al., (1997) however; few other authors stated some contradictory report. The fate of resin acid discharged by P & P mills in the environment has been studied by Makris and Banerjee (2002). A serious concern has been raised and reported by Baruah (1997) on change in the population of surface plankton in Elengabeel's wetland, India because of the untreated discharge of P & P mill effluent into the environment.

In northern Arizona, some serious changes in the soil chemistry have been detected by Howe and Wagner (1999) due to the P & P mill treated effluent discharge on the irrigation soil. Study conducted by Singh et al., (1996) and Yadan and Chandra (2018) reported the presence of high load of organic pollutants and coliform count in various effluents in Punjab and Tamil Nadu, India. However, another researcher Archibald (2000) reported that coliform presence in the P & P effluent can not necessarily impose health hazard until the presence of pathogens has been observed. Existence of several trace metals in the P & P industrial effluent was detected by Holmbom et al., (1994) and Haq et al., (2017). Manganese accumulation at elevated levels in Crayfish coming in contact with P & P wastewater has been observed by King et al., (1999). Mandal and Bandana (1996) reported that humans coming in contact with environmental discharged P & P industrial effluent faces health problems like headaches, eye irritation, diarrhea and nausea. High CO_2 level contributed by P & P mill effluent has been studied by O'connor et al., (2000) and found to be a potential cause of toxicity and distress in rainbow trout fishes. Dutta (1999) demonstrated the toxicity effects of treated P & P mill effluent on paddy field in Assam, India. The presence of chlorinated compounds such as phenols and resin acids in hardwood kraft mill has been observed to be 3 to 8 folds lower than that in softwood kraft mill effluent (Mohamed et al., 1989).

Table 2.1 P & P mill wastewater characteristics at different processes involved in paper making (Bajpai, 2000)

Process	Parameter								
	pH	SS	BOD_5	COD	Acetic acid	Meth-anol	N	P	S
TMP(1)	-	383	2800	7210	235	25	12	2.3	72
TMP(2)	4.2	810	2800	5600	-	-	-	-	-
CTMP	-	500	3000-4000	6000-9000	1500	-	-	-	167
Kraft bleaching	10.1	37-74	128-184	1124-1738	0	40-76	-	-	-
Kraft foul (1)	8.0	16	568	1202	-	421	-	-	5.9
Kraft foul (2)	10.2	0	10,700	16,000	-	-	306	1	91
Kraft foul (3)	9.5-10.5	0	5500-8500	10000-13000	-	7500-8500	350-600	0.02-1.55	120-375
Sulfite condensate (1)	2.5	-	2000-4000	4000-8000	-	250	-	-	800-850
Sulfite condensate (2)	2.8-5.9	-	3700-5110	9800-27100	-	-	-	-	840-1270
Pulping:									
Spent liquor	-	253	13300	39800	3200	90	55	10	868
Chip wash	-	6095	12000	20600	820	70	86	36	315
Paper mill	-	800	1600	5020	54	9	11	0.6	97

Pollution caused by P & P making sector can be reduced by modifying several internal processes and adopting certain management techniques like the use of Best Available Technology (BAT). In the effluent, 60 % BOD reduction has been observed by Dube et al., (2000) when an internal process was modified in Irving P & P Limited, Canada. Several researchers indicated the reduction in COD, BOD, and colour by internal process change (Raghuveer and Sastry, 1991; Hossain and Ismail, 2015; Vashi et al., 2017). However, treatment of P & P industry by various other processes is mandatory as it discharges pollutants of different variety which are highly toxic and recalcitrant in nature.

2.2 AOPs: Current status and Prospects

AOPs has been defined as the water treatment technique performed at room temperature and pressure, dependent on the in-situ generation of oxidative species specifically $^{\bullet}OH$ radicals to degrade contaminants (Glaze et al., 1987). AOPs are gaining increasing interest worldwide, as shown by several research groups due to their attractive performance against the degradation of highly recalcitrant compounds present in water

(Herrmann et al., 1999; Laine and Cheng, 2007; Changotra et al., 2017; Kaur et al., 2018). In different types of AOPs, $^{\bullet}OH$ radicals are formed by different reactions like, photochemical, chemical, electrochemical or sonochemical. The different reactions involved in the generation of $^{\bullet}OH$ in different AOPs has been shown in Table 2.2.

Table 2.2 Different reactions involved in the generation of $^{\bullet}OH$ radicals in different AOPs (Sirés et al., 2014)

	Reactions
Dark AOPs	
Ozone + catalyst	$O_3 + Fe^{2+} + H_2O \longrightarrow Fe^{3+} + OH^- + {}^{\bullet}OH + O_2$
Ozone + H_2O_2	$2O_3 + H_2O_2 \longrightarrow 2{}^{\bullet}OH + 3O_2$
Ozone at elevated pH	$3O_3 + OH^- + H^+ \longrightarrow 2{}^{\bullet}OH + 4O_2$
Fenton	$Fe^{2+} + H_2O_2 \longrightarrow Fe^{3+} + OH^- + {}^{\bullet}OH$
Photo-assisted AOPs	
H_2O_2/UV	$H_2O_2 + h\nu \longrightarrow 2{}^{\bullet}OH$
Ozone/UV	$O_3 + H_2O_2 + h\nu \longrightarrow O_2 + H_2O_2$
TiO_2/UV	$TiO_2 + h\nu \longrightarrow TiO_2\ (e^- + h^+)$
	$h^+ + H_2O \longrightarrow {}^{\bullet}OH + H^+$
	$e^- + O_2 \longrightarrow O_2^{-\bullet}$
Photo-Fenton	$Fe^{2+} + H_2O_2 + h\nu \longrightarrow Fe^{3+} + OH^- + {}^{\bullet}OH$
	$Fe(OH)^{2+} + h\nu \longrightarrow Fe^{2+} + {}^{\bullet}OH$
	$Fe(OOCR)^{2+} + h\nu \longrightarrow Fe^{2+} + CO_2 + R^{\bullet}$
Electro-oxidation	$MO_x + H_2O \longrightarrow MO_x({}^{\bullet}OH) + H^+ + e^-$
	$2Cl^- \longrightarrow Cl_2 + 2\ e^-$

Fenton's process is the oldest type of AOP technique in which a mixture of iron source and H_2O_2 are required to generate $^{\bullet}OH$ radicals. This technique has been widely employed for treating persistent organic pollutants (POPs) (Andreozzi et al., 1999; Parsons, 2004; Gan and Ng, 2012). However, the major drawbacks associated with this technique are the requirement of chemicals and generation of iron sludge which further needs treatment. For bleaching kraft mill effluent, combination of Fenton and photo-Fenton process has been observed to be highly efficient by Perez et al., (2002). The activity of Fenton's treatment process can be further improved by providing simultaneous irradiations like UV irradiation

(photo- Fenton process), or solar irradiation (solar mediated photo- Fenton process) (Changotra et al., 2018a). To remove the colour of kraft mill effluent, horseradish peroxide has been utilized by Peralta-Zamora et al., (1998). The authors reported 50 % decolourization of effluent within 3 h of reaction time.

Some other AOP based techniques such as heterogeneous photocatalysis employing TiO_2 as photo-catalyst (Černigoj et al., 2007; Etacheri et al., 2015; Marinho et al., 2017; Cai and Hu, 2018), ozonolysis (Mehrjouei et al., 2015; Vatankhah et al., 2018) has also been frequently investigated. Heterogeneous photocatalysis often faces limitations like recombination of e^-/h^+ at high rate, separation of catalyst after treatment, limited reusability potential of photo-catalyst (Dong et al., 2017; Zhao et al., 2018).

Recently, electrochemical assisted AOPs have come into picture and reported by several researchers for treating polluted water (Panizza and Cerisola, 2009; Rocha et al., 2012; Radjenovic et al., 2015; Agnihotri et al., 2018). In this process, generation of $^{\bullet}OH$ occur by the means of electrochemistry. It is an emerging technology and is considered as environmental friendly process since it greatly inhibits the need of chemical reagents. This technology has major advantage like high inhibition of e^-/h^+, no need for catalyst separation, degradation of recalcitrant pollutant in shorter duration of time (Nidheesh et al., 2018).

2.2.1 Photocatalysis for wastewater treatment

Semiconductor photocatalysis has been considered among one of the promising techniques for the degradation and complete mineralization of organic contaminants (Solomon et al., 2012; Ayekoe et al., 2017). Heterogeneous photocatalysis has been widely used for treating several types of organic contaminants such as antibiotics (Kanakaraju et al., 2014; Hwangbo et al., 2019), aldehydes (Ding et al., 2018), dyes (Wang et al., 2015; Vaiano et al., 2017), chloroanilines (Szczepanik et al., 2017), insecticides (Mir et al., 2013; Joseph and Thiripuranthagan, 2018), herbicides (Tang et al., 2013), polymers (Singh et al., 2013), and phenols (Shet and Vidya, 2016; Vaiano et al., 2018). Recently, photocatalysis has been found to be effective for the real water samples taken from Agbo river (Ayekoe et al., 2017). The wide application of heterogeneous photocatalysis has been shown in Figure 2.1.

Fig. 2.1 Potential applications of Heterogeneous photocatalysis (Ahmed and Haider, 2018)

2.2.1.1 Photocatalytic treatment of P & P mill pollutants

Photocatalytic treatment of kraft mill effluent has been observed to be largely dependent on the effluent strength in terms of COD and chloride content (Balcioğlu and Cecen, 1999). The pollutant responsible for odour problems, total reduced sulphur (TRS) was catalytically oxidized by Dufresne et al., (2000) to obtain odour free products. The recalcitrant phenolic compounds from bleaching stage effluent has been treated by advanced oxidation techniques using TiO_2/O_2/UV, ozone, ozone/UV and ZnO/O_2/UV and found out TiO_2/O_2/UV and ZnO/O_2/UV to be the best treatment option among others to treat effluent in short time period. UVA-LED based photoreactor has been used by Levchuk et al., (2015) for the degradation of formic acid and phenol by using commercial TiO_2 as a photocatalyst. Heterogeneous photocatalysis for the treatment of P & P mill effluent have been adopted by using magnetically separable Fe_2O_3-TiO_2 photocatalyst. The activity of synthesized catalyst has been observed to be better than the commercial P25 (Subramonian et al., 2017). TiO_2/Polystyrene composite has been utilized for the P & P industry wastewater treatment under UV-LED irradiations. Effective COD, lignin and toxicity removal has been observed after the treatment time of 120 min (Haghighi et al., 2018). The PC treatment for the synthetic wastewater comprising of biorecalcitrant chlorinated phenols such as: 4-CP; 2,4-

DCP; 2,4,6-TCP, and PCP have been studied and significant TOC reduction have been observed (Singh and Garg, 2019).

Considering the target pollutants, few studies have been reported for the efficient degradation of PCP using photocatalysts like RGO/PbS-TiO_2 NTs (Zhang et al., 2013); TiO_2 sol–gel catalysts; $Bi_{12}SiO_{20}$ (Li et al., 2011); Ti-Doped β-Bi_2O_3 (Yin et al., 2010); $Bi_2O_3/TiO_{2-x}B_x$ (Su et al. 2012) and α-Fe_2O_3/ ZnO (Xie et al. 2015). However, limited studies are available for 4-CG degradation including UV/TiO_2 and UV/TiO_2/H_2O_2 process (Kumar et al., 2011a); ZnO/TiO_2 photocatalysts (Dhir et al., 2012a) and CuO·ZnO/Al_2O_3 catalyst (Hamoudi et al., 2001).

Upon comparison, TiO_2 has been observed to be more effective than ZnO in terms of mineralization of effluent from bleaching section of kraft pulp mill (Yeber et al., 2000). The authors observed 55 % TOC reduction with TiO_2 and only 31 % reduction of TOC with ZnO. Kansal et al., (2008), has also reported TiO_2 as a better catalyst for treating acid effluent from kraft mill utilizing agro waste as its raw material. TiO_2 has also been observed to be an efficient catalyst in immobilized form (immobilized on glass surface) (Yeber et al., 1999). The studies have suggested that the treatment utilizing TiO_2 in immobilized form to be as effective as when it utilized in suspended form, but TiO_2 in immobilized form requires longer reaction duration to achieve similar treatment targets. The immobilization step facilitates the utilization of photo-catalyst in continuous mode reaction eliminating the need of catalyst separation and recovery step (Bhatia et al., 2018). Several researchers combine H_2O_2 with UV-TiO_2 photocatalytic process to additionally supply $^{\bullet}OH$ radicals to the reaction system as an additional oxidizing species. All the studies reported improved COD reduction when H_2O_2 was added in addition to UV-TiO_2 treatment particularly at near neutral pH (Chang et al., 2004; Catalkaya and Kargi 2008; Kumar et al., 2011; Affam et al., 2018).

2.2.1.2 Solar mediated photocatalytic treatment

Solar light for the activation of semiconductor photo-catalyst has also been investigated extensively in order to reduce the treatment cost by utilizing naturally available resources. Amat et al., (2005) have studied efficient COD reduction of board industrial effluent in the presence of solar irradiations and observed 40% reduction at pilot scale while, 50% at laboratory scale. Kansal et al., (2008) reported solar mediated PC treatment of bleach section effluent and observed ZnO to be better catalyst as compared to TiO_2 in the presence of solar light which was contradictory in case the of UV radiations. Dhir et al., 2012 studied role of ZnO photocatalyst for the treatment of chlorinated effluent from agriculture based P &

P industry in combination with biological treatment. The overall 92% COD reduction has beeb observed when solar mediated ZnO photocatalysis was employed as pre-treatment before biological process and 95% COD removal has been observed when photocatalysis was used as post treatment to biological process. $CdSe/TiO_2$ nanocatalysts have been synthesized for the PC treatment of phenol under solar irradiations. The results demonstrate that a CdSe nanoparticle extend the spectral response of TiO_2 into visible region and reduces the recombination of e^-/h^+ pair (Ghodrati et al., 2011). Dye-sensitisation method using methylene blue and rhodamine B has been used for the modification of TiO_2 catalyst. The modified catalyst has been then employed for the solar light mediated photocatalytic degradation of P & P industry wastewater (Priya et al., 2015). Hydrothermal process has been employed for preparing C-modified TiO_2 material by utilizing lignin as precursor and providing a possibility of lignin valorization (Gómez-Avilés et al., 2019).

2.2.2 Electro catalysis for wastewater treatment

Electrochemical methods are gaining increasing interest due to their technical and economic feasibility for large scale functioning in comparison to several other physicochemical treatment techniques (Soloman et al., 2009; Montiel et al., 2018). EC process is based on either direct degradation of pollutants on the surface of electrode or indirect degradation by oxidative radicals in the solution itself. Removal of various contaminants by employing these methods significantly depends upon the used process operational conditions. The main treatment conditions which affect the treatment process are characteristics of wastewater, material of electrode, current density and treatment time. Electrochemical oxidation methods have fetched considerable attention as they are capable in complete mineralization of contaminants such as dyes (De Aragao Umbuzeuro et al., 2005; Florenza et al., 2014; Labiadh et al., 2015), pharmaceuticals (Sopaj et al., 2015; Ganzenko et al., 2018), pesticide (Landeros et al., 2017), herbicide (Dos Santos et al., 2015), chlorinated compounds (Zazou et al., 2016). Electro-Fenton technique has been adopted by Olvera-Vargas et al., (2018) to treat pharmaceutical (acetaminophen) contaminated aqueous solution. It has been observed that, optimum current has a positive effect on the degradation and mineralization of pharmaceutical compound. The electro-Fenton degradation of phenol has been studied by Khatri et al., (2018) by using iron electrodes and activated carbon as a co-catalyst. The enhanced degradation was observed due to the synergestic effect of adsorption and electro-oxidation reactions.

The wide applicability of electrochemical oxidation technique has been shown in Figure 2.2.

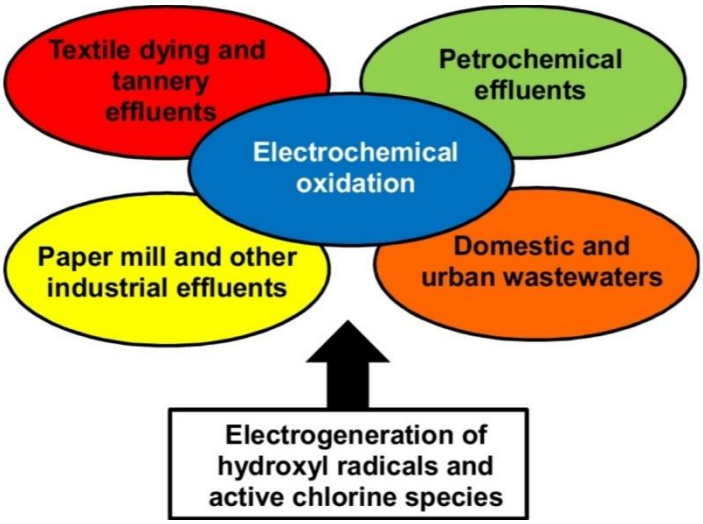

Fig. 2.2 Wide applications of electrochemical oxidation **(**Garcia-Segura et al., 2018)

2.2.2.1 Electrochemical treatment of P & P mill pollutants

A significant COD reduction (63%) of cellulose pulp mill effluent has been observed by Buzzini et al. (2006), at 22.5 Adm^{-2} after a time period of 180 min. Commercially available iron and aluminium electrodes have been tested against COD reduction of P & P mill effluent by Boroski et al., (2008) and the both type of electrodes were found to exhibit similar COD removal trends. When the other P & P mill pollutants like phenol, lignin and BOD were treated using these electrodes, Al electrodes showed higher removal efficiency when compared to Fe electrodes (Uğurlu et al., 2008). The influence of pH on the treatment of paper mill effluent has been studied by Perng et al., (2008) and concluded that 28% COD reduction and 94% decolourization was achieved at pH 9, current density 187 Am^{-2}, gap between the electrodes 15 mm and retention time as 57 s. Domínguez-Ramos et al., (2008) reported 80% TOC reduction of lignosulfonate by electrochemical oxidation. The decolourization and COD reduction of effluent has been evaluated and the concentration of polyelectrolytes has been optimized by Khansorthong and Hunsom, (2009). Selvabharathi and Kanmani, (2010) combined electrochemical oxidation with Fenton's process commonly known as electro-Fenton treatment process, and checked its efficiency against the treatment of biologically treated paper mill effluent and observed 90% COD removal and 95 % of decolourization. Treatment at higher pH resulted into decreased efficiency of electro-Fenton process due to the precipitation of $Fe(OH)_3$ as observed by previous published reports of Fenton treatment. It has been suggested that the use of polyacrylamide, sodium silicate and

calcium carbonate as electrolytes can be neglected due to their insignificant contribution in decolourization and COD removal of the effluent, saving down the operational cost of the treatment process.

Moodley et al., (2011) reported the electrochemical conversion of lignin into vanillin, a by-product of commercial value. Antony and Natesan, (2012) reported the COD removal of bleaching effluent of bagasse based paper mill to be 53 % at 0.87 Adm^{-2} in 1.75 h as operating conditions. Elevated COD reduction (87%) of similar bleaching effluent of bagasse based paper mill has also been reported, when electro-oxidation was combined with post biological treatment. The probable reason might be that, after electro-oxidation of effluent its biodegradability gets increased which on further undergoing biological treatment resulted in increased COD reduction as compared to electro-oxidation process alone. Furthermore, when authors studied combined electro-coagulation (1 Adm^{-2} for 34.4 min), electro-oxidation (1.5 Adm^{-2} for 90.5 min) followed by biological treatment for 521 min, 95% reduction in the COD values has been noticed. Treatment of model compounds present in P & P industry effluent also showed significantly effective results. The two types of granular electrodes (bentonite and hydroxy-aluminum pillared bentonite) has been prepared by Chu et al., (2016) for the COD and colour removal of P & P mill wastewater. The significant reduction in COD (84.3 %) and colour (93.0 %) was observed. Buftia et al., (2018) utilized electro-Fenton process for the successful treatment of non-recoverable lignin and other contaminants present in acid black liquor of P & P mill. Recently, electrochemical based treatment techniques have been adopted for the management of P & P mill industrial wastewater (Zainith et al., 2019).

Few authors have reported the degradation of target pollutant PCP using different electrochemical oxidation methods using simple electrochemical treatment (Patel and Suresh, 2008); electro-Fenton (Hanna et al., 2005; Song-Hu and Xiao-Hua, 2005; Govindan et al., 2014); Ti/SnO_2–Sb electrodes; diamond electrodes (Codognoto et al., 2003) and anatase TiO_2/Ti nanotube electrodes (Yang et al., 2006); and Nb/PbO_2 electrodes for electrochemical oxidation of 4-CG. However, these reports face limitation like high treatment cost, use of expensive electrodes, longer treatment time and insufficient knowledge of intermediates generated during the degradation process.

2.2.3 Photoelectrocatalysis: A combination of photocatalysis and electrooxidation

The high recombination of photo-generated e^-/h^+ rate in the case of TiO_2 photocatalysis leads to reduced photonic efficiency imposing a major limitation to the photocatalytic process (Waldner et al., 2003). Zanoni et al., (2003) used photoelectrocatalysis

technique to degrade the reactive dye RBO (Remazol Brilliant Orange) using TiO_2 thin film photoelectrode in the presence of UV light achieving nearly complete mineralization of the dye. PEC treatment is fetching considerable attention in the field of wastewater treatment due to its remarkable efficiency towards the degradation of wide variety of recalcitrant pollutants present in aqueous phase which are not degraded by conventional treatment methods (He et al., 2003; 2006; Daghrir et al., 2012a). Electrochemical anodization of silicon doped titania nanotube array by Chemical Vapour Deposition (CVD) resulted in significant blue shift in the UV spectrum (Su et al., 2008). Yu et al., (2008) fabricated TiO_2 nanostructured thin films having large surface to volume ratio using an anodization technique and investigated the influence of different electrolytes like HF-containing or neutral electrolyte and different substrates such as silicon or silicon carbide substrate on the formed structure of the anodized thin films.

Due to the major drawback of recombination, PEC, a combination of photocatalysis and electrolytic processes has been employed as an alternative cost effective treatment process (Liu and Du, 2011). Previous research suggested the applied external current as a key factor in PEC technique as it accelerates the photo-catalytic reactions (Daghrir et al., 2012b). The reaction mechanism of PEC is almost similar as of PC except the involvement of external current. Cheng et al., (2016) studied microwave reduction to prepare photoelectrodes of reduced TiO_2 nanotubes and tested its photoelectrocatalytic degradation efficiency against Diclofenac achieving better degradation rates under visible light.

2.2.3.1 Laboratory synthesized electrodes for the PEC degradation of pollutants

A thin film photocathode having corrosion resistant property has been developed by Siripala et al., (2003) using TiO_2 cathode surface electrochemically deposited on cuprous oxide and demonstrated that corrosion limitations of Cu_2O while maintaining high photoelectrolysis efficiency. Shaogui et al., (2004) synthesized nanocrystalline Fe_2O_3/TiO_2, ZnO/TiO_2, and $Fe_2O_3/ZnO/TiO_2$ electrodes and found that Zn^{2+} doped electrodes were most efficient towards pentachlorophenol degradation. Li et al., (2006a) synthesized PbO_2 electrode by TiO_2 co-deposition, which were found to be more uniform when compared with unmodified PbO_2 electrode for PEC degradation of Acid Orange 7. A TiO_2/Ti mesh electrode using laser calcinations has been prepared and photo-degradation has been tested against Methylene Blue (Li et al., 2007). Paulose et al., (2007) synthesized self-aligned titania nanotube arrays of around 1000 µm length by potentiostatic anodization of titanium. Two Sb-

doped SnO_2 films were prepared (Ti/SnO_2-Sb_2O_4/SnO_2-Sb_2O_4 and Ti/SnO_2-Sb_2O_4) on titanium substrate using electro-deposition and dip-coating, and the results showed that Ti/SnO_2-Sb_2O_4 electrode with sub-layer exhibited enhanced PEC degradation efficiency against phenol when compared to Ti/SnO_2-Sb_2O_4 electrode. (Yan et al., 2009). Sadek et al., (2008) performed Ti film deposition onto the Indium Tin Oxide substrate by anodization process and studied the role of temperature in anodization process as well as on the structure of the film. It has been reported that high temperature anodization films resulted in the nano tube type structures, while anodization at room temperature resulted in irregular pores. Esquivel et al., (2011) achieved electrophoretic deposition of TiO_2 doped with varying amounts of Co and Ni on Indium Tin Oxide electrodes and results indicated higher colour removal efficiency of Methyl Orange dye when compared to the commercially used TiO_2. Lin et al., (2012) investigated that PEC degradation efficiency of persistent pollutant perfluorooctanoic acid in aqueous medium by employing Ti/SnO_2-Sb/MnO_2, Ti/SnO_2-Sb/PbO_2 and Ti/SnO_2-Sb were found to be 90.3, 91.1, and 31.7%, respectively. The combination of these two techniques provides the opportunity of photo-generated e^-/h^+ separation thereby, preventing their recombination. In the recent study, Yao et al., (2016) prepared Ti/Sb-SnO_2 and Ti/F-PbO_2 electrodes using electrodeposition and thermal decomposition process; their electrocatalytic performance was compared against Malachite Green dye and it has been observed that higher oxygen evolution capability was possessed by Ti/Sb-SnO_2 electrodes over Ti/F-PbO_2 electrodes, whereas, corrosion resistance property and stability of latter was much higher. For improving the photo-catalytic degradation of salicylic acid, Momeni and Hosseini, (2016) studied the fabrication of TiO_2 nanotube arrays (TNTAs) by two-step anodization method followed by their treatment in methanol solution under the influence of UV light irradiation which exhibited better photo-catalytic activity than the electrodes prepared in one-step anodization process. Tantis et al., (2016) degraded dye in the presence of Sodium chloride by coupling electrochemical process with photocatalytic degradation and observed that coupling of these two processes accelerated the mineralization process. A novel petaline NiO@polyaniline-carbon felt anode has been prepared by in-situ polymerization (Zhong et al., 2018). The synthesized electrodes exhibited significant colour (95.9 %) and COD (64.2 %) removal of dye wastewater.

2.2.3.2 PC, EC and PEC comparison

TiO_2 has been used in both photocatalytic and photoelectrocatalytic studies to assess the influence of current on the improvement of the photocatalytic reaction efficiency and observed that degradation rates of photocatalytic reaction were proportional to the thickness of TiO_2 film (Kim and Anderson, 1994). Xie and Li (2006) prepared TiO_2/Ti film electrode by anodiziation at low voltage where the TiO_2 thick film was synthesized in H_2SO_4-H_2O_2-H_3PO_4-HF based electrolyte while the TiO_2 thin film was prepared in H_3PO_4-HF solution. The reactivity of prepared films for PC and PEC degradation of Bisphenol A in aqueous solution showed the degradation efficiency of TiO_2/Ti thin film to be higher with PEC oxidation (Li et al., 2007). Li et al., (2009) synthesized an electrode by combining TiO_2 photocatalyst and Sb-doped electrocatalyst (SnO_2), which exhibited high PC and EC oxidation efficiency at the same time. This research enabled to enlighten the PEC theory on the electrode's microstructured interface and lead to exploration of highly efficient PEC technology. He et al., (2010) prepared TiO_2 nanocrystalline structure by depositing metals like Pt, Ag and Cu and concluded that degradation efficiency against formic acid has been higher of metal deposited TiO_2 film when compared to TiO_2 film in both PEC and PC process. Chai et al., (2011) prepared a novel electrode using a block co-polymer soft template method and the synthesiezed electrode exhibited significant PC and EC performances against the degradation of p- Nitrophenol wastewater. The band gap of the synthesized electrode i.e. Mp-SnO_2/TiO_2NTs has been observed to be 2.93 eV and it showed good light absorption properties. Nurdin, (2014) fabricated TiO_2/Ti nano tube electrodes through anodization method and degraded Acid Orange 7 dye.

2.2.3.3 Role of co-catalyst

It was suggested that by using co-catalyst on the surface of photoelectrode, the over potential can be reduced which is necessary for occurance of redox reactions and in some cases promotes separation and diffusion of carrier species (Costi et al., 2008; Meekins and Kamat, 2011). Study performed by Wang and Zang, (2012) revelead that modification of TiO_2 nanorod with graphite-like carbon nitride by chemical vapour deposition (CVD) method had dramatically improved the electron-transfer rate to the electrode surface from electrolyte and showed high activity towards PEC degradation of Rhodamine B. Chen et al., (2011a) studied the oxidation resistance of CVD mediated coating of graphene with Cu and Cu/Ni alloy and found that graphene layer acts as a barrier for Cu and Cu/Ni alloy against air and chemical oxidation in the solution of 30% H_2O_2. Zhai et al., (2014) modified TNTAs

electrodes with RGO-TNTs and utilized for PEC degradation of Methyl Orange (MO) under visible light illumination. Results showed RGO–TNT arrays electrodes were more stable and provided improved PEC activity against the degradation of MO in comparison to bare TNTAs electrode. Zheng et al., (2016) combined in-situ anodization and electro-deposition process for the fabrication of Graphene/TiO_2 nanotube arrays photoelectrodes and reported 99.5% of degradation of alachlor (herbicide) after 15 cycles with 60 min irradiation for each cycle. Similar work has been reported by Zheng et al., (2016) for degrading Rhodamine B which showed degradation of 75% with GR/TNAs photoelectrodes within 60 min of irradiation at pH 6.

The fabrication of graphene on anodized Ti soft wire bearing TiO_2 nanotubes using CVD followed by electrochemical deposition of Cu_2O was performed by Yang et al., (2016). The fabricated mesh of TiO_2/graphene/Cu_2O has been successfully applied in effective PEC oxidation of Bisphenol A. Almeida et al., (2015) synthesized a novel nanocomposite of TiO_2 and Cu_2O nanoparticles combined with RGO and studied the activity of nanocomposite against the photodegradation of Methylene Blue dye under solar irradiation. Li et al., (2016) fabricated nano-graphite/TiO_2 photoelectrode through sol-gel method followed by the hot-press approach and observed enhanced degradation efficiency of 99.2% towards the PEC degradation of phenol when compared to 29.1 and 58.3% removal effieicncy with TiO_2 and Nano-G electrode, respectively. Liu et al., (2016) developed a PEC system for the removal of Ofloxacin in which electrodeposited Cu^{2+} ions on titanium plate served as the cathode and highly ordered TiO_2 nanotubes served as a highly active photoanode. Zhang et al., (2017) used Ti sheet as precursor in NaOH solutions to synthesize highly ordered TiO_2NTs nanotubes by a low-temperature hydrothermal process. Further, deposition of gold nanoparticles was done on the surface of TiO_2NTs by a microwave-assisted chemical reduction route, which exhibited higher degradation effificency in the PEC treatment of Methylene Blue. Cobalt doped black TiO_2 nanotube array electrode has been synthesized and exhibited higher performance as compared to IrO_2 anode for the treatment of organic rich wastewater (Yang et al., 2018).

Literature analysis revealed that P & P industries are facing improper reforms in environmental performances considering the wastewater treatment. At industrial scale, several physicochemical methods including adsorption, coagulation, membrane processes and biological methods are being employed to treat the recalcitrant pollutants in effluents, but still

they are unable to degrade the recalcitrant organic pollutants present in P & P effluents. The reviewed literature studies have demonstrated that use of several advanced oxidation processes including photoelectrocatalysis technique have been explored as an effective method in treatment of wide range of toxic and recalcitrant compounds in different aqueous solution. However, more studies related to PEC treatment are requisite to improve the degradation of recalcitrant pollutants found in P & P effluents.

2.3 Research Gaps

AOP treatments for the oxidation of pollutants have been observed to be a proficient and effective method to mineralize the organic matters. It has been observed that all the AOPs have few drawbacks for utilization in industrial sector which include:

- Due to the high rate of electron−hole pair recombination and difficulty in catalyst separation from aqueous solutions for reusability, the practical applications of TiO_2 as photocatalyst are found to be significantly restricted.
- Most of the semiconductors are active in the range of UV region and the efficacy of degradation is low in visible light so, doping is needed to extend the absorption spectra in visible region.
- Few scattered reports exists which employed electrochemically assisted photocatalytic degradation for the degradation studies of real and simulated industrial effluent.
- In photoelectrocatalytic process, electrodes often face limitations like creep, substrate corrosion, lead contamination of the electrolyte, high over potential for oxygen evolution. Loss of electrode activity is observed when used for long time, so durability studies are needed.
- Commercially available electrodes have the limitation of their high cost so development of novel working electrodes with good electrochemical and catalytic properties with moderate cost needs to be explored.
- The reaction mechanisms alonwith the complete mineralization of organic pollutants and the characterization of intermediates/secondary by-products have not been frequently explored using PEC treatment.
- Enhancement of treatment efficiency in short time durations by synthesizing new electrode has not been extensively studied.

- To the best of author's knowledge, no report manifests the application of PEC processes using laboratory synthesised doped Cs, Ag, Ag/GO based titania electrodes for the degradation of P & P industrial and simulated effluents.

2.4 Objectives of research work

Keeping in view of these gaps, the proposed study aims to utilize PEC, a synergistic approach of photocatalysis and electrooxidation for the treatment of P & P industry pollutants. Different dopants (GO, Cs, Au, Ag-GO) has been anodized on the surface of synthesized TiO_2 electrodes and their contribution in the degradation activity enhancement has been assessed. Characterization of prepared electrodes has been performed to justify the successful synthesis and doping of electrodes. The synthesized electrodes has been tested against the treatment of recalcitrant compounds present in P & P mill effluents i.e. PCP and 4-CG. For assessing the practical applicability of PEC process using laboratory synthesized electrodes, the treatment efficacy has been observed against the treatment of simulated effluent.

In order to reuse the wastewater, it is essential to remove the recalcitrant compounds like chlorinated organic, dyes etc. which the conventional treatment technologies (mainly biological treatment) fails to do. Hence, this study aims at exploring the effectiveness of PEC process using laboratory synthesized electrodes under solar/UV light for the degradation of model compounds and simulated wastewater. Hence, the study has been focused at the fabrication of titania based electrodes for the photoelectrocatalytic degradation of few model compounds present in P & P mill effluents; use of various dopants to enhance the activity of synthesized electrodes under UV/solar irradiations; and treatment of simulated effluent with solar induced photoelectrocatalytic process under optimized conditions.

The following objectives were followed and achieved during the course of this study:

- Fabrication of Titania based electrodes for the photoelectrocatalytic degradation of few model compounds present in pulp & paper mill effluents;
- Use of various dopants to enhance the activity of synthesized electrodes under UV/solar irradiations; and
- Treatment of simulated effluent with solar induced photoelectrocatalytic process under optimized conditions.

Chapter 3

Materials and Methods

This chapter deals with all the details of materials (chemicals and reagents) used in the photoelectrocatalytic degradation of model compounds and simulated P & P mill effluent. The methodology used for the synthesis of different electrodes has been explained. All the details of characterization techniques adopted for the physicochemical study of synthesized electrodes has been elucidated.

3.1 Chemicals and materials

Titanium (Ti) sheet (thickness 1.0 mm, purity 99.5 %) was purchased from Sanghvi Steel Co., Ltd., New Delhi, India. D.C. Power supply (Output: 30 V, 5 A) was supplied by Batra Trading Company, Ambala, India. Pentachlorophenol (>99%), 4-chloroguaiacol (4-chloro-2-methoxyphenol, 98%), Cesium nitrate (99%), Terephthalic acid (98%), graphite flakes (>99%) were purchased from Sigma Aldrich. Sodium sulphate (>99%), silver nitrate (>99%) and terephthalic acid (98%) were procured from Merck. 2-Hydroxyterephthalic acid (>98%) was procured from TCI Chemicals. Analytical grade reagents were used in this study without any purification. Experimental solutions were prepared using ultrapure water (Milli-Q^{TM} system).

3.3.1 Model compounds

Pentachlorophenol (>99%) and 4-chloroguaiacol (4-chloro-2-methoxyphenol, 98%), were purchased from Sigma Aldrich. The PCP stock solution (20 mg L^{-1}) was prepared by mixing 20 mg L^{-1} of PCP in distilled water overnight. The 4-CG stock solution (20 mg L^{-1}) was prepared by mixing 20 µL of 4-CG in 1 L of distilled water overnight.

3.3.2 Simulated Effluent

P & P industrial effluent has been collected after bleaching stage from the representative industry located in Punjab, India. The sample has been collected in plastic containers and stored at -4 °C in a cold room. The simulated effluent has been prepared by diluting the real effluent collected from the bleaching section of P & P mill with tap water in 50:50 (v/v). In previously reported studies, simulated effluent has also been prepared by diluting the real P & P mill effluent (Yadav and Garg, 2017; Yadav and Garg, 2018).

3.2 Synthesis methodology of different electrodes

Various novel Titanium based electrodes were synthesized using anodization technique at laboratory scale and their efficacy towards the degradation of model compounds and simulated P & P mill effluent was assessed.

3.2.1 Synthesis of TiO_2 nanotube electrode

TiO_2 nanotube electrodes were fabricated by anodization method (Yun et al., 2012) followed by calcination. Ti sheet was firstly gently rubbed using different sized abrasive paper, ultrasonically cleaned in acetone and double distilled water for 20 min each, chemically etched in HF:HNO_3:H_2O solution (1:4:10,v/v/v) for 10 second and then rinsed with acetone and double distilled water. Anodization was performed using Ti sheet as positive, while Cu (copper) sheet as negative electrode at 2 cm distance apart in 200 ml HF (4%) based electrolyte. The anodization was performed for duration of 20 min at a constant voltage of 20V. The freshly prepared electrode was then washed with double distilled water, air dried and calcined in muffle furnace at 500 °C for 3 h.

3.2.2 Synthesis of Cs-TiO_2 nanotube electrode

The synthesized TiO_2 nanotube electrode as discussed in section 3.2.1, has been used as a cathode and Ti sheet as an anode for the electro-deposition of cesium to yield Cs-TiO_2 nanotube electrodes. The anodization with varying concentration of cesium nitrate ($CsNO_3$) was executed for 15 min at 15 V and annealed at 300 °C for 1 h to get Cs-doped TiO_2NT electrode. The schematic diagram illustrating the synthesis process has been show in Figure 3.1.

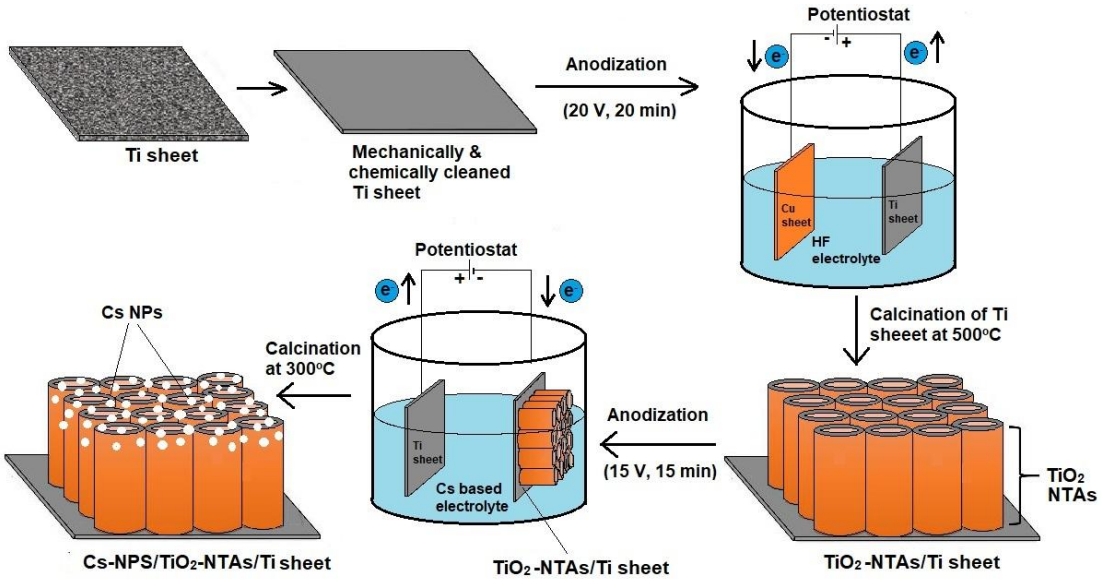

Fig. 3.1 Schematic representation of synthesis of Cs doped TiO_2 nanotubes photoelectrode

3.2.3 Synthesis of Au doped TiO_2 nanotube electrode

The synthesized TiO_2 nanotube electrode was used as a cathode and Ti sheet as an anode for the electro-deposition of Au to yield Au-TiO_2 nanotube electrodes. The anodization with varying concentration of chloroauric acid ($HAuCl_4$) was executed for 15 min at 15 V and annealed at 300 °C for 1 h to get Au-doped TiO_2NT electrode. The schematic diagram illustrating the synthesis process has been show in Figure 3.2.

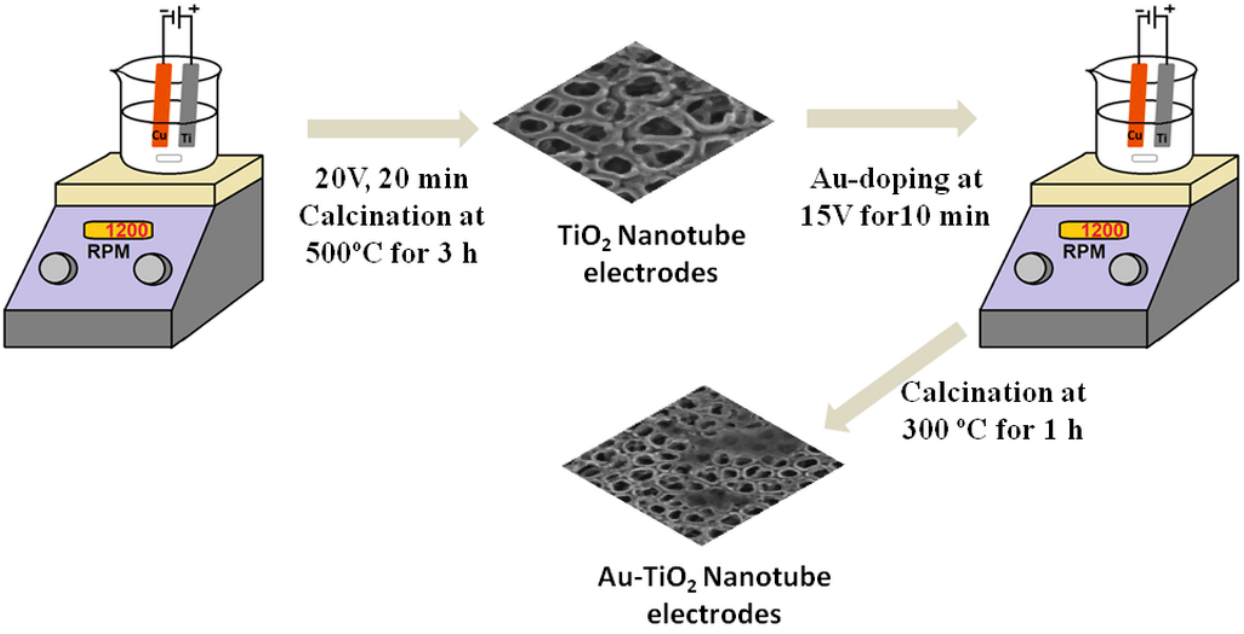

Fig. 3.2 Schematic representation of synthesis of Au doped TiO_2 nanotubes photoelectrode

3.2.4 Synthesis of GO/TiO_2 nanotube electrodes

GO was synthesized from graphite flakes using modified Hummers method (Marcano et al., 2010). The schematic process of GO synthesis from graphite flakes has been shown in Figure 3.3. GO/TiO_2 nanotube electrodes were prepared by electrodeposition of GO at different concentrations on the TiO_2 electrode surface. TiO_2 nanotube electrode was used as anode while Cu as cathode, and anodization was executed at a constant voltage of 15 V for 15 min followed by calcination of prepared electrode at 300 °C for 1 h.

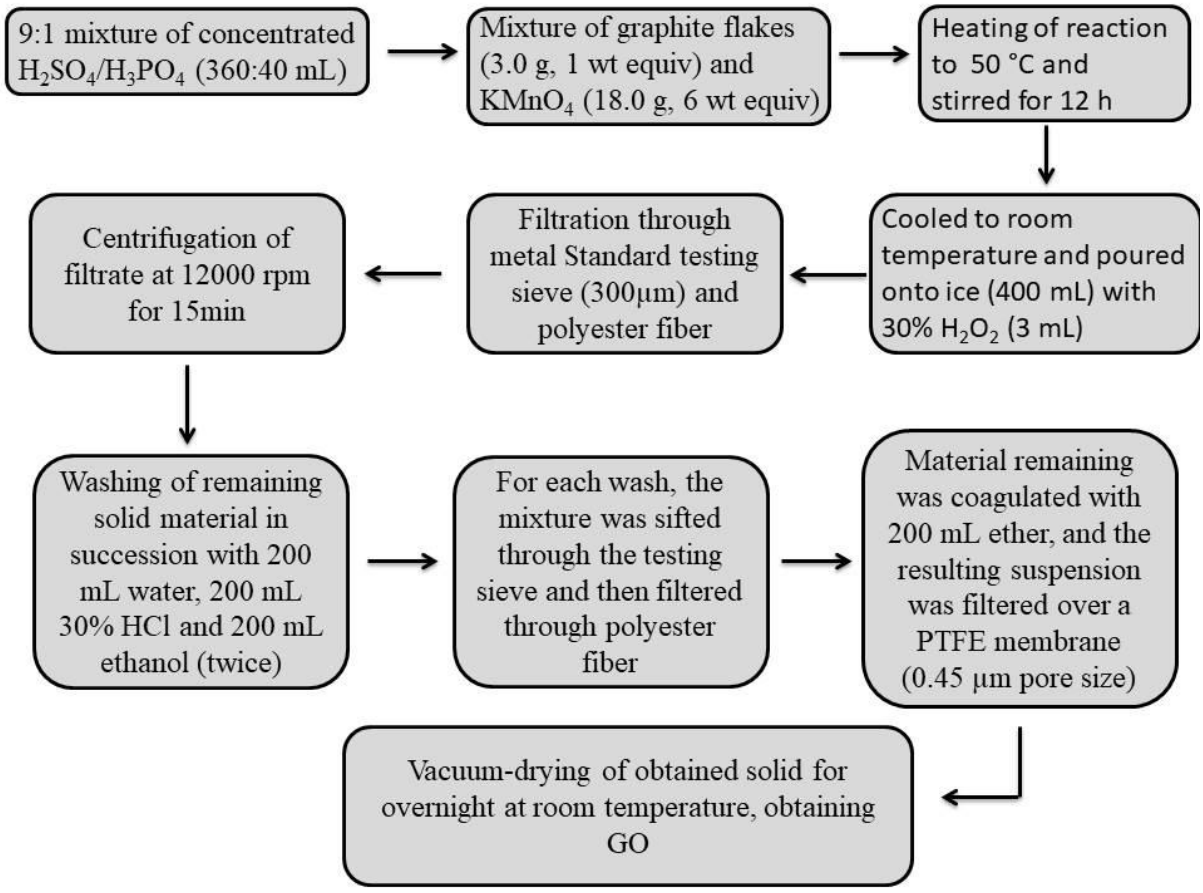

Fig. 3.3 Synthesis procedure of Graphene oxide (Marcano et al., 2010)

3.2.5 Synthesis of Ag loaded GO/TiO_2 nanotube electrode

TiO_2 and GO/TiO_2 nanotube electrodes were prepared as discussed in section 3.2.1 and 3.2.4. For the synthesis of Ag loaded GO/TiO_2 nanotube electrode, anodization was performed at 15 V for 15 min followed by calcination at 300 °C for 1 h. During this process, GO/TiO_2 nanotube electrodes was taken as anode and deposition of varying quantity of Ag was carried out in 200 ml silver nitrate (25, 50, 75 and 100 mg/L) electrolyte at 15 V for 10 min. Annealing was performed at 300 °C for 1 h.

3.3 Characterization of synthesized electrodes

The physicochemical properties of synthesized electrodes like structure, composition, morphology, crystalline structure, bonding etc. has been examined using various techniques. The morphology of synthesized electrodes has been characterized using Field Emission-Scanning Electron Microscopy (FE-SEM, Nova Nano FE-SEM 450) with an accelerating voltage of 15 kV associated with Energy Dispersive Spectrometry (EDS). The crystalline structure has been confirmed using X-ray diffractometer (XRD, PanAlytical) using Cu Kα

radiation source (α = 1.5406 Å) operated at an applied current of 40 mA and accelerating voltage of 45 kV. Raman measurements has been performed using a confocal micro Raman Spectrophotometer (STR 500, Airix Corporation, Japan) with a 532 nm diode green laser. The Ultraviolet-vis diffuse reflectance spectroscopy (UV-vis DRS) measurements has been performed on UV-2600 (Shimadzu, Asia-Pacific) and were recorded in the range of 400-700 nm. The composition and surface properties of electrodes has been analysed by X-ray photoelectron spectroscopy (XPS, Omicron Nanotechnology, Oxford Instruments). Fourier Transform Infrared spectrum (FTIR) has been obtained using a FT-IR Spectrum 2 (Perkin Elmer). Photoluminescence (PL) spectrum has been acquired using a Fluorescence spectrophotometer (LS 55, Perkin Elmer).

3.4 Experimental

The degradation experiments have been performed using synthesized electrodes and their PEC activity has been assessed against the removal of model compounds i.e. pentachlorophenol, 4-chloroguaiacol and simulated effluent. The initial concentration kept throughout the study was 20 mg L^{-1} for both the model compounds

3.4.1 Batch experiments of PEC, PC and EC

The photoelectrocatalytic degradation experiment in batch mode has been carried out in a cylindrical glass reactor (9.5 x 7 cm) using synthesized electrode (4.6 x 6.5 cm) serving as a photo anode and Cu electrode serving as cathode. The diagrammatic representation of PEC batch reactor has been shown in Figure 3.4. Model compound's solution (20 mg/L, 250 mL) has been magnetically stirred with optimized concentration of Na_2SO_4 as a supporting electrolyte. All the UV radiation based experiments have been performed in a chamber consisting of two long wave UV tubes (Philips, 36 W, λ_{max} = 365 nm) each having intensity of 1.6 W/m^2. Solar radiation based experiments have been performed on the roof top of Thapar Institute of Engineering and Technology, with solar light at an average intensity of 941W m^{-2}. External current has been applied using a DC regulated power supply. The solution pH has been adjusted with 1 M solution of HCL and NaOH. For each experiment run, freshly anodized electrodes has been prepared and used. All the experiments have been performed in triplicate and the average values are reported.

Photocatalytic experiments has been carried out using synthesized electrodes as immobilized catalyst and rest of the reaction conditions has been kept similar in the absence of supplied current. However, while performing Electrocatalytic experiments novel

synthesized electrodes has been used under the influence of externally applied current but in the absence of UV/solar irradiations.

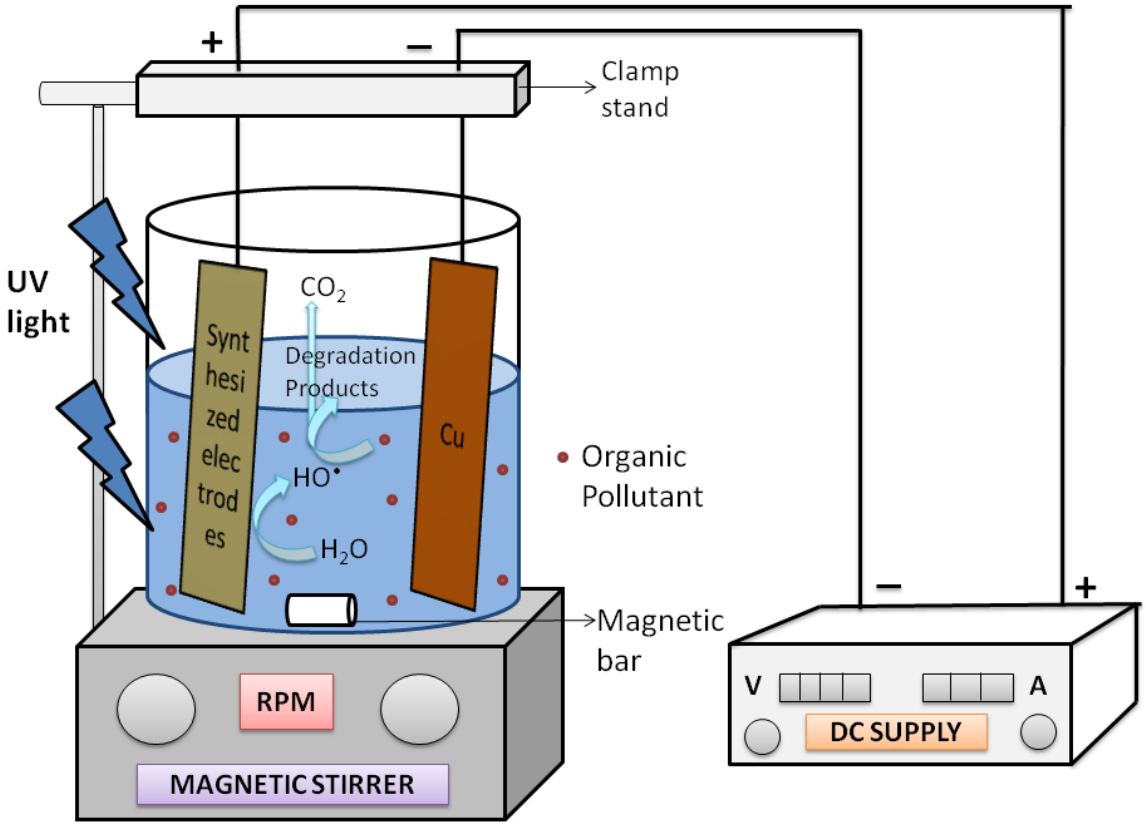

Fig. 3.4 Diagrammatic representation of PEC batch reactor

3.4.2 Response surface Methodology (RSM) and Box-Benkhen Design (BBD)

The widely exploited statistical tool, RSM on the basis of BBD has been utilized in this study for the optimization of process parameters in context to the treatment of model compound PCP by using TiO_2 and GO/TiO_2 nanotube electrodes in PEC degradation process. Design Expert v.6.0.8 (Stat-Ease, Inc., Minneapolis, USA) software has been used for the regression analysis and process optimization. The experiments were performed as suggested by BBD. The correlation between independent variables and the responses were obtained by quadratic polynomial model as presented in Eq. 3.1:

$$Y = \beta_o + \sum\beta_i X_i + \sum\beta_{ij} X_i X_j + \sum\beta_{ii} X_i^2 \quad (3.1)$$

Where, Y is the response output, X_1(i = 1,2,3,4) are controlling independent variables; β_o, β_i(i = 1,2,3,4) and β_{ij}(i = 1,2,3,4 and j = 1,2,3,4) are the coefficient model parameters. The

desirability functional approach has been used for the parametric optimization. The desirability value resides between 0 and 1, showing the proximity of response towards its ideal value (Hiwarkar et al., 2017).

3.5 Analytical techniques used for the assessment of degradation efficacy

The concentration value of PCP and 4-CG before and after irradiations has been determined using spectrophotometer (T60 LabIndia) and high-performance liquid chomatography (HPLC, Shimadzu, SED 20A). HPLC system has been equipped with C_{18} reversed- phase column and Diode array detector (SPD-M20A). A mixture of 1% acetic acid and methanol/water, 80:20 (v/v) at 1.0 mL/min has been used as mobile phase for PCP while for 4-CG, 70:30 % (v/v) HPLC grade methanol: water at 1 mL/min has been used as mobile phase. Sample injections have been held at 20 µL using a fixed volume injection loop. The detection wavelength for PCP and 4-CG has been 210 nm and 281.5 nm, respectively.

The PCP degradation products have been identified using LC-MS (Micromass Q-TOF micro, Waters, USA) equipped with Unisol YVR C_{18} reverse-phased column. The sample injection volume has been kept 25 µL and mobile phase was similar as used in the analysis of PCP in HPLC system. The ESI-MS analysis has been performed in positive mode using electro spray ionization source with source temperature at 110 °C and spray voltage of 3000 V. Nitrogen has been used as sheath gas at a flow rate of 30 L/h and pressure of 6-7 bar. The spectrum has been acquired in negative scan mode over the 60-400 *m/z* range. The degradation intermediates and by-products of 4-CG has been identified by GC-MS (Micromass Q-TOF micro, Waters, USA).

Mineralization of PCP and 4-CG solution has been studied using Total organic carbon (TOC) analyzer by Multi N/C 2100 BU (Analytic Jena AG Corporation, Germany). Standard methods from APHA manual (1989) has been followed for the determination of COD (APHA- 5220, C), chloride (APHA- 4500), sulphate (APHA- 4500-SO_4^{2-}, E), nitrite (APHA- 4500- NO_2, B), nitrate (APHA- 4500- NO_3, E), phosphate (APHA- 4500, P), Total solids (APHA-2540, B).

The active species generated during the PEC degradation process have been investigated by the scavenger quenching experiments using, iso-propyl alcohol (IPA) as a $^{\bullet}OH$ scavenger (Li et al., 2009a), disodium ethylenediaminetetra acetate (EDTA) as h^+ scavenger (Cui et al., 2014) and $_L$-ascorbic acid as scavenger of $^{\bullet}O_2^-$ (Xu et al., 2016).

The $^{\bullet}OH$ formed during the PEC treatment has been studied by fluorescence method.

In this method, terephthalic acid (TA) was used as probe molecule which rapidly reacts with $^{\bullet}OH$ to generate highly fluorescent compound i.e. 2-hydroxyterephthalic (2-HTA) having fluorescence signal at 425 nm (Ishibashi et al., 2000). For the estimation of $^{\bullet}OH$ concentration, UV/solar irradiations based experiments were conducted using synthesized electrodes in 250 mL of 0.5 mM TA and 5 mM NaOH solution. The fluorescent intensity of 2-HTA at 425 nm was measured using a fluorescent spectrophotometer (LS 45, Perkin Elmer). Standard curve of 2-HTA was made and used to determine the concentration of $^{\bullet}OH$ generated during the PEC, PC and EC process for the degradation of PCP and 4-CG. The samples were diluted with distilled water before the analysis due to very high peak intensity at 425 nm.

3.6 PEC treatment of simulated effluent

The batch experiments for the treatment of simulated experiments have been conducted as described in section 3.4.1. The pH and conductivity of prepared simulated effluent has not been altered and the treatment time has been fixed to 6 h for all the electrodes. All the reactions have been conducted under the influence of solar irradiations with solar light at an average intensity of 941W m^{-2}. External current has been selected as 0.05 A, on the basis of experiments conducted on different current values as explained in section 4.5. An overall framework of resesrch work performed has been shown in Fig. 3.5.

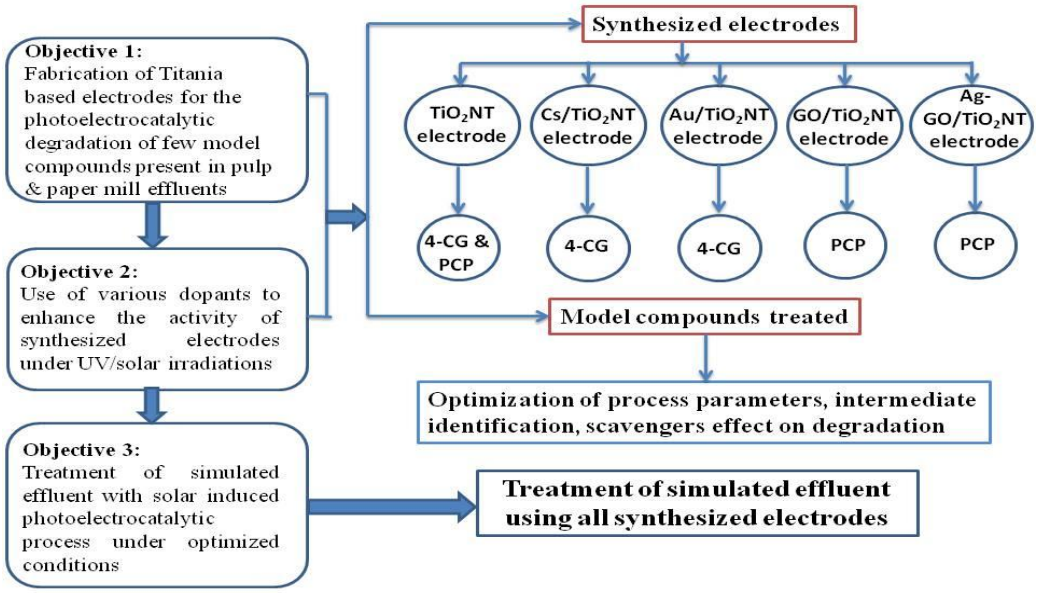

Fig. 3.5 An Overall framework of research work performed

Chapter 4

Results and Discussion

This chapter deals with the results and observations of photoelectrocatalytic degradation of recalcitrant and hazardous compounds commonly present in P & P mill effluents using laboratory synthesized titania based electrodes. Several electrodes like TiO_2, GO/TiO_2, Cs/TiO_2, Au/TiO_2 and $Ag\text{-}GO/TiO_2$ have been fabricated and their PEC efficacy has been tested against the degradation of model compounds, i.e. PCP and 4-CG. The simulated effluent which has been prepared by diluting real effluent collected at the bleaching stage of P & P mill has also been treated using the synthesized electrodes.

4.1 PEC degradation of 4-CG using Cs/TiO_2 nanotube electrodes

4-CG is a widespread recalcitrant pollutant present in pulp and paper effluents (Kringstad and Lindström, 1984). Softwood pulp effluents contain abundant amount of chlorinated derivatives like catechol, vanillin, phenol and guaiacol (Tam et al., 1994). The problems associated with these compounds have been their carcinogenic and mutagenic impacts on environment, resistance to biodegradation, toxicity, drinking water pollution, adverse impacts on human respiratory and nervous system like altered pulmonary function and chronic bronchitis (Tsutsui et al., 1997; Yan et al., 2009). The physicochemical properties of 4-CG have been presented in Table 4.1.

Table 4.1 Physicochemical properties of 4-CG

Name of the compound	4-Chloroguaiacol
IUPAC Name	4-Chloro-2-methoxyphenol
Molecular weight	158.581 g/mol
Molecular formula	$C_7H_7ClO_2$
Boiling point	241 °C
Melting Point	16-17 °C
Structure	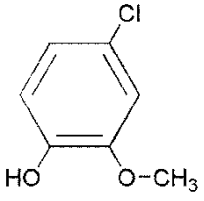

For effective photocatalysis, oxides containing Cs have been receiving increasing investigations and incorporation of Cs^+ has shown many folds increased photocalatylic activity of semiconductor than the pure sample (Luo et al., 2010). Hence, Cs- TiO_2 nanotube electrodes have been synthesized and their PEC efficiency have been assessed against the degradation of 4-CG.

4.1.1 Characterization of TiO_2 and Cs/TiO_2 nanotube electrodes

The structural and surface morphological evaluation of TiO_2 and Cs-doped TiO_2 nanotube electrodes have been performed using Field Emission-Scanning Electron Microscopy (FE-SEM), Raman Spectroscopy, X-ray Diffraction pattern, Ultraviolet-vis diffuse reflectance spectroscopy and Fourier Transform Infrared spectra analysis.

4.1.1.1 FE-SEM and EDS analysis

A typical FE-SEM top-view image of porous TiO_2 nanotubes has been shown in Figure 4.1(a). The TiO_2 nanotubes over Ti sheet have been found to be ordered structure and their top-view orientation has been used as a substrate to deposit Cs nanoparticles. Figure 4.1(b) displays the FE-SEM images of Cs sitting over TiO_2NTs. The results suggest that Cs has been present in scattered form over TiO_2 nanotube electrode. The elemental analysis of TiO_2 and Cs/TiO_2 nanotube electrode has been assessed using EDS analysis and presented in Table 4.2.

Table 4.2 EDS analysis of (a) TiO_2 and (b) Cs/TiO_2 nanotube electrodes

Element	**O**	**Ti**	**Cs**	**Totals**
		Weight (%)		
(a)	24.67	75.33	0.00	100.00
(b)	27.28	70.94	1.78	100.00

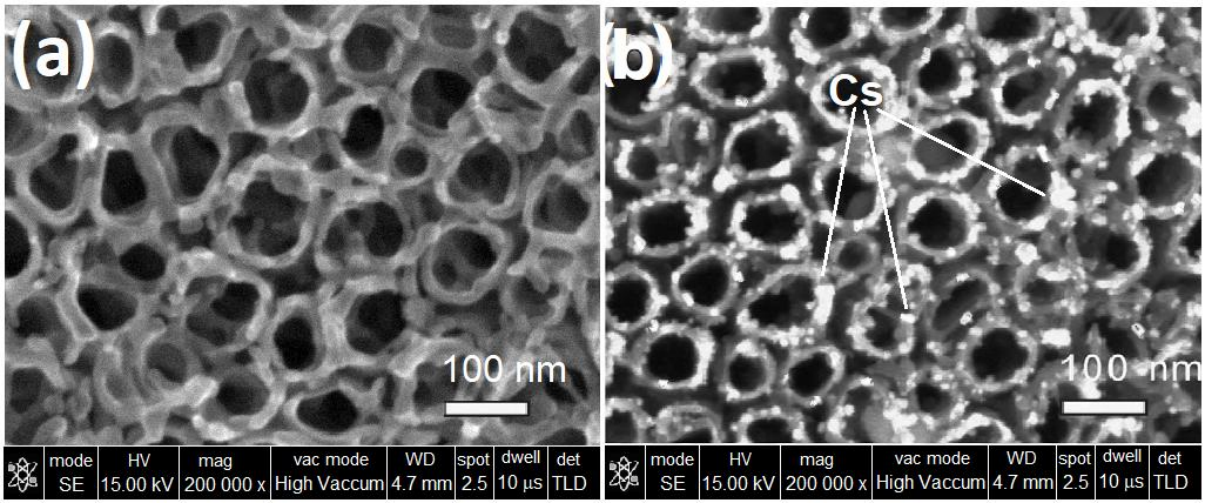

Fig. 4.1 FE-SEM images of (a) TiO_2 and (b) Cs/TiO_2 nanotube electrodes

4.1.1.2 X-ray diffraction study

Figure 4.2 displays the XRD pattern of synthesized electrodes. The diffraction pattern of the TiO_2 nanotubes electrodes showed several peaks assigned to crystalline phases of anatase, predominantly the formation of peak at 38.2° corresponding to (112) plane and several other peaks at 25.6° (101), 48.2° (200), 63.2° (204), 72.1° (220) and 76.4° (215) (JCPDS No. 21-1272). The XRD pattern exhibits a weak peak of rutile at 27.5° corresponding to (110) plane. It is necessarily notable that the rutile peak is much lesser than the anatase peak, so it is justifiable to overlook the effect of such trace content of rutile on the PEC activity. When compared to TiO_2, XRD pattern of Cs/TiO_2 nanotube electrode exhibits the intense peak of metallic Cs at 35.1° (002) (JCPDS No. 080-2257). Moreover, the separate peaks have not been witnessed probably due to very less concentration of Cs (<2.5 mM), though decrease in the intensity of 25.6°, 27.7° and 48.2° peak can be attributed to the presence of Cs (JCPDS No. 080-2257).

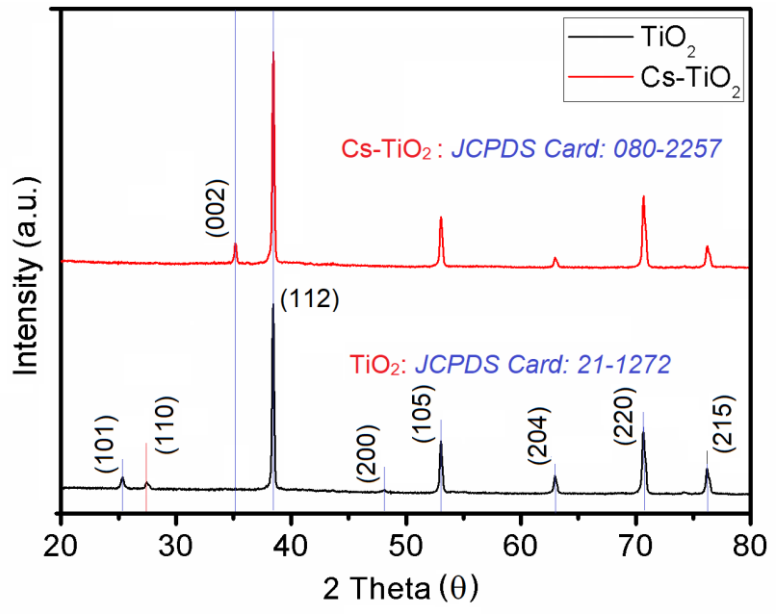

Fig. 4.2 XRD pattern of TiO_2 and Cs/TiO_2 nanotube electrodes

4.1.1.3 UV-vis diffuse reflection spectrum

UV-vis/DRS spectroscopy of TiO_2 and Cs/TiO_2 nanotube electrodes has been shown in Figure 4.3. The major absorbance at wavelengths less than 400 nm might be due to the intrinsic band gap absorption of titanium dioxide. The parent TiO_2 electrode exhibits maximum absorbance at 245 nm which corresponds to the charge transfer from O 2p to Ti 3d of TiO_2 (Yu et al., 2008). For Cs/TiO_2 electrodes, the absorption edge showed a significant red-shift and displayed stronger and broader absorption in the range of 390 to 700 nm in comparison to the parent TiO_2 electrode. The shown UV-vis/DRS results indicate that introduction of Cs onto TiO_2 electrode has a significant influence on coordination framework of TiO_2 crystalline structure, resulting in the red shifts of the absorption band. It has been expected that the Cs-doped TiO_2 nanotubes could exhibit a higher PEC oxidation capability as compared to bare TiO_2 electrodes for the degradation of organic pollutants under solar irradiation.

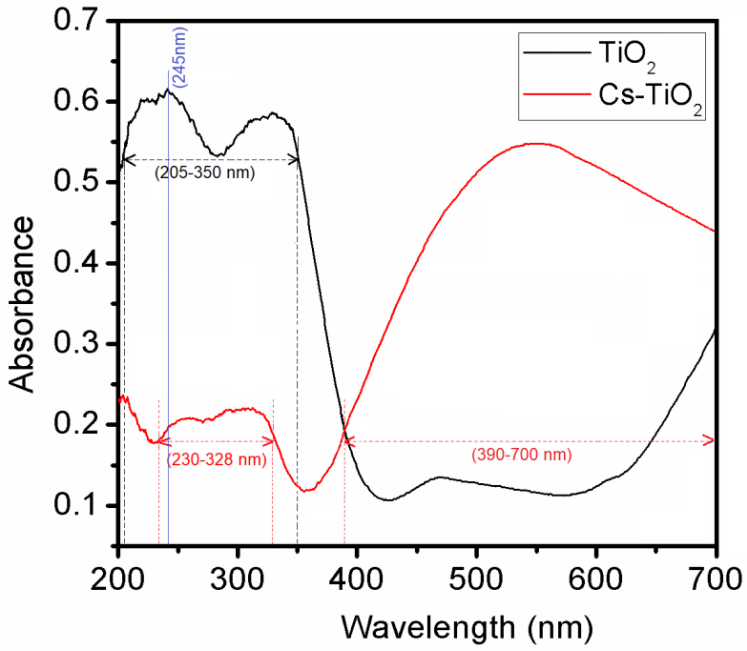

Fig. 4.3 UV-vis diffuse reflection spectrum of TiO_2 and Cs/TiO_2 nanotube electrodes

4.1.1.4 FTIR spectrum

FT-IR spectra of TiO_2 and Cs/TiO_2NTs electrode have been shown in Figure 4.4. In case of TiO_2, the peak at ~1216 cm^{-1} and a broader peak at ~3308 cm^{-1} may be due to O-H stretching of hydroxyl groups. Peak present at 1367 cm^{-1} corresponds to carboxyl groups. The peak emerging at ~591 cm^{-1} might be due to the bending and stretching of Ti-O-Ti bond (McDevitt and Baun, 1964). Peak approximately observed at 1635 cm^{-1} has been assigned to the O-H-O bending on the TiO_2 surface (Zhou et al., 2016). In the case of Cs/TiO_2, shifting of absorption peak at 424 cm^{-1} towards reduced wave numbers might be due to the formation of Ti-O-Cs bridges. The main differences between TiO_2 and Cs doped TiO_2 spectra begin at the low wave number region, where the influence of Cs can be seen. In this region, the peak at 591 cm^{-1} disappears with Cs adsorption, while the peaks at 661 and 724 cm^{-1} become more intense as shown in Fig. 4.4 (Inset1), which might be due to vibrational modes of O-Ti-O bonds. The peak at 3364 cm^{-1} in Cs/TiO_2 reflects the adsorption of hydroxyl groups on the electrode surface with Cs doping onto TiO_2; and thus it signifies that doping of Cs nanoparticles has been advantageous for the adsorption of hydroxyl groups on TiO_2 nanotube electrode which will subsequently improve the PEC activity.

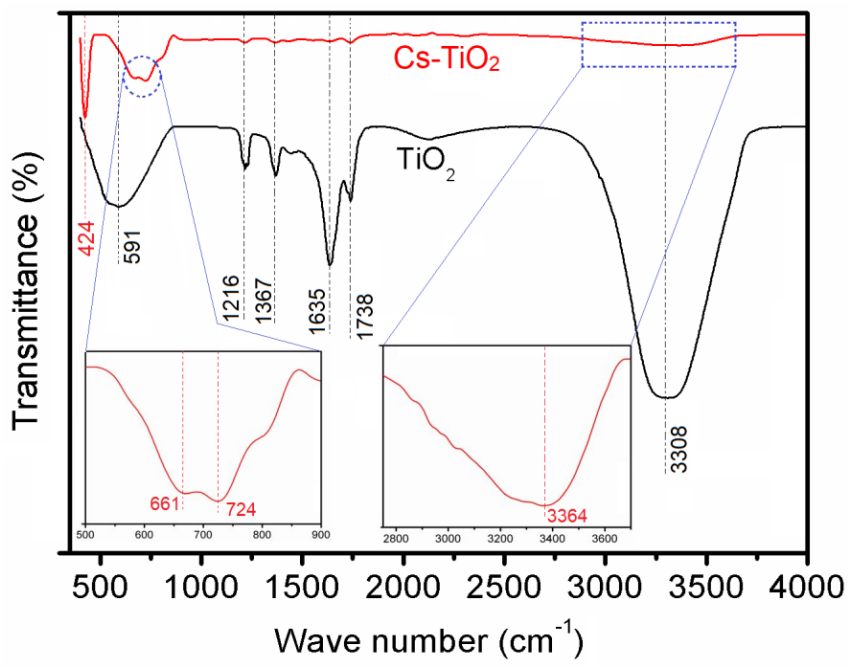

Fig. 4.4 FTIR spectrum of TiO_2 and Cs/TiO_2 nanotube electrodes

4.1.1.5 Raman measurement

The Raman spectra of TiO_2 and Cs/TiO_2 nanotube electrode obtained after calcination has been measured at room temperature and shown in Figure 4.5. The E_g peaks corresponds to symmetric stretching vibration of O–Ti–O at 142 and 639 cm^{-1}, the B_{1g} peak at 396 cm^{-1} is due to symmetric bending vibration of O–Ti–O, and the A_{1g} peak at 514 cm^{-1} correspond to anti-symmetric bending vibration of O–Ti–O (Tian et al., 2012). The absence of Raman bands at 235, 447 and 612 cm^{-1} could be due to the TiO_2 rutile phase which further confirms the phase purity of synthesized electrodes (Li et al., 2007). In comparison to TiO_2, the Cs/TiO_2 peak widths displayed more obvious changes, thus indicates that doping of Cs plays a significant role in decreasing the dimensions of TiO_2 crystallites. As shown in figure, the peak intensity of E_g at 142 cm^{-1} increase, indicating less exposure of TiO_2 facets on doping with Cs ions (Tian et al., 2012). The results showed that doping of TiO_2 with Cs marginally shifts in the absorption towards higher wave numbers which could be ascribed to the generated structural changes by substitutional or interstitial impurities (Sibu et al., 2002).

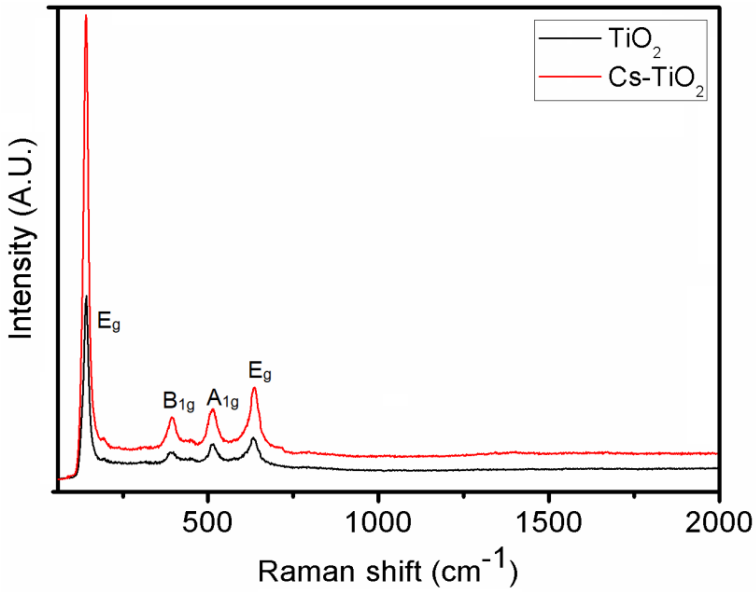

Fig. 4.5 Raman spectrum of TiO_2 and Cs/TiO_2 nanotube electrodes

4.1.2 PEC degradation of 4-CG and effect of parameters

The PEC activity of Cs/TiO_2 system has been evaluated against the degradation of 4-CG (20 mg L^{-1}) aqueous solutions under solar light. The effect of various process parameters such as Cs concentration, conductivity of electrolyte, external current and pH have been studied.

4.1.2.1 Effect of Cs concentration

The effect of Cs loading onto TiO_2 nanotube electrode for the PEC degradation of 4-CG has been shown in Figure 4.6 demonstrates. As the concentration of cesium has been varied at 1.3, 1.9, 2.5 and 3.2 mM, the degradation of 4-CG has been measured as 48.8, 66.6, 83.3 and 76.3%, respectively. Hereafter, the increase in degradation rate constant could be ascribed to development of Schottky barrier at the interface of metal and semiconductor facilitating the reduction in recombination rate of charged species (Bannat et al., 2009). However, after a limit (2.5 mM) Cs loading reversed the rising trend in degradation which could be attributed to the active site blockage by excessive Cs and also might be due to reduced photons invasion inside the porous layer of TiO_2 (Gao et al., 2015). As suggested by the results, 2.5 mM has been considered as the optimal Cs loading for efficient PEC degradation of 4-CG.

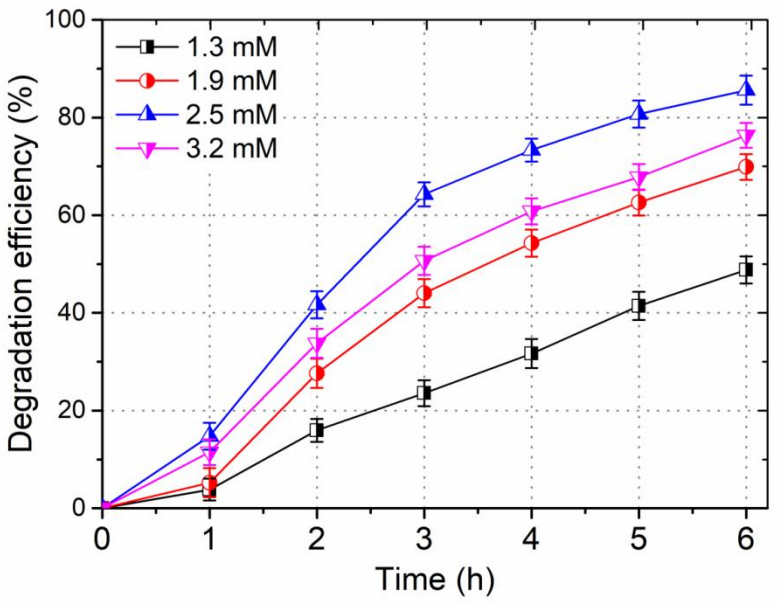

Fig. 4.6 Effect of Cs loading on PEC degradation of 4-CG

4.1.2.2 Effect of conductivity

The effect of sulphate concentration, which has been directly related to the conductivity of the electrolyte, on 4-CG degradation efficacy has been investigated and shown in Figure 4.7. With increasing amount of supporting electrolyte, initially degradation of 4-CG increased, however, after reaching a certain limit increased concentration of sulphate ions did not favour removal of pollutant. This can be ascribed to the fact that at elevated concentrations of the electrolyte some side reactions involved in oxygen evolution have been favoured rather than the oxidation of organic contaminant (Tiwana et al., 2011). However, at lower concentrations of sulphate ions, diminished 4-CG removal has been noticed which might be due to the higher solution resistance occurred at low concentration of electrolyte (Hu et al., 2016). The results showed that 160 mg L^{-1} was observed to be the optimum electrolyte concentration for the PEC degradation of 4-CG.

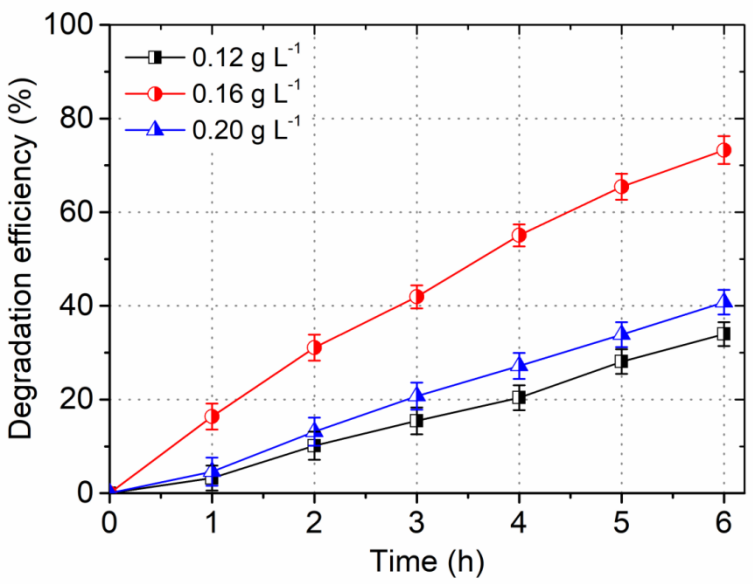

Fig. 4.7 Effect of sulphate concentration on PEC degradation of 4-CG

4.1.2.3 Effect of applied current

The effect of applied current on PEC reaction system for the oxidative removal of 4-CG has been investigated within the range of 0.02 to 0.04 A and the obtained results have been shown in Figure 4.8. Participation of current in the PEC process enhances the degradation of organic contaminants as the electric field facilitates the separation of photo-generated charged species, thereby resulting in reduced recombination. 4-CG degradation has been observed to be highest at 0.03 A. With increasing external current, reaction rate increased which could be due to the decreased recombination of e^- and h^+. However, further increase in applied current did not yield high degradation of 4-CG which may be attributed to the competitive side reactions which include evolution of hydrogen and cathodic reduction of in-situ generated H_2O_2 to H_2O. Moreover, oxygen generated due to water splitting at current higher than the optimum value can also interfere in the catalytic oxidation process (Zhang et al., 2012; Ramirez et al., 2015).

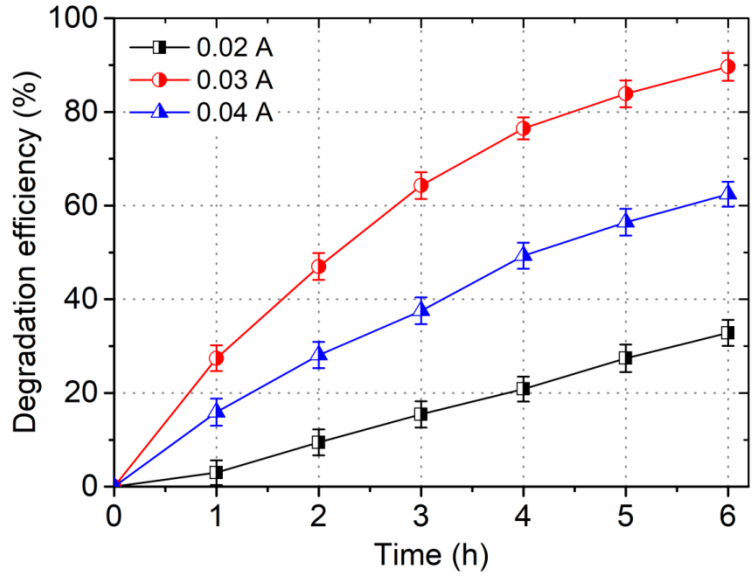

Fig. 4.8 Effect of applied current on PEC degradation of 4-CG

4.1.2.4 Effect of pH

The influence of pH on degradation efficiency of 4-CG has been shown in Figure 4.9. Under acidic condition, specifically, pH 3 favours the degradation of 4-CG, whereas degradation reduced both at alkaline and neutral conditions due to the insufficient quantity of active hydrogen formation under alkaline and neutral environment. Under acidic conditions, the formation of active hydrogen could be accelerated due to the electro-reduction of hydrogen ions. However, under alkaline or neutral environment, H_2O molecules could not be electrolyzed to generate active hydrogen. The in-situ generated active hydrogen under acidic environment evolved from H^+ ions could effectively degrade 4-CG due to their high reactivity (Cui et al., 2008). Moreover, at pH smaller than the point zero charge of TiO_2 (pH 6.5), the surface of TiO_2 becomes positively charged and results in easy transfer of photogenerated electrons consequently, reducing recombination rates and facilitating photocatalytic treatment (Leng et al., 2006).

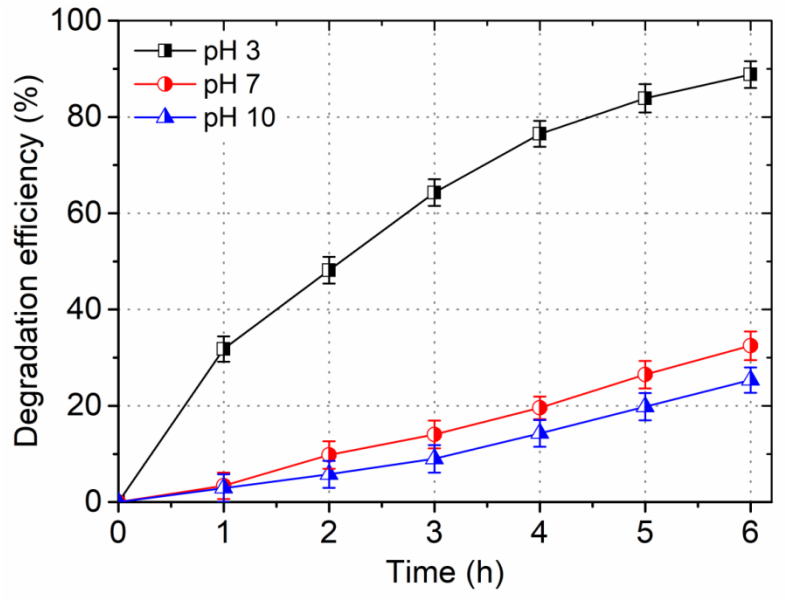

Fig. 4.9 Effect of pH on PEC degradation of 4-CG

4.1.3 PC, EC and PEC efficacies

A comparative assessment between the PEC, PC and EC process for the degradation of 4-CG (20 mg L^{-1}) under the optimized conditions viz. 2.5 mM Cs, 160 mg L^{-1}, Na_2SO_4, 0.03 A current at pH 3 has been performed.

4.1.3.1 Degradation efficacy with different treatment process

When compared with EC, PEC and PC processes, the degradation of 4-CG through direct photolysis and dark adsorption has been quite low (<6%) which could be neglected. The EC process for 4-CG degradation has been observed to be slower when compared to PEC and PC processes, demonstrating the possibility of enhanced degradation efficacy in the presence of visible irradiation. Additionally, PC performance (53%) of Cs/TiO_2 nanotube electrodes has been found to be higher than that of bare-TiO_2 nanotube electrodes (31%) within 6 h under visible light irradiation, which could be primarily ascribed to the improved charge separation efficiency and enhanced visible light absorption with Cs loading, as evident from UV-vis/DRS results (Figure 4.3). Low PC performance of bare-TiO_2 nanotube photoelectrode might be owing to the higher recombination rate of photogenerated charged species and relatively weaker light absorption capacity (Cheng et al., 2016). For elucidating the enhanced light driven PEC performance, ability of Cs/TiO_2 nanotube photoelectrode has been assessed under optimized conditions which led to almost 92% degradation within 6 h as shown in Figure 4.10. The Cs/TiO_2 nanotube electrode showed higher PEC activity for the

degradation of 4-CG than the TiO_2 nanotube electrode, as a result of synergistic effect of the large surface areas, enhanced mass and electron transfer. Moreover, the higher PEC performance of Cs doped TiO_2 nanotube electrode has been probably because the external current hinders the recombination of photogenerated electron–hole pairs and leads to prolonged life of photogenerated carrier's. Accordingly, deposition of suitable Cs concentration on TiO_2 nanotube, an effective charge separation of the photogenerated electron–hole pairs can be achieved.

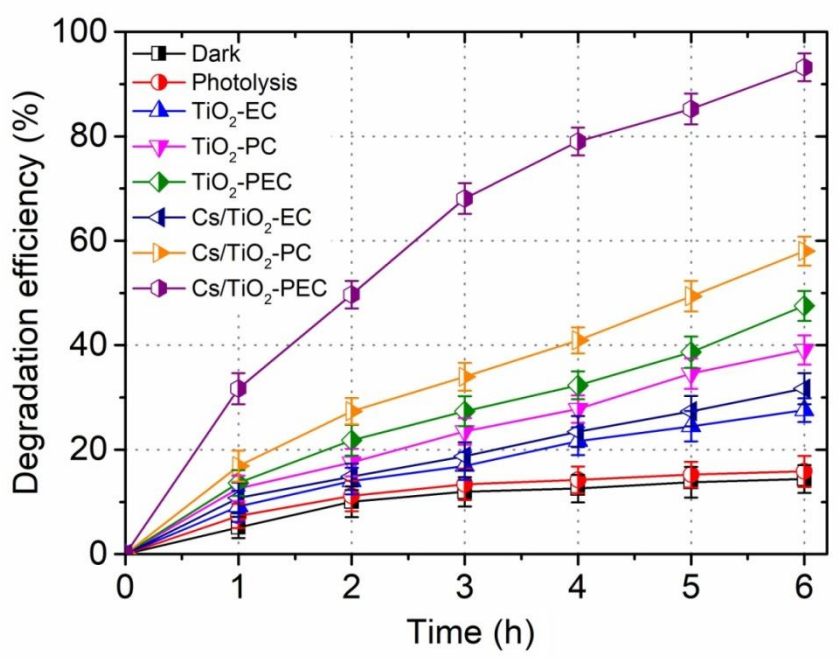

Figure 4.10 Degradation profile of 4-CG under different conditions

4.1.3.2 Mineralization study

In order to verify the results obtained after comparative assessment of Cs/TiO_2 nanotube electrode for PC, EC and PEC degradation, total organic carbon (TOC) removal has been assessed to evaluate the mineralization extent of 4-CG. The mineralization results demonstrate that TOC removal efficiency reached 70.2, 42.3 and 12% for PEC, PC and EC process, respectively as shown in Figure 4.11.

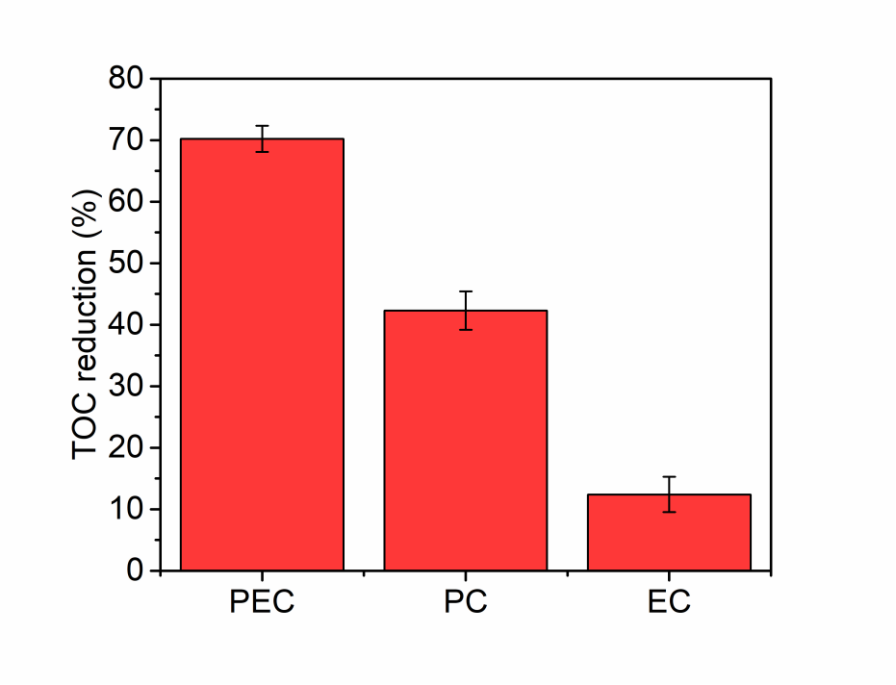

Fig. 4.11 TOC removal of 4-CG after PEC, PC and EC treatment

4.1.3.3 Hydroxyl radical quantification

The quantification of •OH radicals has been conducted to further validate the obtained results. The results as shown in Figure 4.10 and 4.11 depicts that PEC led to efficient degradation and mineralization when compared to EC and PC processes. Figure 4.12 displayed the formation of •OH radicals in PEC, PC and EC process. Noticeably, it can be evidently observed that the as-fabricated Cs/TiO_2 nanotube photoelectrode exhibited increasing pattern of •OH radical concentration with time in PEC process when compared to EC and PC process. PEC yielded of 118.7 mM with Cs/TiO_2 nanotube electrode; whereas the •OH radical concentration for PC and EC process has been found to be 34.1 and 0.64 mM, respectively, after 6 h irradiation time. The •OH radical concentration was observed to be 30.84 mM when TiO_2 nanotube electrodes were used. The results suggested that doping of Cs over TiO_2 nanotube electrodes results in generation of higher amount of •OH radicals. Thus, Cs/TiO_2 nanotube photoelectrode exhibited higher activity in terms of degradation and mineralization of organic pollutant when compared to EC and PC process.

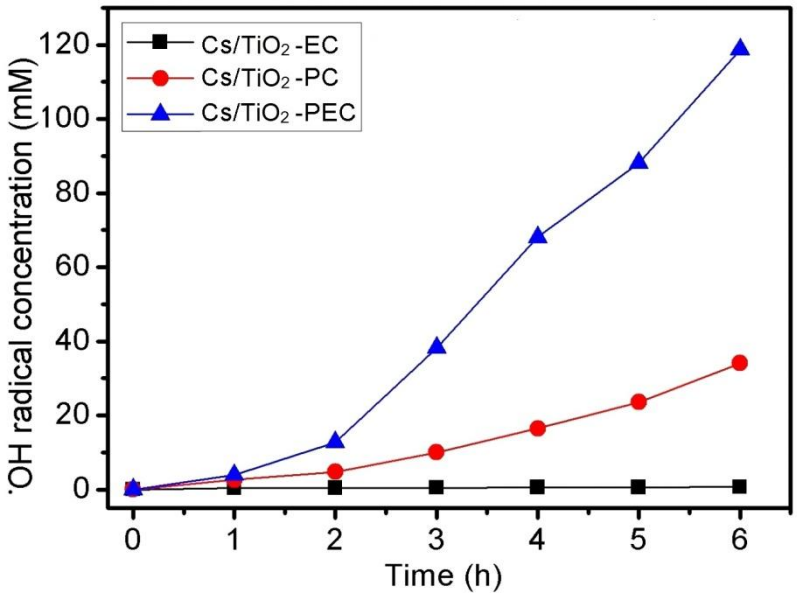

Fig. 4.12 ·OH radical concentration with PEC, PC and EC process

4.1.4 PEC degradation mechanism of 4-CG

The mechanism of enhanced degradation of 4-CG under visible light has been proposed and illustrated in Figure 4.13. The electrons (e_{cb}^{-}) get excited excited from the valence band (VB) to conduction band (CB) leaving behind the holes (h_{vb}^{+}). The defined work-function is as follows (Chatterjee et al., 2005):

$$W = E_0 - E_F \quad (4.1)$$

Where, E_0 and E_F are vacuum energy and Fermi energy, respectively. TiO_2 work-function is lesser than Cs and hence, the Fermi energy of Cs is lower when compared to TiO_2. The Schottky barriers have been formed between TiO_2 nanotubes and Cs nanoparticles after Cs loading over TiO_2 surface (Traversa et al., 2000) which facilitates the smooth transfer of photo-generated electrons from CB of TiO_2 to Cs (solid black arrow shown in Figure 4.13(b). Therefore, the doped Cs nanoparticles could effectively separate the photo-generated charged species, resulting in reduced recombination. During PC, the photo-generated electrons could rapidly transfer to surface-absorbed oxygen in order to generate superoxide radical, $\cdot O_2^-$, (Figure 4.13b, dotted arrows). The $\cdot O_2^-$ then generates ·OH radicals through photo-reduction process involving reactions with H^+ ions. The ·OH radicals have also been produced from the photo-generated holes (h^+) on reaction with H_2O, which is the photo-oxidation process (red arrow shown in Figure 4.13b). The ·OH radicals accountable for degrading organic pollutants have been generated by both photo-reduction and photo-oxidation processes. Thus, the

significant improvement of the photocatalytic activity could be assigned to the lower recombination rate of charged species. When external current is supplied to Cs/TiO_2 nanotube electrode, the electrons (e^-) forcefully get transferred to the counter electrode via potential gradient thereby, reducing the absorbed oxygen on its surface to form $^{\bullet}O_2^-$, which further generates $^{\bullet}$OH radicals. The PEC reactions could be summarized as follows (Eq. 4.2–4.3):

$$TiO_2 \rightarrow TiO_2 - e_{cb}^- + TiO_2 - h_{vb}^+ \quad (4.2)$$

$$TiO_2 - h_{vb}^+ + H_2O \rightarrow TiO_2 - OH_{ads} + H^+ \quad (4.3)$$

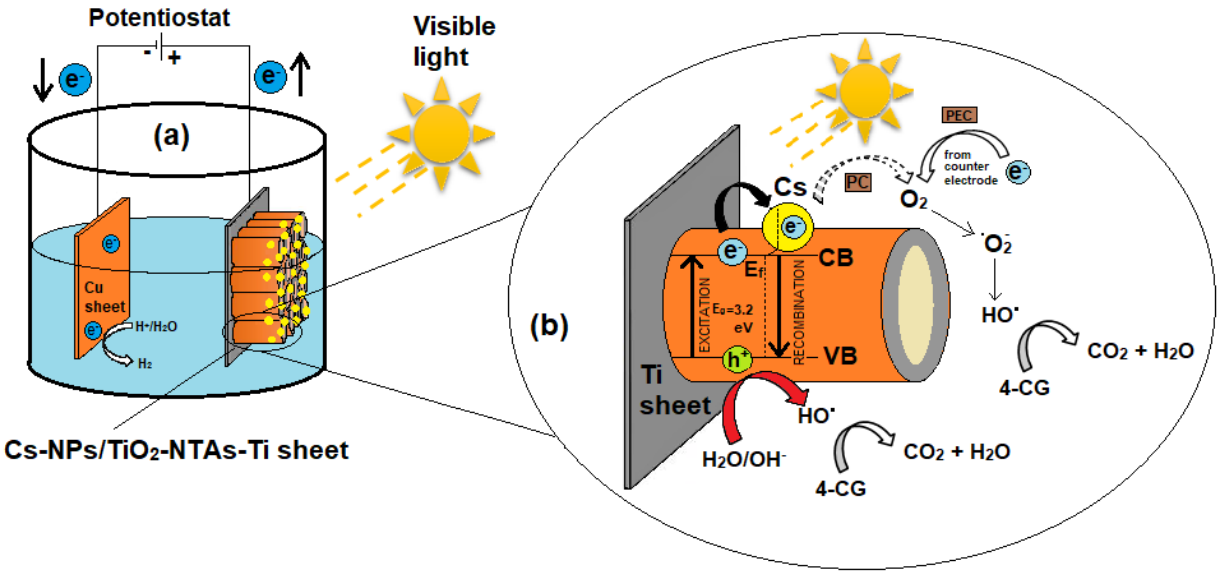

Figure 4.13 (a) Experimental set-up of PEC and; (b) Schematic diagram representing the transfer of charged species with Cs/TiO_2 nanotube electrode under visible light

4.1.5 GC-MS Analysis

The intermediate products formed during the PEC degradation of 4-CG using Cs/TiO_2 NTs have been identified through GC-MS analysis and are shown in Figure 4.14. Based upon these identified intermediates (**a-m**), a tentative pathway has ben proposed for the degradation of model compound 4-CG. Dehydroxylation of the parent compound (**a**) lead to the formation of by product (**b**). Further the removal of methoxy group could possibly generate (**c**) which could undergo hydroxylation to form (**d**). The cleavage of benzene ring in (**d**) could possibly leads to the generation of by product (**e**) which could further form (**f**) after undergoing dehydroxylation. The formed intermediate (**f**) could lead to the generation of (**g**) after undergoing dechlorination through route (**1**). The successive oxidation and

hydroxylation of (**g**) could lead to the formation of (**i**). Demethylation of (**i**) followed by its hydroxylation could finally lead to the end product (**l**). On the other hand by product (**f**) could get fragmented into (**j**) through route (**2**). By product (**j**) on further getting demethylated could lead to the formation of (**k**) which could finally yield the end product (**l**) after undergoing dechlorination followed by hydroxylation.

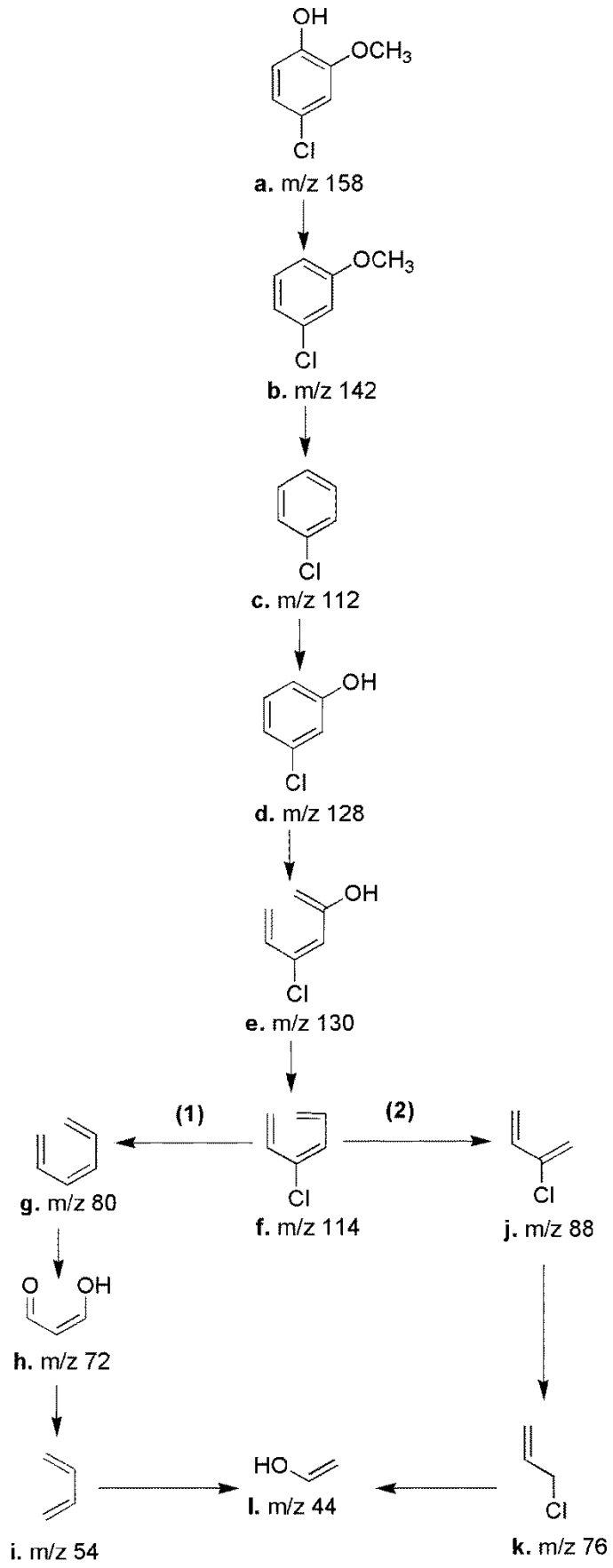

Fig. 4.14 Proposed pathway for the degradation of 4-CG through PEC

4.2 PEC degradation of 4-CG using Au/TiO_2 nanotube electrode

After the doping of Cs on TiO_2 nanotubes electrode, gold particles were doped on TiO_2 electrode for the PEC treatment of 4-CG and was characterized for its physical and chemical properties. The optimization of process parameters has been carried out for 4-CG degradation. The quantitative analysis of hydroxyl radical generated during the reaction process has been estimated and their concentration has been reported.

4.2.1. Characterization of Au/TiO_2 nanotube electrodes

The physicochemical properties of Au/TiO_2 nanotube electrodes have been studied using FE-SEM, Raman Spectroscopy, XRD and UV-vis DRS analysis techniques and compared with TiO_2 nanotube electrodes.

4.2.1.1 FE-SEM and EDS analysis

The morphology of TiO_2 and Au loaded TiO_2 nanotube electrodes have been examined by FE-SEM and the images have been shown in Figure 4.15(a) and (b). Figure 4.15(a) shows the formation of uniform framework of nanotubes with the top end open and the bottom end attached to the surface of Ti substrate. Furthermore, irregular shaped scattered clusters of Au nanoparticles have been clearly visible in Figure 4.15(b). The image shows that the TiO_2 nanotubes serve as substrate and carrier for Au nanoparticles. The elemental analysis of synthesized electrodes has been performed by EDS analysis and the results have been shown in Table 4.3.

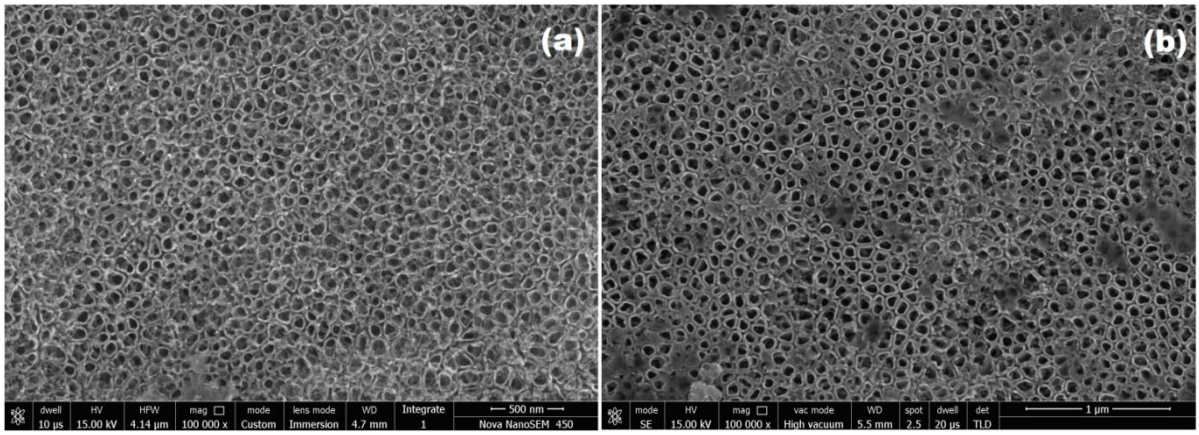

Fig. 4.15 FE-SEM images of (a) TiO_2 and (b) Au/TiO_2 nanotube electrodes

Table 4.3 EDS analysis of TiO_2 and Au/TiO_2 nanotube electrodes

Element	**O**	**Ti**	**Au**	**Totals**
		Weight (%)		
TiO_2	26.63	73.37	0.00	100.00
Au/TiO_2	28.51	70.69	0.81	100.00

4.2.1.2 X-ray diffraction study

The phase composition and crystalline structure of synthesized TiO_2 and Au/TiO_2 nanotube electrodes have been examined by XRD spectra as shown in Figure 4.16. The TiO_2 anatase peaks have been evident at 25.31° (310), 38.61° (111), 53.92° (432), 63.31° (204) and 72.1° (220) (JCPDS No. 21-1272). The diffraction peaks at 35.16° (101) and 41.1° (111) corresponds to the rutile phase of TiO_2 (JCPDS No. 21-1276). The separate peaks for Au in the XRD spectrum of Au-TiO_2NTs electrode has not been observed probably due to its low concentration i.e. 0.15 mM and/or the probable overlapping of Au and TiO_2 characteristic peaks. This finding also indicates that the deposition of Au did not considerably alter the crystal phase of TiO_2. The obtained results are in accordance with the previous findings (Ghanem et al., 2018).

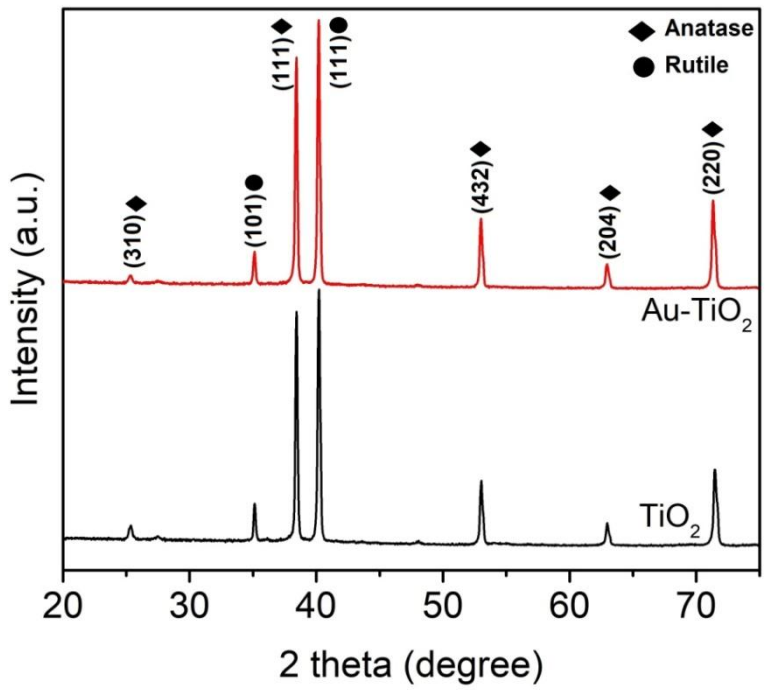

Fig. 4.16 XRD pattern of TiO_2 and Au/TiO_2 nanotube electrodes

4.2.1.3 UV-vis diffuse reflection spectroscopy

The UV-vis absorption pattern of synthesized electrodes has been presented in Figure 4.17. It can be clearly seen that after the doping of Au, Au/TiO_2 nanotube electrode exhibited strong absorption in the range 400 nm to 550 nm causing the red-shift of spectrum in visible region (Wu et al., 2015). However, TiO_2NTs electrode showed its absorption in mainly ultraviolet region i.e. less than 400 nm. Based on the outcome, it can be concluded that the doping of Au exhibited significant influence on the crystalline structure of TiO_2 which resulted in the red shift of adsorption band. It can also in inferred that, Au-TiO_2NTs electrode can perform higher PEC degradation under solar irradiation when compared to TiO_2NTs electrode.

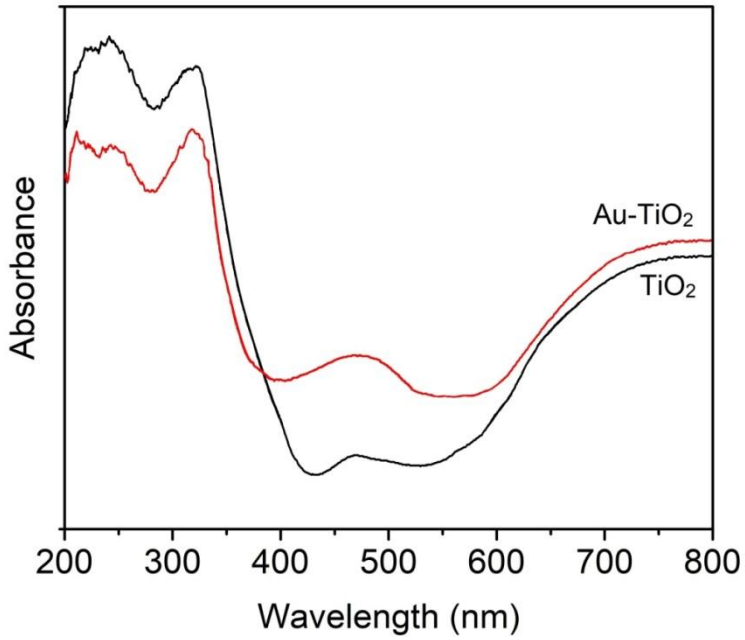

Fig. 4.17 UV-vis diffuse reflection spectrum of TiO_2 and Au/TiO_2 nanotube electrodes

4.2.1.4 Raman measurements

The synthesized TiO_2 and Au-TiO_2NTs electrodes have been investigated by Raman spectroscopy and the results have been shown in Figure 4.18. TiO_2NTs electrodes exhibited four Raman bands at around 142, 397, 516 and 639 cm^{-1} corresponding to anatase phase of TiO_2 in Eg, B_1g, A_1g and Eg modes, respectively. The Eg peaks in the spectrum are due to symmetric stretching vibrations of O–Ti–O bonds, B1g peak corresponds to the symmetric bending vibrations of O–Ti–O bonds while, A1g peak is due to the anti-symmetric bending vibrations of O–Ti–O bonds (Tian et al., 2012). Upon modification with Au, no distinct change in the number of peaks has been noticed. However, Eg peak of TiO_2NTs electrode

shift towards higher wavenumber after doping which indicates the enhanced crystalline defects within TiO_2 (anatase) which can influence its vibrational frequency and can act as photoelectrons trapping sites (Li et al., 2013).

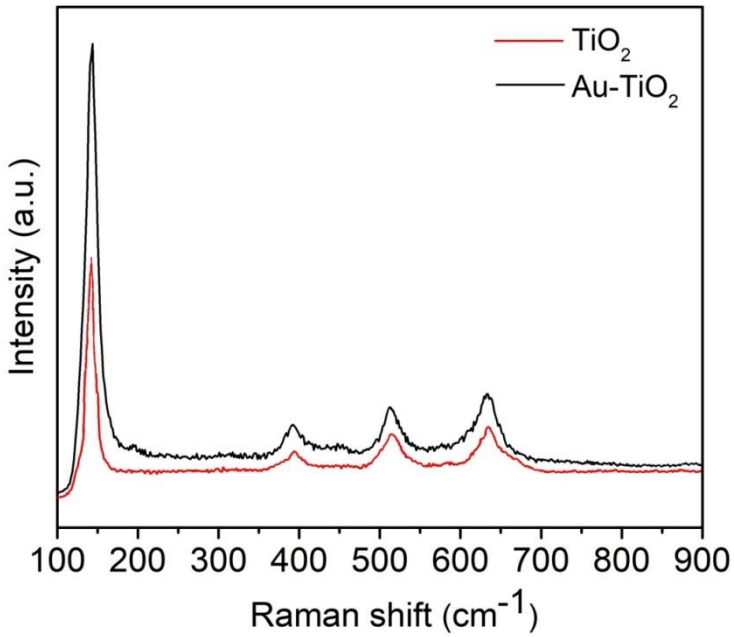

Fig. 4.18 Raman spectrum of TiO_2 and Au/TiO_2 nanotube electrodes

4.2.2 PEC degradation of 4-CG and optimization of process parameters

PEC degradation of model compound 4-CG (20 mg L^{-1}) has been studied in batch mode using synthesized Au/TiO_2 nanotube electrodes and parametric optimization has been performed.

4.2.2.1 Effect of Au loading

The PEC removal of 4-CG has been observed to be 56, 74, 54 and 48% after 6 h, when the concentration of Au on TiO_2 nanotube electrode was kept 0.075, 0.15, 0.225 and 0.3 mM, respectively. However, only 46% 4-CG degradation after 6 h has been achieved with un-doped TiO_2 nanotube electrodes which indicated significant improvement in the PEC activity of electrodes after incorporation of Au. With increasing Au concentration, increased degradation has been observed till a certain value and then, a decreased degradation trend was observed as shown in Figure 4.19. The probable reason behind the increasing trend might be the formation of schottky barrier at Au/TiO_2 interface because of the high work function of Au, resulting into the smooth transfer of photo-generated e^- to the conduction band of TiO_2 nanotubes (Tian and Tatsuma, 2005). Through the external circuit, the photo-generated e^- gets

transferred from TiO_2 nanotubes to Ti sheet and ultimately to the counter electrode (Cu) where, the electrons reduce the electrode surface absorbed oxygen molecules to produce reactive species superoxide anions, hydroxyl radicals etc. which further contributes towards the degradation of contaminants (Xie et al., 2010). Above the optimum dopant concentration, the degradation performance decreases, as the recombination of e^-/h^+ might increase above the optimum value (Ni et al., 2007) and also the excessive dopant concentration can cause active site shielding effect resulting in decreased PEC activity (Gao et al., 2015). The optimal concentration of Au has been determined to be 0.15 mM for the highest PEC degradation efficiency of 74% after 6 h which was 28% higher than that of un-doped TiO_2 nanotube electrode under the similar conditions.

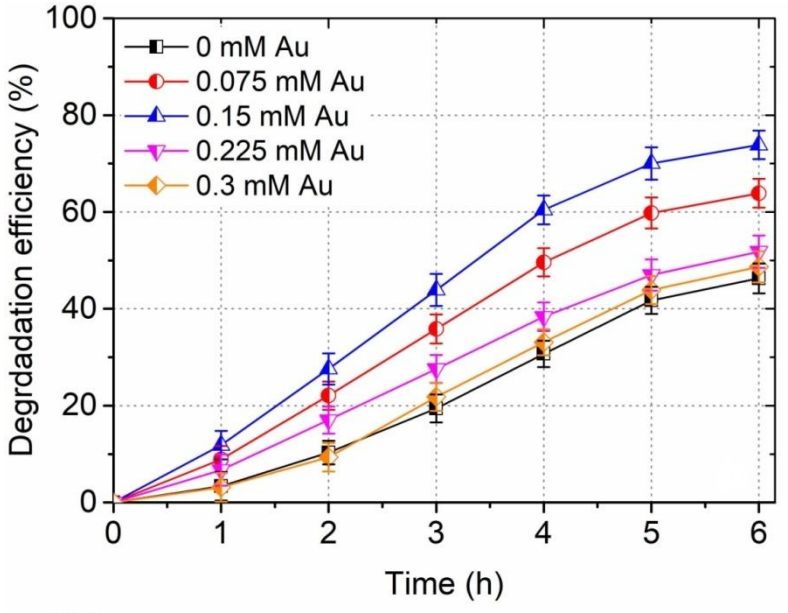

Fig. 4.19 Effect of Au concentration on PEC degradation of 4-CG

4.2.2.2 Effect of electrolyte concentration

The concentration of electrolyte plays a vital role in the electrochemical processes hence, the effect of sodium sulphate concentration i.e. conductivity of electrolyte has been studied and presented in Figure 4.20. Na_2SO_4 has been selected as a supporting electrolyte and its concentration has been varied from 0.04 to 0.16 g L^{-1} to investigate its effect on 4-CG degradation. 4-CG degradation has been initially enhanced in the presence of Na_2SO_4 till it reaches optimum value i.e. 0.08 g L^{-1} and afterwards downfall in the degradation efficiency was observed. The electrolyte increases the conductivity of reaction solution and poses positive impact on degradation rates (Quan et al., 2007). However, after reaching a certain concentration, SO_4^{2-} exhibit inhibition effect on catalytic oxidation as it causes blocking of

active sites of photo-catalyst accordingly reducing the adsorption of pollutant on catalyst surface (Mahmoodi et al., 2011).

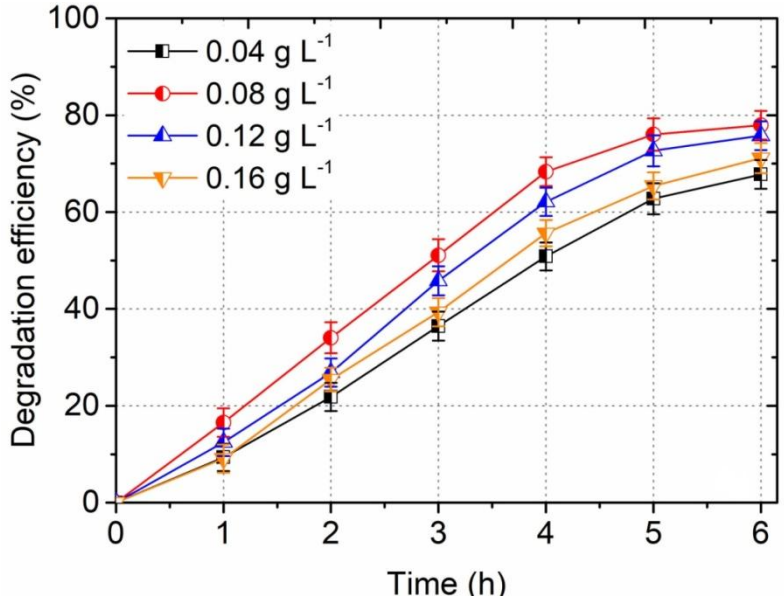

Fig. 4.20 Effect of electrolyte concentration on PEC degradation of 4-CG

4.2.2.3 Effect of external current

The effect of external current on PEC degradation of 4-CG has been investigated from 0.01 to 0.04 A. The photodegradation of 4-CG versus various external applied current has been shown in Figure 4.21. An obvious positive effect of external current till a certain value was observed on PEC degradation of 4-CG as it facilitates the transfer of e^-/h^+ leading to reduced recombination rates. The highest degradation using Au/TiO_2 nanotube electrodes has been observed when the external current was 0.03 A. When the current exceeding 0.03 A has been supplied, gradual decrease in the degradation was observed which might be due to the initiation of several side reactions (Zhang et al., 2012).

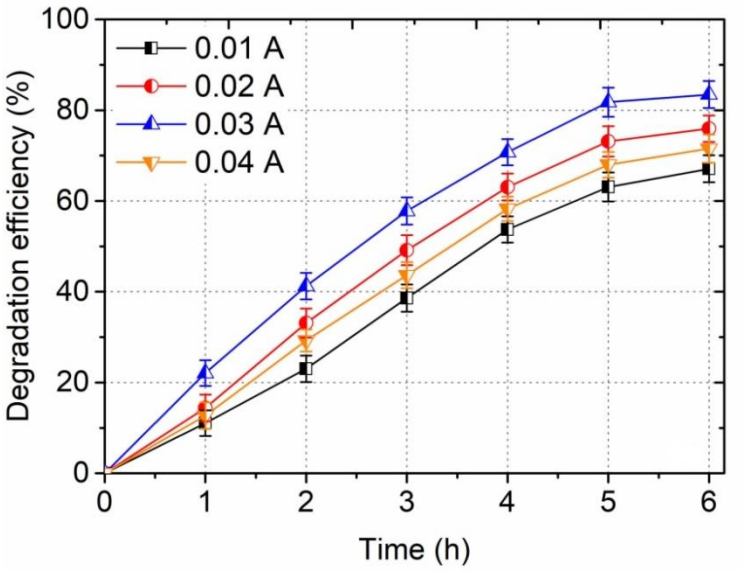

Fig. 4.21 Effect of external current on PEC degradation of 4-CG

4.2.2.4 Effect of pH

The influence of pH from 3 to 11 on the PEC degradation of 4-CG has been studied and illustrated in Figure 4.22. Acidic conditions (pH 3) have been observed to favour the degradation of 4-CG however, reduced degradation was observed under neutral (pH 7) and alkaline (pH 11) conditions. The reduced degradation efficiency under neutral and alkaline conditions might be due to the insufficient generation of active hydrogen under these circumstances (Cui et al., 2008). Also, pH values lower than the TiO_2 (pH 6.5) point of zero charge imparts positive charge to the catalyst surface and facilitates the transfer of photo-generated charged species (Leng et al., 2006).

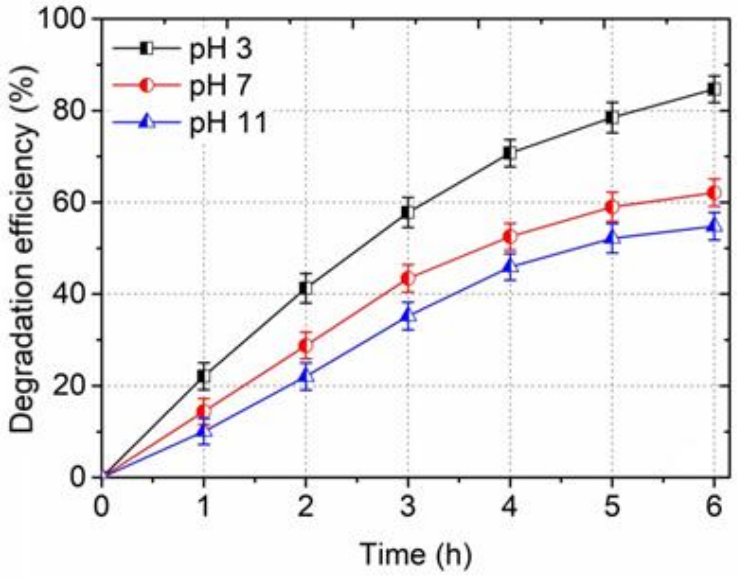

Fig. 4.22 Effect of pH on PEC degradation of 4-CG

4.2.3. Hydroxyl radical detection and quantification

The detection and quantification of •OH radicals have been performed to further validate the obtained results. The intensity of hydroxyl radical production has been measured at 425 nm and the results are presented in Figure 4.23. It can be clearly seen that Au/TiO_2 nanotube electrode exhibited many folds increased performance towards the production of radicals when compared to bare TiO_2 nanotube electrode after 6 h of exposure time. Furthermore, the concentration of hydroxyl radical has been determined by the standard curve of 2-HTA. Au/TiO_2 electrode yielded 105 mM of •OH radical concentration however, the yield was merely 30.84 mM, when bare TiO_2 nanotube electrode has employed. Thus, Au/TiO_2 nanotube photoelectrode exhibited higher activity in terms of degradation and mineralization of organic pollutant when compared to TiO_2 nanotube electrode.

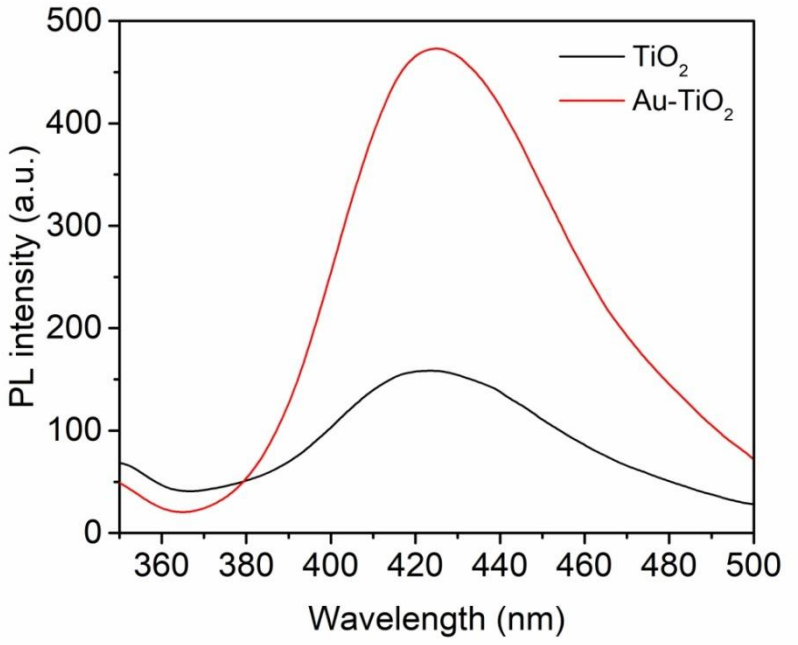

Fig. 4.23 •OH radical production using TiO_2 and Au/TiO_2 nanotube electrode

4.2.4. GC/MS analysis for intermediates identification

The intermediate products formed during the PEC degradation of 4-CG using Au/TiO_2 nanotube electrode have been identified through GC-MS analysis and are shown in Table 4.4. On the basis of GC/MS analysis intermediates (**A**-**K**) have been identified and are presented along with their molecular formula and structure.

Table 4.4 Identified intermediate compounds for 4-CG photoelectrocatalytic degradation under optimized conditions

Compound (m/z)	**Main Fragment**	**Molecular formula**	**Molecular structure**
4-CG	158	$C_7H_7ClO_2$	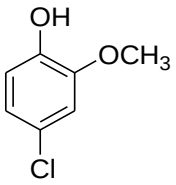
A	142	C_7H_7ClO	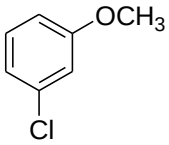
B	112	C_6H_5Cl	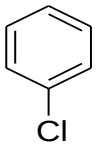
C	128	$C_6H_5ClO_2$	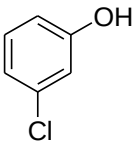
D	130	C_6H_7ClO	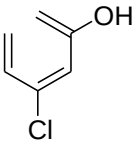
E	114	C_6H_7Cl	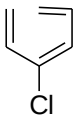
F	88	C_4H_5Cl	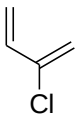
G	80	C_6H_8	
H	76	C_3H_4Cl	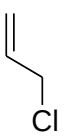

I	72	$C_3H_4O_2$	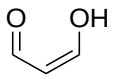
J	54	C_6H_4	
K	44	C_2H_4O	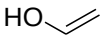

When compared to TiO_2 and Au/TiO_2, Cs/TiO_2 nanotube electrodes exhibited higher degradation efficiency of 92% against the degradation of 4-CG after 6 h treatment time under solar irradiations. The probable reason might be that the yield of $^{\bullet}OH$ radical concentration was higher in the case of Cs/TiO_2 nanotube electrodes (118.7 mM), when compared to Au/TiO_2 (105 mM) and TiO_2 (30.84 mM) nanotube electrodes. A comparative assessment of TiO2, Cs/TiO2 and Au/TiO2 nanotube electrodes have been shown in Table 4.5.

Table 4.5 Comparative assessment of synthesized electrodes in terms of 4-CG degradation and $^{\bullet}OH$ radical generation

Type of electrode	**Degradation efficiency (%)**	**Average treatment time (min)**	**Light source**	**$^{\bullet}OH$ radical concentration (mM)**
TiO_2	48	360	UV	30.84
Cs/TiO_2	92	360	Solar	118.7
Au/TiO_2	84	360	UV	105

4.3 Photoelectrocatalytic degradation of PCP using GO/TiO_2 nanotube electrodes

After achieving the significant degradation efficinecy of 4-CG using Cs/TiO_2 and Au/TiO_2 electrodes, PCP was selected for the PEC degradation. PCP is a highly-chlorinated hydrocarbon widely used as a broad-spectrum biocide and wood preservative (Lewandowski and Filippi, 1998; Hong and Zeng, 2002). PCP has been regarded as a priority pollutant on the United States Environmental Protection Agency (USEPA) list due to its toxic and carcinogenic nature. It has been widely present in the ground water and soil due to its poor handling and disposal techniques (McGinnis et al., 1991). Due to the persistence of PCP in soil, its migration to groundwater aquifers may pose risk to human beings (Lee et al., 1991; Rao, 2013). The adverse effects of PCP on ecological receptors and human may include: alteration in the electrical conductivities of biomembranes and inhibition of cellular enzymes (Umemura et al., 1999); exhibition of carcinogenic, teratogenic and reproductive effects in animal and humans due to cell mutations (Lewis and Irving, 2003); and adverse effects on terrestrial and aquatic flora and fauna (Repetto et al., 2001). The physicochemical properties of PCP have been presented in Table 4.6.

Table 4.6 Physicochemical properties of PCP

Name of the compound	Pentachlorophenol
IUPAC Name	2,3,4,5,6-pentachlorophenol
Molecular weight	266.323 g/mol
Molecular formula	C_6Cl_5OH or C_6HCl_5O
Boiling point	309-310 °C
Melting Point	174 °C
Structure	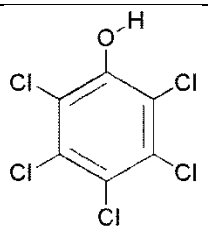

4.3.1 Characterization of GO/TiO_2 nanotube electrodes

GO/TiO_2 photoelectrodes have been synthesized by the in-situ anodization method and used for the PEC degradation of PCP (20 mg L^{-1}) as discussed in section 3.2. It has been reported that incorporation of graphene oxide on TiO_2 nanotubes array could highly promote photocatalysis on contaminants (Cheng et al., 2014; Kusumwati et al., 2014). The synthesized

TiO_2 and GO/TiO_2 nanotube electrodes have been characterized using FE-SEM, XRD, Raman spectra, UV-vis DRS, XPS, FTIR and PL spectra.

4.3.1.1 FE-SEM and EDS analysis

FE-SEM images of TiO_2 nanotube electrodes and GO/TiO_2 electrodes have been shown in Figure 4.24(a) and (b), respectively. Table 4.7 presents the EDS analysis of synthesized electrodes. TiO_2 nanotube electrode displayed porous surface and well aligned TiO_2 nanotubes with top end open formed onto the surface of Ti sheet with tube diameter ranging from ~ 20 to 25 nm and thickness of wall ~ 2 to 5 nm. It has been observed that the morphology of TiO_2 nanotube electrodes has greatly changed when decorated with GO particles. On comparing Figure 4.24(a) and 4.24(b), it can be observed that after electro-deposition, GO particles have been located at TiO_2 nanotubes covering most of its surface and has been seen to coexist with the rest of the uncovered region. The obtained FE-SEM results have been observed to be in good agreement with the previously reported studies (Yun et al., 2012).

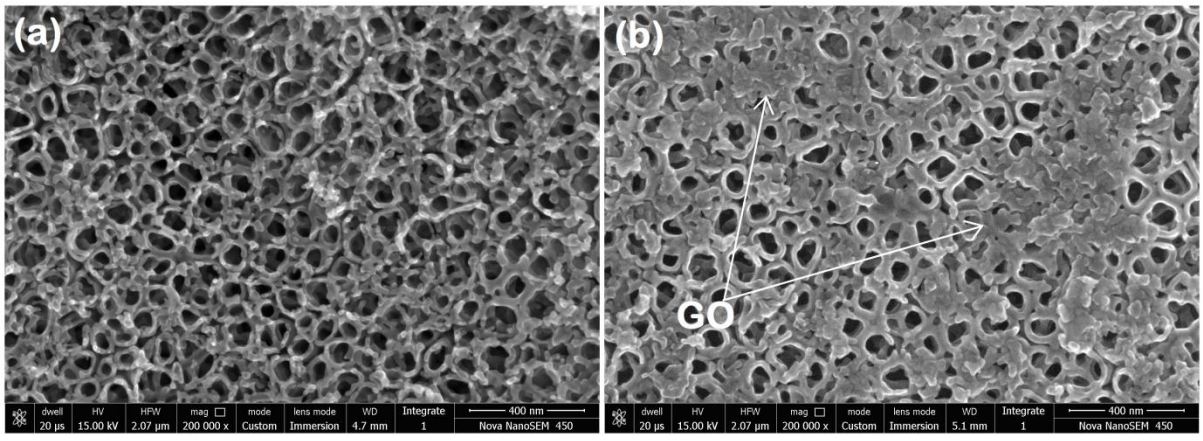

Fig. 4.24 FE-SEM images of (a) TiO_2 and (b) GO/TiO_2 nanotube electrodes

Table 4.7 EDS analysis of (a) TiO_2 and (b) GO/TiO_2 nanotube electrodes

Element	**C**	**O**	**Ti**	**Totals**
Weight (%)				
(a)	0.00	29.74	70.26	100.00
(b)	10.45	32.62	56.93	100.00

4.3.1.2 X-ray diffraction study

The X-ray diffraction patterns of TiO_2 and GO/TiO_2 nanotube electrodes have been shown in Figure 4.25. TiO_2 nanotube electrodes have been observed to be mostly comprised of anatase TiO_2 and their characteristic peaks have been obtained at 25.33° (310), 38.40° (331), 48.00° (530), 53.99° (432), 62.91° (641), 74.14° (204) and 76.17° (652) (JCPDS No. 21-1272). The diffraction peak at 25.33° has been allocated to the characteristic diffraction peak of (002) plane of graphite (JCPDS No. 41-1487). GO/TiO_2 nanotube electrodes possessed the characteristic peaks of anatase TiO_2 and Graphite. Very small difference in the diffraction peaks and angle has been observed after GO doping indicating the unchanged crystal phase of TiO_2 nanotube electrodes.

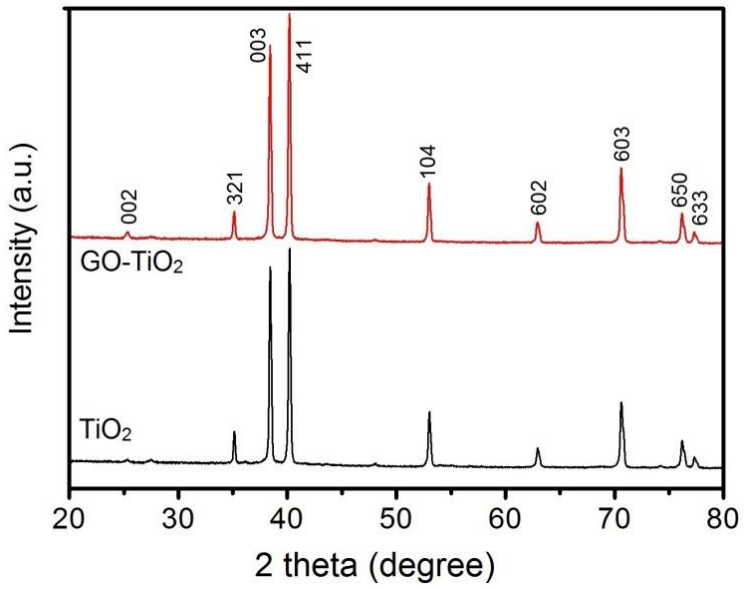

Fig. 4.25 XRD pattern of TiO_2 and GO/TiO_2 nanotube electrodes

4.3.1.3 Raman measurements

For the further confirmation of the presence of GO in GO/TiO_2 nanotube electrodes, Raman measurements has been conducted and the obtained spectra has been shown in Figure 4.26. TiO_2 nanotube electrodes displayed four characteristic peaks at round 142 (A), 396 (B), 514 (C) and 639 (D) cm^{-1}, attributed to the presence of anatase TiO_2 in A1g + 2B1g + 3Eg modes (Cheng et al., 2014). Two additional peaks at 1347 cm^{-1} (G1) and 1603 cm^{-1} (G2) were observed in GO/TiO_2 nanotube electrodes which correspond to the band peaks of graphite. G1-peak indicates the presence of certain impurity atom or defect in the graphitic hexagonal layers, while G2-peak indicated the E_{2g} graphite mode accounted to the sp^2 bonded

C atom in hexagonal two-dimensional graphitic layer (Li et al., 2016). The intensity ratio of G1-band to G2-band (I_D/I_G) in GO/TiO_2 nanotube electrodes was ~0.198.

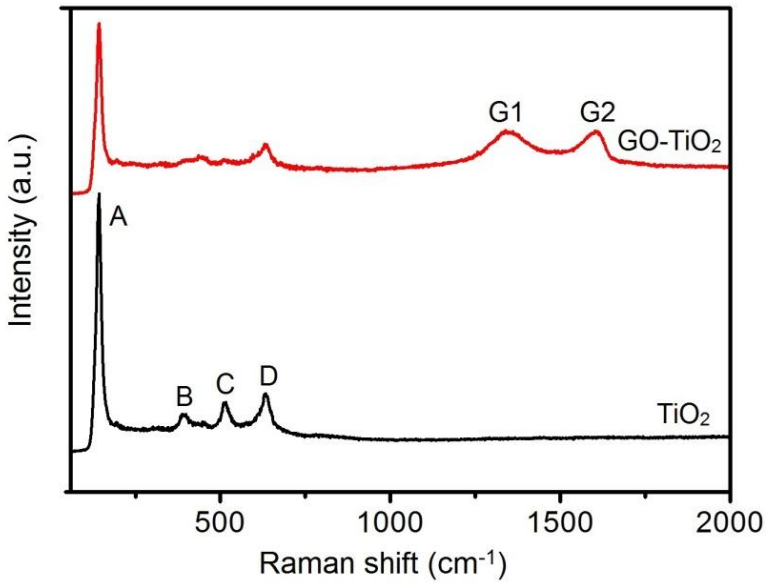

Fig. 4.26 Raman spectrum of TiO_2 and GO/TiO_2 nanotube electrodes

4.3.1.4 XPS analysis

The oxidation state of TiO_2 and GO/TiO_2 nanotube electrodes have been studied using XPS analysis. The XPS survey as shown in Figure 4.27 depicts that both contain three main peaks of O 1s, Ti 2p and C 1s. The significant C 1s peak assigned to C-C (sp^2) graphite bond can be observed at round 285.2 eV in the case of GO/TiO_2 nanotube electrodes. The two additional peaks, one of Ti 2p at 460.2 eV and other of O 1s at 533.1 eV have also been observed indicating the presence of titanium at Ti^{4+} and O as crystal lattice oxygen confirming the formation of O-Ti-O (Yun et al., 2012). Hence, the XPS analysis supports the successful synthesis of GO/TiO_2 nanotube electrodes. Small peak of C 1s in the TiO_2 nanotube electrodes can be due to the presence of adventitious hydrocarbons from the instrument itself.

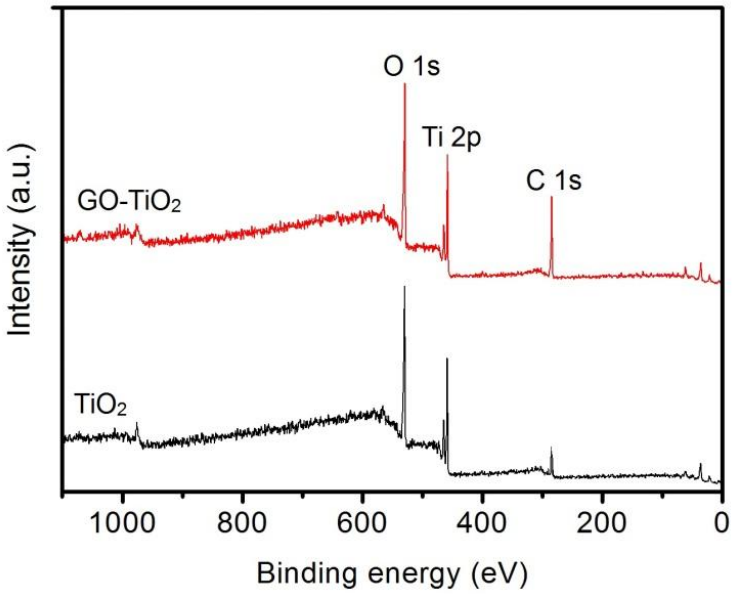

Fig. 4.27 XPS analysis of TiO_2 and GO/TiO_2 nanotube electrodes

4.3.1.5 UV-vis diffuse reflection spectrum

The UV-vis DRS of TiO_2 and GO/TiO_2 nanotube electrodes have been presented in Figure 4.28. TiO_2 electrodes exhibited intense photoabsorbance in UV region while GO/TiO_2 nanotube electrodes showed photoabsorbance in visible region. GO/TiO_2 nanotube electrodes displayed a red-shift to higher wavelength might be due to the presesnce of Ti-O-C bond between GO and TiO_2 which alters the optical absorption edge (Zhang et al., 2009).

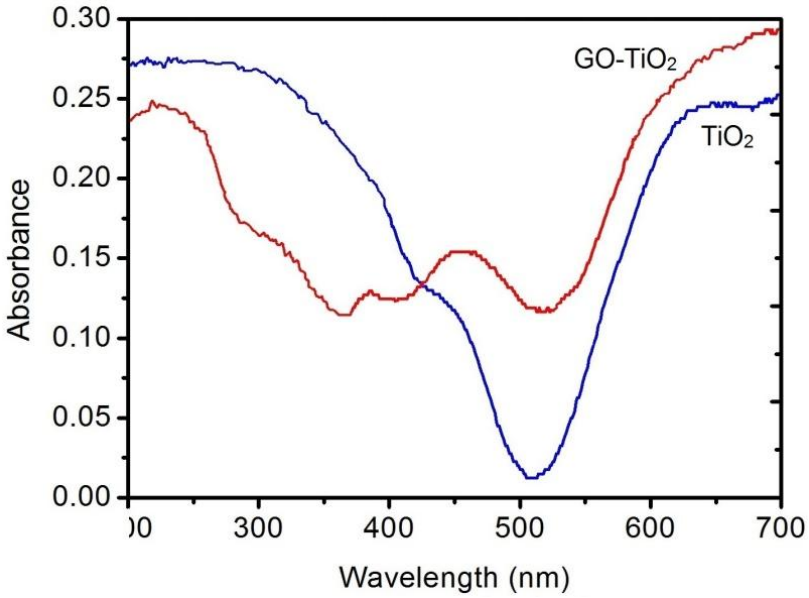

Fig. 4.28 UV-vis diffuse reflection spectrum of TiO_2 and GO/TiO_2 nanotube electrodes

4.3.1.6 Photoluminescence spectrum

The photoluminescence (PL) spectra have been widely used to determine the surface structure, stoichiometry and the efficiency of transfer, trapping and migration of charge carrier, additionally to figure out the fate of e^--h^+ pairs in semiconductors (He et al., 2013; Sellappan et al., 2013; Gu et al., 2013). The intensity of PL spectrum gives a direct estimation of electron-hole recombination rate i.e. more intense the spectrum, faster will be the recombination and lower intensity of spectrum indicates more trapping of excited electrons and their stable transfer through the interface. To study the effect of graphene doping on the electron-hole recombination rate, the PL spectra of TiO_2 and GO/TiO_2 has been determined and shown in Figure 4.29. Band at ~422 nm is due to the excitonic PL peaks trapped by surface states and defects (Liu et al., 2007). The emission signal at ~486 and ~545 nm may be attributed to the charge transfer from Ti^{3+} to oxygen vacancies present at the surface and presence of Ti site vacancies created in TiO_2, respectively (Liu et al., 2008; Sasaki and Watanabe, 1997). After the binary composite GO/TiO_2 has been formed, the PL intensity reduced markedly and few of the above mentioned peaks disappeared due to the photo-excited electrons trapping by graphene oxide which could suppress the recombination rate resulting in higher PEC activity.

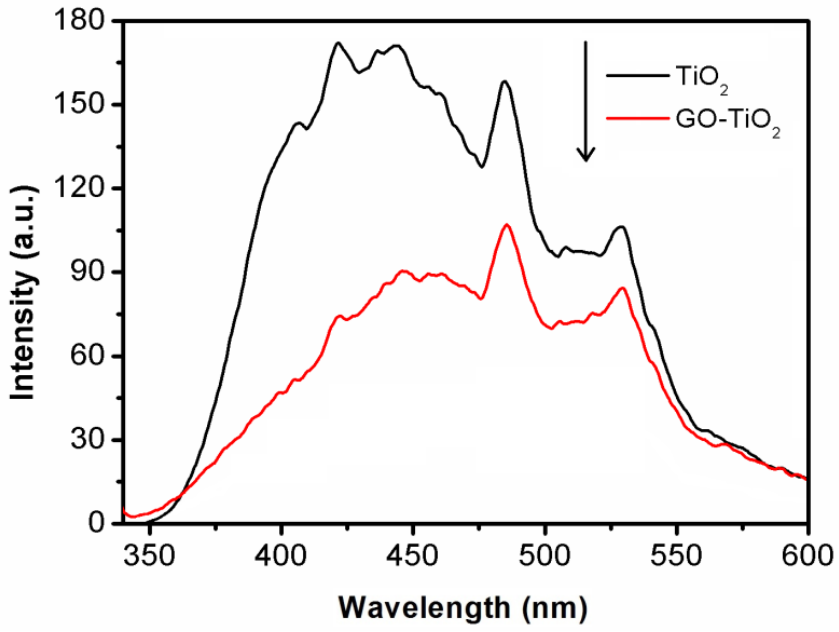

Fig. 4.29 PL spectrum of TiO_2 and GO/TiO_2 nanotube electrodes

4.3.1.7 FTIR spectrum

The FTIR spectra of TiO_2 and GO/TiO_2 have been shown in Figure 4.30. Graphene oxide exhibits a peak at ~1738 cm^{-1} for C=O groups. The peaks at ~1216 cm^{-1} and a broad peak at ~3308 cm^{-1} have been designated to hydroxyl groups. Peak appearing at 1367 cm^{-1} corresponds to carboxyl groups (Nethravathi and Rajamathi, 2008). The peak near ~591 cm^{-1} has been assigned to Ti-O-Ti stretching (lattice vibration). The IR spectrum of TiO_2 has been observed to be almost similar to GO/TiO_2, this might be due to the low quantity of GO (15 mg L^{-1}) used in synthesizing the electrodes as well as non-uniform deposition of GO layer on the TiO_2 surface as evident from FE-SEM images. The results are in agreement with the previous published findings wherein the IR spectrogram of TiO_2 and GO-TiO_2 nanoparticles has been reported to be almost similar (Liu et al., 2016).

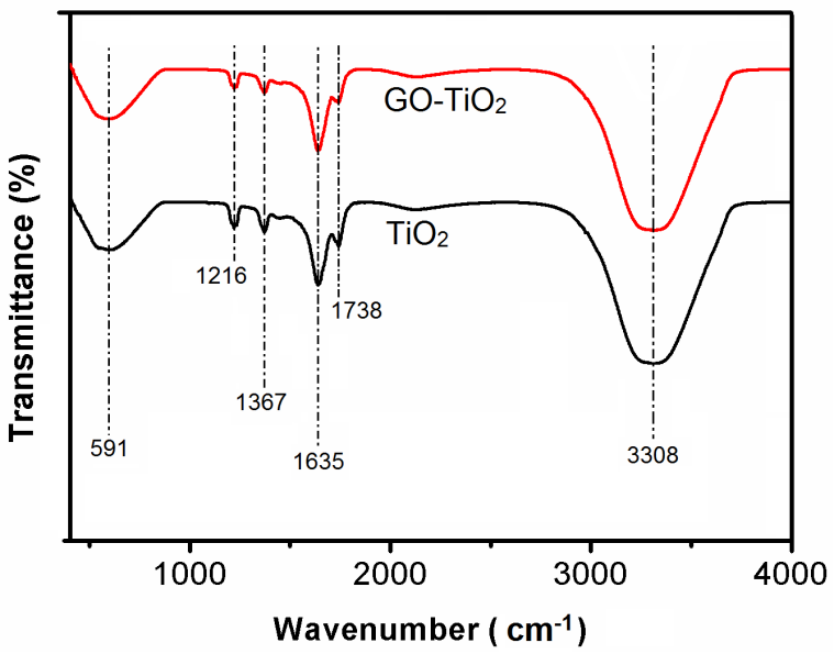

Fig. 4.30 FTIR spectrum of TiO_2 and GO/TiO_2 nanotube electrodes

4.3.2 Parametric optimization for the degradation of PCP

The Box-Behnkem design (BBD) has been applied to find out the optimum conditions for the PEC degradation of PCP. Degradation efficacy and energy consumption has been taken as the responses. The four independent variables selected were applied current (X_1), pH (X_2), time (X_3) and GO concentration (X_4). The ranges of variables were 20-60 mA current, 3-8 pH, 10-120 min time, 0.005-0.25 g/L GO concentration and their low (-1), centre (0) and high (+1) levels and have been illustrated in Table 4.8.

Table 4.8 BBD based experimental levels for independent variables

Variables	**Symbols**	**-1**	**0**	**+1**
Applied current (mA)	X_1	20	40	60
pH	X_2	3	5	8
Time (min)	X_3	10	65	120
GO concentration (g/L)	X_4	0.005	0.15	0.25

4.3.3 Model fitting and ANOVA analysis

Experiments performed as suggested by BBD have been shown in Table 4.9. The outputs have been fitted by using a second-order polynomial equation as shown in Eq.4.4 and Eq.4.5:

$$Y_1 = +4.00 - 4.98X_1 - 27.42\ X_2 + 16.00X_3 + 4.95X_4 + 4.84X_1^2 + 38.75X_2^2 + 13.87X_3^2 + 11.79\ X_4^2 + 6.43X_1X_2 - 10.25X_1X_3 + 1.75X_1X_4 + 5.75X_2X_3 + 0.92X_2X_4 + 10.00X_3X_4 \quad (4.4)$$

$$Y_2 = +\ 7.470E\text{-}004 + 5.861E\text{-}004X_1 + 1.425E\text{-}004X_2 + 6.059E\text{-}004X_3 + 3.348E\text{-}004X_4 + 1.316E\text{-}004X_1^2 + 8.455E\text{-}005X_2^2 + 2.392E\text{-}004X_3^2 + 1.068E\text{-}004X_4^2 + 4.838E\text{-}\ 005X_1X_2 + 5.301E\text{-}004X_1X_3 - 3.519E\text{-}005X_1X_4 - 3.349E\text{-}004X_2X_3 + 2.813E\text{-}004X_2X_4 + 8.156E\text{-}005X_3X_4 \quad (4.5)$$

Where Y_1 is the degradation efficacy; Y_2 is the energy consumption (kWh); X_1, X_2, X_3, X_4 are the coded parameters i.e. applied current, pH, degradation time and GO concentration, respectively.

Table 4.9 Coded levels and real values for the BBD design experiments along with their actual and predicted degradation efficacy and energy consumption (kWh)

Run	Coded levels				Degradation efficacy (Y_1)		Energy Consumption (kWh, Y_2)	
	X_1	X_2	X_3	X_4	Actual	Predicted	Actual	Predicted
1	0.000	0.000	0.000	0.000	4.00	4.00	7.470E-004	7.470E-004
2	1.000	0.000	-1.000	0.000	9.00	11.98	6.380E-004	5.679E-004
3	0.000	0.000	0.000	0.000	4.00	4.00	7.470E-004	7.470E-004
4	0.000	1.000	0.000	1.000	35.00	32.98	1.761E-003	1.697E-003
5	1.000	0.000	0.000	1.000	27.00	22.35	1.863E-003	1.871E-003
6	0.000	0.000	0.000	0.000	4.00	4.00	7.470E-004	7.470E-004
7	0.000	1.000	1.000	0.000	46.00	50.96	1.372E-003	1.484E-003
8	0.000	0.000	0.000	0.000	4.00	4.00	7.470E-004	7.470E-004
9	-1.000	0.000	0.000	1.000	25.00	28.80	1.023E-003	7.693E-004
10	-1.000	0.000	-1.000	0.000	6.00	1.43	3.820E-004	4.559E-004
11	0.000	0.000	0.000	0.000	17.00	18.72	2.967E-004	2.339E-004
12	0.000	1.000	0.000	1.000	13.00	22.41	1.900E-005	2.926E-005
13	1.000	0.000	0.000	1.000	91.70	86.41	1.429E-004	2.828E-004
14	0.000	0.000	0.000	0.000	22.00	23.48	3.044E-003	2.840E-003
15	0.000	1.000	1.000	0.000	15.00	7.46	8.090E-004	9.423E-004
16	0.000	0.000	0.000	0.000	74.00	73.80	8.200E-005	-1.255E-005
17	-1.000	0.000	0.000	1.000	64.00	60.61	1.940E-003	2.115E-003
18	0.000	0.000	-1.000	-1.000	18.00	21.62	1.768E-003	1.740E-003
19	-1.000	0.000	0.000	-1.000	4.00	4.00	7.470E-004	7.470E-004
20	-1.000	-1.000	0.000	0.000	14.00	18.72	3.808E-004	4.712E-004
21	1.000	0.000	1.000	0.000	82.00	94.30	1.984E-003	1.869E-003
22	0.000	1.000	-1.000	0.000	28.00	21.26	7.097E-004	4.647E-004
23	0.000	-1.000	-1.000	0.000	65.00	53.93	6.680E-004	6.074E-004
24	0.000	0.000	1.000	1.000	8.00	8.96	9.997E-004	1.272E-003
25	-1.000	1.000	0.000	0.000	35.00	30.72	1.190E-003	1.283E-003
26	0.000	-1.000	1.000	0.000	6.00	8.61	7.200E-004	7.404E-004
27	0.000	1.000	0.000	-1.000	73.00	67.61	1.336E-003	1.358E-003
28	-1.000	0.000	1.000	0.000	79.00	77.93	8.090E-004	7.423E-004
29	1.000	0.000	0.000	-1.000	82.34	85.99	7.350E-004	8.493E-004

The ANOVA (Analysis of variance) analysis from Table 4.10 indicates the response surface quadratic model was statistically significant and appropriate for representing the relation between the responses and variables with high F-value of 41.61 and very small P-value of <0.0001. There is only 0.01% chance that this large "Model F-value" could occur due to noise. In general, if P-value is less than 0.05, the design model is considered to be significant and can be used as statistical predictive model (Singh et al., 2015). Thus, very low P-value in present study indicated that the fitted quadratic model is valid. Coefficient of determination (R^2), the ratio of explained variation to total variation, is also a measure of degree of fitness and has been shown in Table 4.5. In the present study, the R^2 values of quadratic model for degradation efficacy and energy consumption are 0.9655 and 0.9689, respectively. Hence, it can be interfered that the predicted degradation efficacy and energy consumption from model are comparable to experimentally measured values owing to near unity values of R^2.

The residual analysis has been shown in Figure 4.31, which is used to make sure feasibility between the assumptions and practical experimental values. The normal plot of residues Figure 4.31(a) shows that the standard deviation between actual and predicted degradation efficacy are in a reasonable range indicating no abnormal experimental results. The residuals vs. predicted degradation efficacy plot (Figure 4.31b) obtained by quadratic model fitting shows that the actual experimental results are randomly distributed within the ±3.00 range of studentized residuals indicating that the fitted quadratic model is appropriate. Figure 4.31(c) shows the predicted vs. actual plot of degradation efficacy infering that they are in good synergy. All the plots for energy consumption have been observed to be similar as the plots of degradation efficacy.

Table 4.10 ANOVA table for the BBD RSM model

Source	Degradation efficacy					Energy Consumption				
	Sum of Squares	DF	Mean Square	F-value	P-value	Sum of Squares	DF	Mean Square	F-value	P-value
X_1	297.01	1	297.01	4.84	0.0452	4.123E-006	1	4.123E-006	143.81	<0.0001
X_2	9022.28	1	9022.28	146.9	<0.0001	2.438E-007	1	2.438E-007	8.50	0.0113
X_3	3072.00	1	3072.00	50.02	<0.0001	4.405E-006	1	4.405E-006	153.66	< 0.0001
X_4	293.44	1	293.44	4.78	0.0463	1.345E-006	1	1.345E-006	46.92	< 0.0001
X_1^2	151.69	1	151.69	2.47	0.1384	1.123E-007	1	1.123E-007	3.92	0.0678
X_2^2	9741.54	1	9741.54	158.6	<0.0001	4.637E-008	1	4.637E-008	1.62	0.2242
X_3^2	1248.45	1	1248.45	20.33	0.0005	3.711E-007	1	3.711E-007	12.95	0.0029
X_4^2	901.78	1	901.78	14.68	0.0018	7.400E-008	1	7.400E-008	2.58	0.1305
X_1X_2	165.12	1	165.12	2.69	0.1233	9.361E-009	1	9.361E-009	0.33	0.5768
X_1X_3	420.25	1	420.25	6.84	0.0203	1.124E-006	1	1.124E-006	39.21	< 0.0001
X_1X_4	12.25	1	12.25	0.20	0.6620	4.953E-009	1	4.953E-009	0.17	0.6840
X_2X_3	132.25	1	132.25	2.15	0.1644	4.486E-007	1	4.486E-007	15.65	0.0014
X_2X_4	3.35	1	3.35	0.055	0.8187	3.166E-007	1	3.166E-007	11.04	0.0050
X_3X_4	400.00	1	400.00	6.51	0.0230	2.661E-008	1	2.661E-008	0.93	0.3517
Model	24040.8	14	1717.21	27.96	<0.0001	1.249E-005	14	8.919E007	31.11	< 0.0001
Error	0.000	4	0.000			0.000	4	0.000		
Total	24900.7	28				1.289E-005	2			
	R^2 = 0.9655, Adj R^2 = 0.9309, Predicted R^2 = 0.8011, CV = 24, Precision = 16.476					R^2 = 0.9689, Adj R^2 = 0.9377, Predicted R^2 = 0.8206, CV = 17.28, Precision = 23.425				

It has been evident from ANOVA table (Table 4.10) that, X_1 (applied current), X_3 (degradation time) and X_4 (GO concentration) are the significant variables and X_1X_3 is the significant interaction with P-value <0.0001.

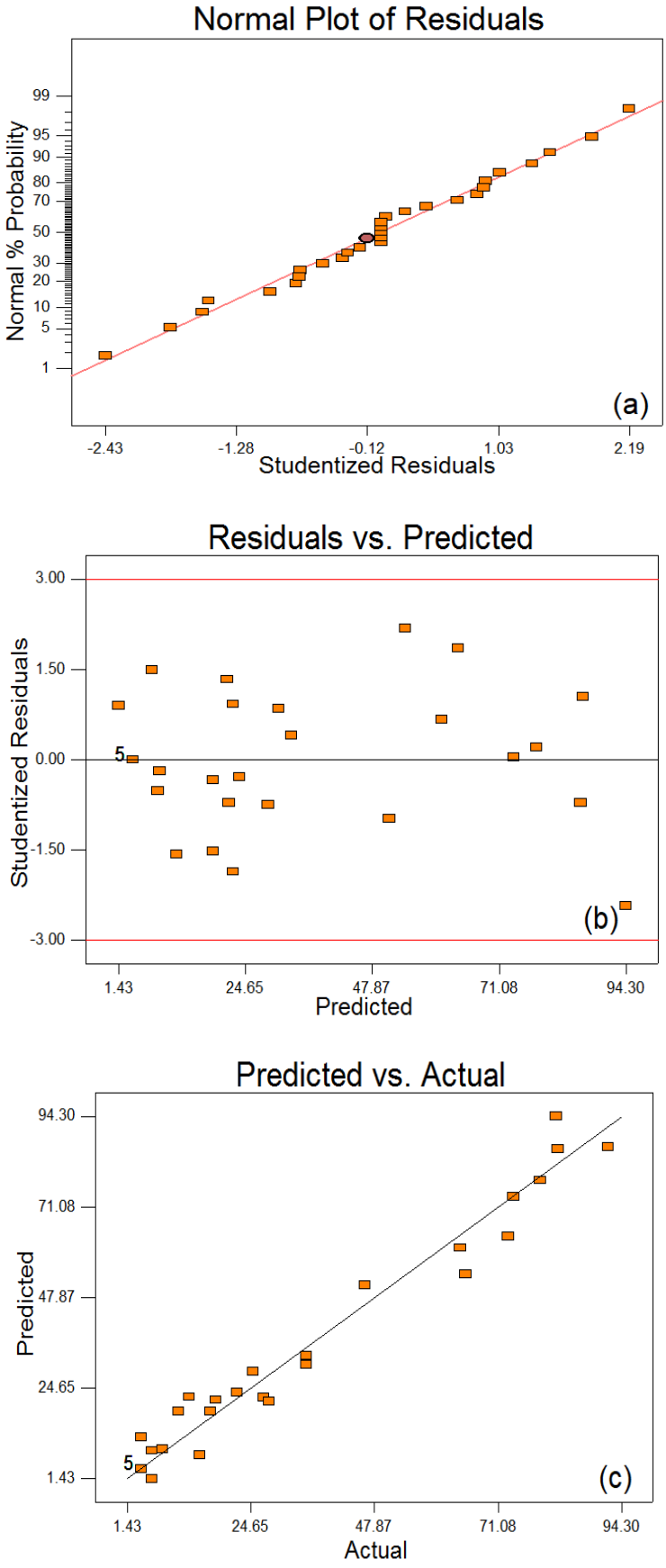

Fig. 4.31 (a) Normal plot of residuals, (b) Residuals vs. predicted plot, (c) Predicted vs. actual plot for percentage degradation

The effect of applied current and GO concentration on PEC degradation of PCP at constant pH 5.5 and degradation time 65 min has been shown in Figure 4.32(a). The GO/TiO_2 nanotube electrodes showed the highest degradation efficiency of PCP when applied current and GO concentration has been kept 34 mA and 0.145 mg L^{-1}, respectively. Application of applied potential improves the oxidation of pollutant on the GO/TiO_2 nanotube photoelectrode. The involvement of an electric field allows separation of photogenerated charge carriers (e^- and h^+) by the movement of charges in different directions via the anode and cathode thereby, reducing the recombination. It has been observed that with the increase in applied potential, PCP degradation increases until a value of 20.68 mA and then, gradually decreases with increasing potential. This could be due to the evolution of hydrogen and cathodic reduction of H_2O_2 to H_2O side reactions which affect electro generation of H_2O_2 at potential higher than 20.68 mA (Bagotskii et al., 1965; Sahoo et al., 2012). The presence of GO improved the conductivity of photoelectrodes so the degradation of PCP was maximum with lower applied potential. Moreover, the use of an external applied field combined with UV light irradiation enhanced the degradation of PCP with time. The H_2O_2 electro generated by O_2 reduction on GO surface has been activated with UV irradiations producing hydroxide radicals, which were responsible for decomposition of PCP in the PEC process.

Figure 4.32(b) and 4.32(c) showed that degradation rate decreased with increasing pH of the PCP aqueous solution from pH 3-8. Higher degradation efficiency has been attained in the acidic environment when compared to alkaline and neutral environment. At pH values lower than the point of zero charge of TiO_2 i.e. 6.5, the surface of catalyst becomes positively charged resulting in easily transfer of photoelectrons (Leng et al., 2006) consequently; recombination of e^-/h^+ has been decreased facilitating the photocatalytic reactions.

The significant enhancement in PEC efficiency with GO/TiO_2 nanotube electrode could be attributed to the synergic effect between electrochemical and photocatalytic process, the decorated GO layer significantly improved the ability of light absorbance in GO/TiO_2 nanotube electrode. Moreover the applied potential and existence of GO in GO/TiO_2 nanotube electrode were favorable in inhibiting the recombination of photogenerated charge carriers and reducing the transfer resistance of electrons (Li et al., 2016).

In the case of energy consumption, highest effect on the response was of degradation time with F value of 153.66. Applied current, GO concentration and pH of the solution have been found to exhibit less effect on energy consumption during the reaction. Figure 4.33 demonstrates the effect of degradation time, applied current, GO concentration and pH on the

energy consumption during PEC process. It can be observed that with increase in applied current and degradation time, energy consumption increases, whereas GO concentration and initial pH of the solution showed marginal effect on the energy consumption.

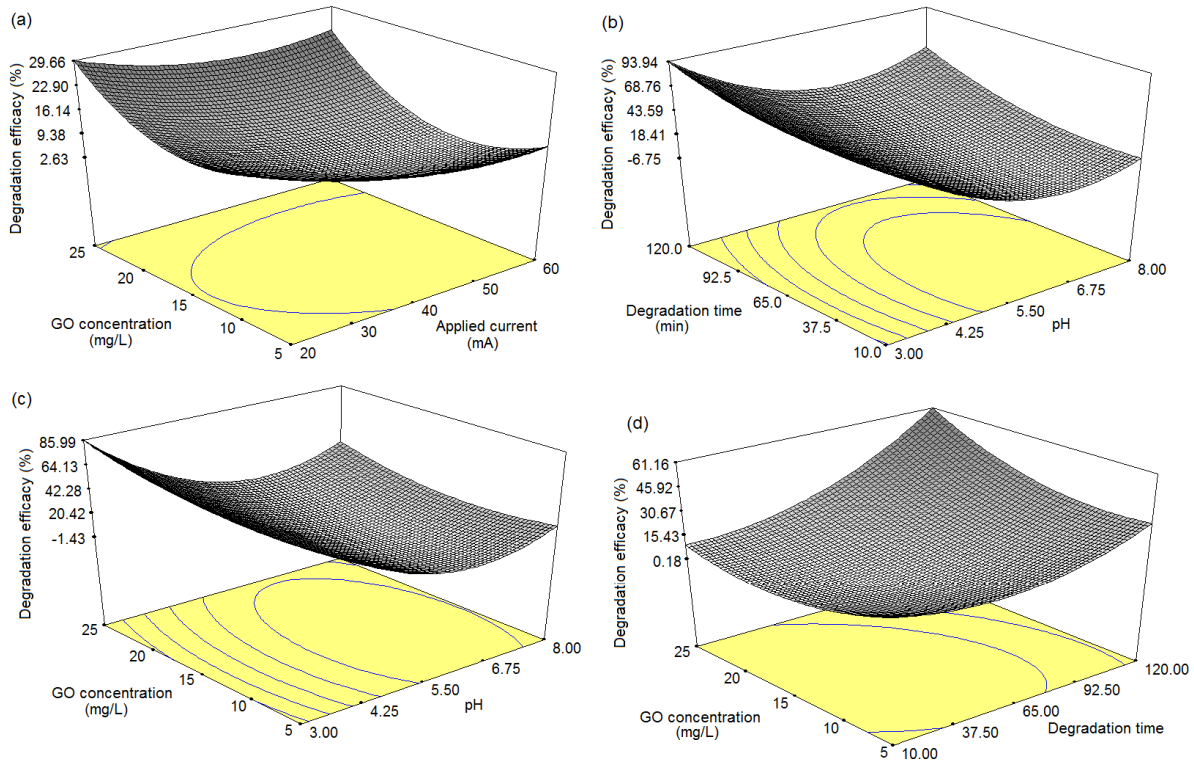

Fig. 4.32 3-D response surface graph for the photoelectrocatalytic degradation of PCP (a) degradation efficacy vs. GO concentration and applied current; (b) degradation efficacy vs. degradation time and pH; (c) degradation efficacy vs. GO concentration and pH; (d) degradation efficacy vs. GO concentration and degradation time.

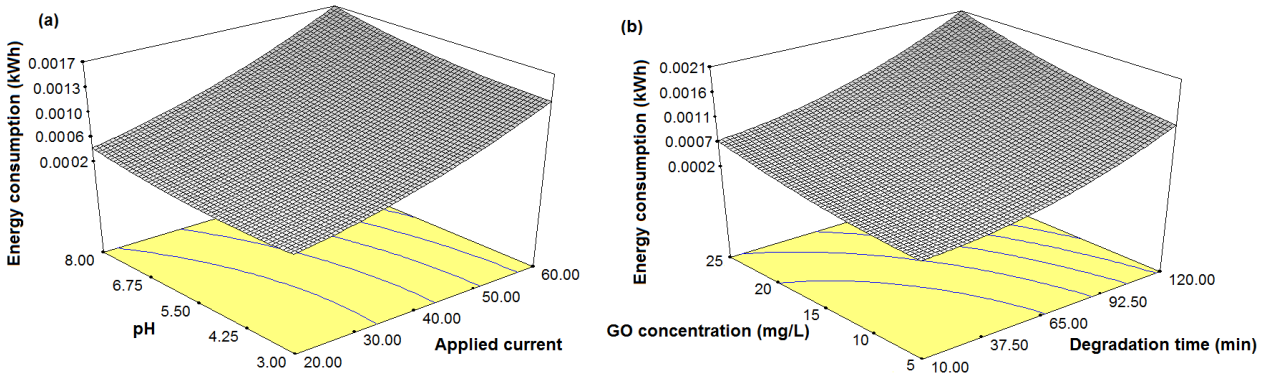

Fig. 4.33 3-D response surface graph for the photoelectrocatalytic degradation of PCP (a) Energy consumption vs. pH and applied current (b) Energy consumption vs. GO concentration and degradation time

4.3.4 Optimum conditions and verification

With the help of BBD, the optimal operational parameter values have been predicted. Table 4.11 presents the optimum values for degradation efficiency (Y_1) and energy consumption (Y_2). The predicted response data for variables have also been presented. Verification experiments have been performed under optimum operating conditions (applied current 20.68 mA; pH 3.14; GO concentration 15 mg L^{-1} and degradation time 93 min). The experiments have been performed in triplicate to authenticate the output and yielded an average PCP degradation efficiency of 91.56%, and energy consumption of 0.0034 kWh L^{-1}. TOC removal of 85% has been achieved under optimized conditions. The good agreement between predicted and actual experimental results verified the existence of an optimal point and validity of model.

Table 4.11 Predicted and actual values for degradation efficacy and energy consumption at optimum conditions (20.68 mA, pH 3.14, 93 min and 15 mg L^{-1} GO)

Degradation Efficacy (%)	***Predicted***	***Experimental***
	93.9	91.56
Energy consumption (kWh)	*0.00056*	0.00068

4.3.5 Scavengers study

In order to further appraise the role of active species like hydroxyl radical ($^{\bullet}OH$), superoxide ions ($^{\bullet}O_2^-$) and holes (h^+), different type of scavengers have been introduced in the reaction system. Figure 4.34 showed the PEC activity of GO/TiO_2 photo-electrode against PCP under the influence of various scavengers. Without any scavengers, PCP degradation efficacy has been 91% after 93 min of irradiation. When IPA as a $^{\bullet}OH$ scavenger has been added into the reaction system, the PCP degradation efficacy (53.7%) has been suppressed significantly. Furthermore, when EDTA and $_L$-ascorbic acid have been supplemented in the system, the PCP degradation decreased moderately. By the observation, it can be concluded that each selected reactive species performed significant role in regulating PEC process, and involvement of $^{\bullet}OH$ has been majorly responsible for PCP removal.

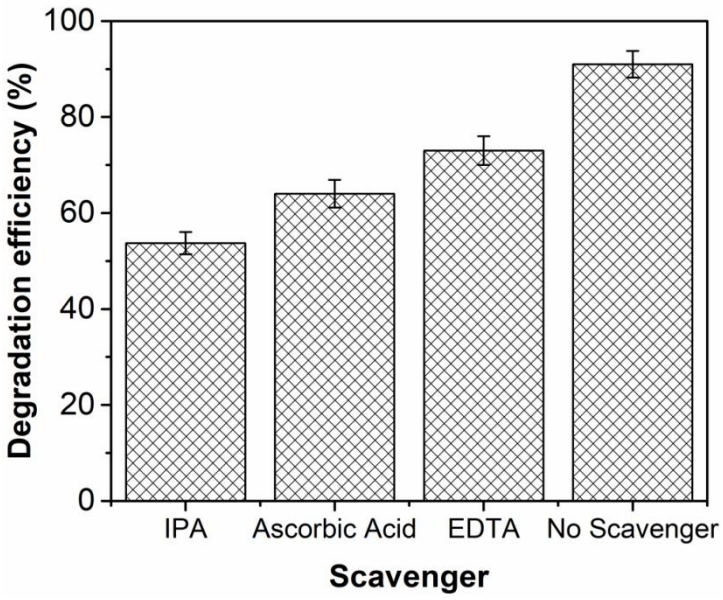

Fig. 4.34 Effect of different scavenger on PEC degradation of PCP

4.3.6 Quantification of ˙OH radicals

It has been a well known fact that produced as major species are responsible for the oxidative degradation of pollutants (Li et al., 2012). As can be seen in Figure 4.35, the PL intensity at around 425 nm of GO/TiO_2 electrode has been much higher than TiO_2 electrode indicating the higher contribution of GO/TiO_2 (135 mM) anode in ˙OH production as compared to TiO_2 nanotube electrode (32.46 mM). It can also be observed that the exposure to irradiation could increase the generation of hydroxyl radicals, which could improve the degradation efficacy.

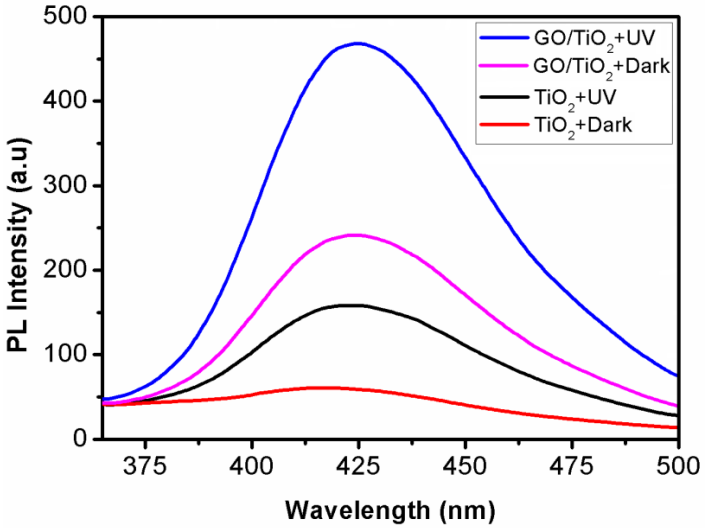

Fig. 4.35 PL spectra of GO/TiO_2 and TiO_2 photoelectrodes with and without UV irradiation

4.3.7 PCP decomposition pathway and intermediate identification

The intermediates formed during the decomposition process have been identified using LC/MS (Figure 4.36) and has been shown in Figure 4.37. Identification of primary degradation products allowed the prediction of tentative interlinking pathways for PCP decomposition. The pathway begins with the oxidative dechlorination of PCP (a, *m/z* 265.84, C_6HCl_5O) at para position and the mass pattern was found to be matching with tetrachlorohydroquinone (b) having *m/z* 247.87 with empirical formula $C_6H_2Cl_4O_2$. Formation of (b) has also been reported previously in photocatalytic degradation process of PCP (Mill and Hoffmann, 1993; Silva et al., 2012). As the decomposition reaction precedes, the isomers of dichlorohydroquinone (c), (d) and (f) have been obtained, which on further decomposition furnished (g). 2,6-dichlorohydroquinone (f) came from the reductive dechlorination at ortho position, while 2,5-dichlorohydroquinone (c) has been formed by the substitution of chlorine atom by hydrogen atom at ortho and meta positions. It has been documented in the literature that, presence of hydroquinones can be detected when $^{\bullet}OH$ exists in the PCP aqueous solution (Jardim et al., 1997). Formation of chlorohydroquinone (e, *m/z* 143.99, $C_6H_5ClO_2$) took place by the reductive dechlorination of (d). C_6H_6O (g, m/z 93.46) has been formed by further removal of Cl from the compound. Furthermore, the decomposition reaction of (e) leads to the formation of (h) (*m/z* 175.96, $C_6H_3ClO_4^{\bullet-}$) and (i) (*m/z* 83.04, $C_5H_7O^{\bullet}$). The formed end products clearly indicate the breakdown of PCP which has been otherwise considered recalcitrant in nature.

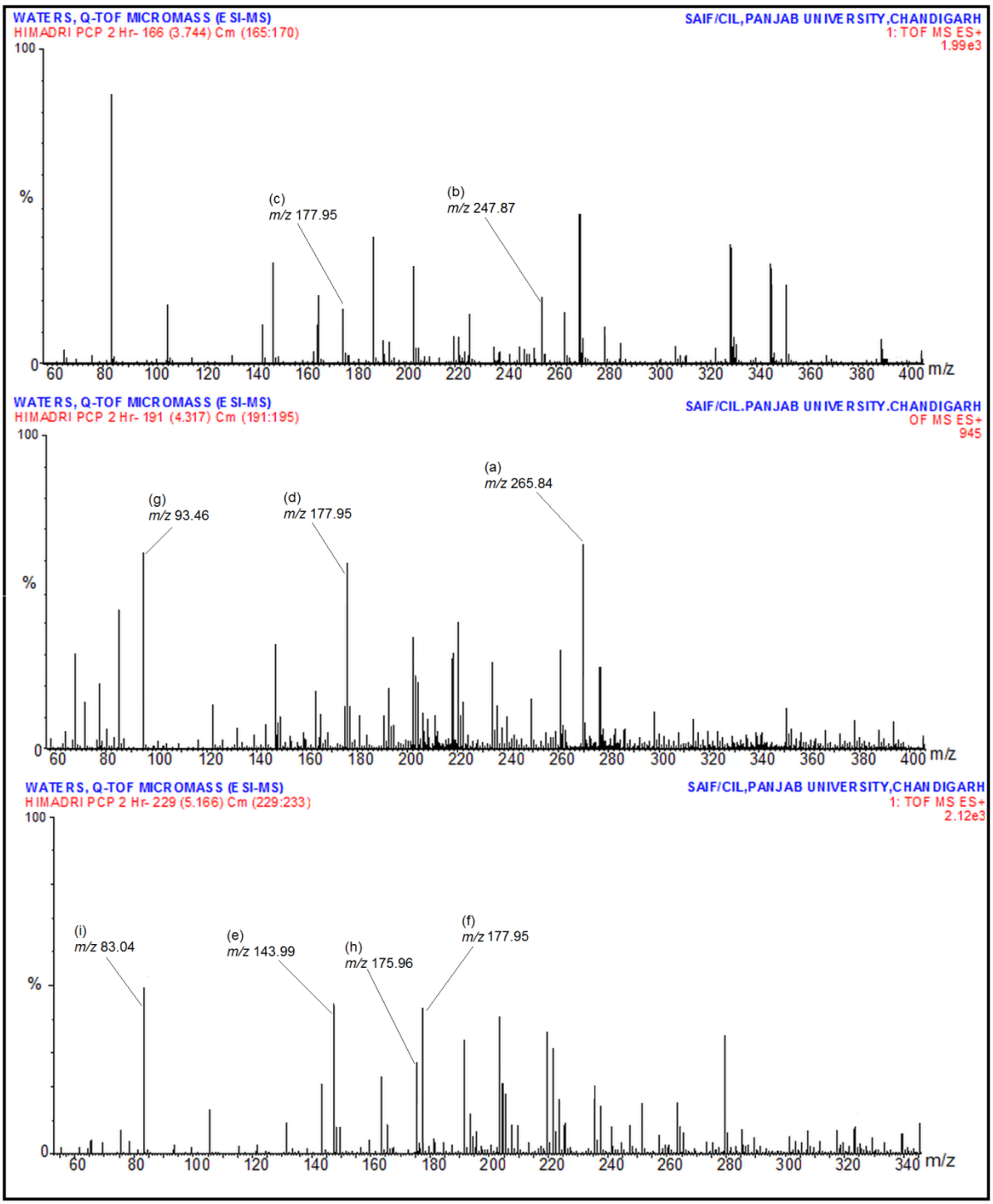

Fig. 4.36 Mass spectrum of intermediates formed during the PEC degradation

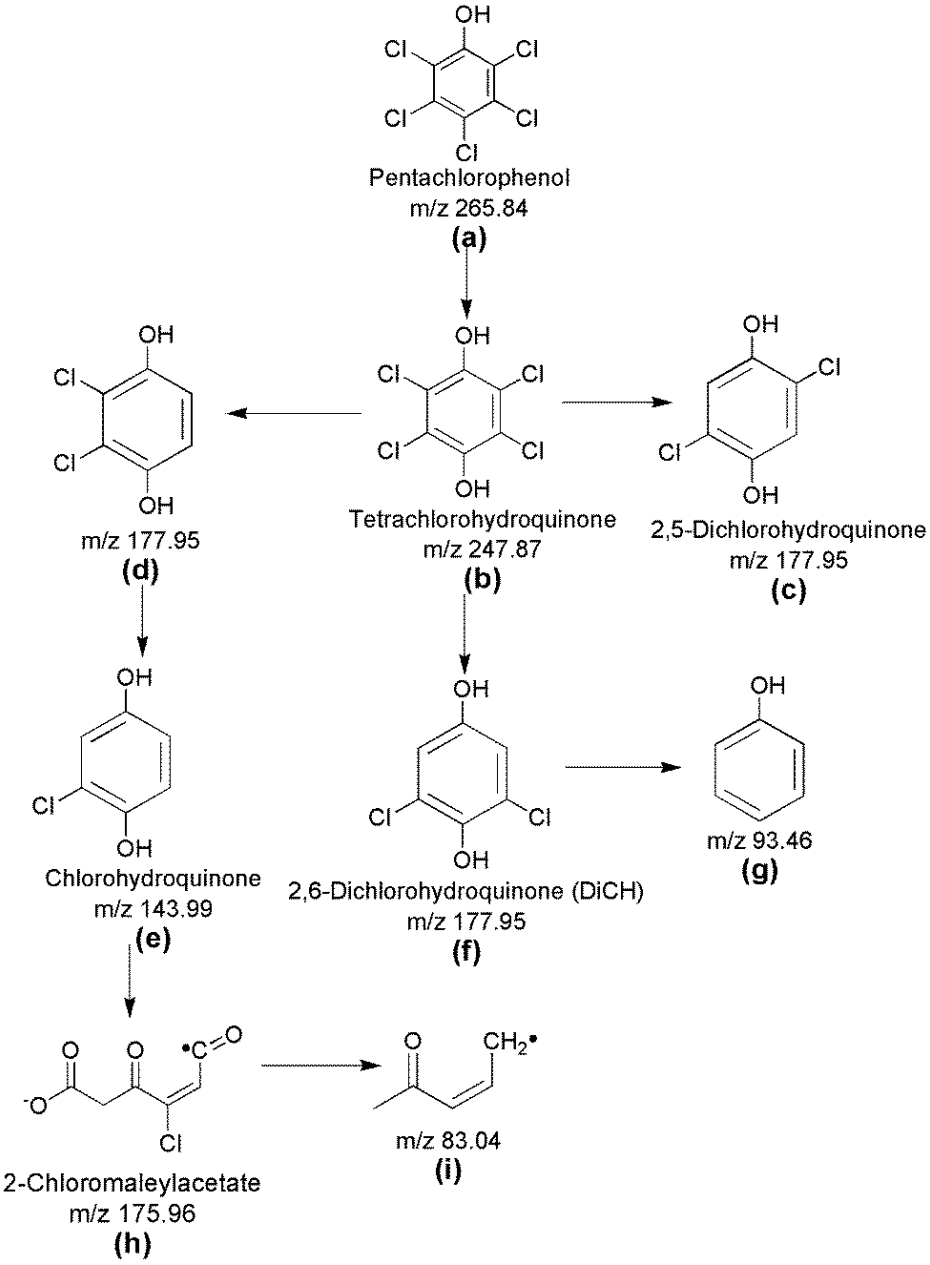

Fig. 4.37 Identified intermediate products and proposed degradation pathway of PCP

On the basis of detailed study as described above, photoelectrocatalytic degradation of PCP using GO-TiO_2 nanotube electrodes can be summarized as shown in Figure 4.38.

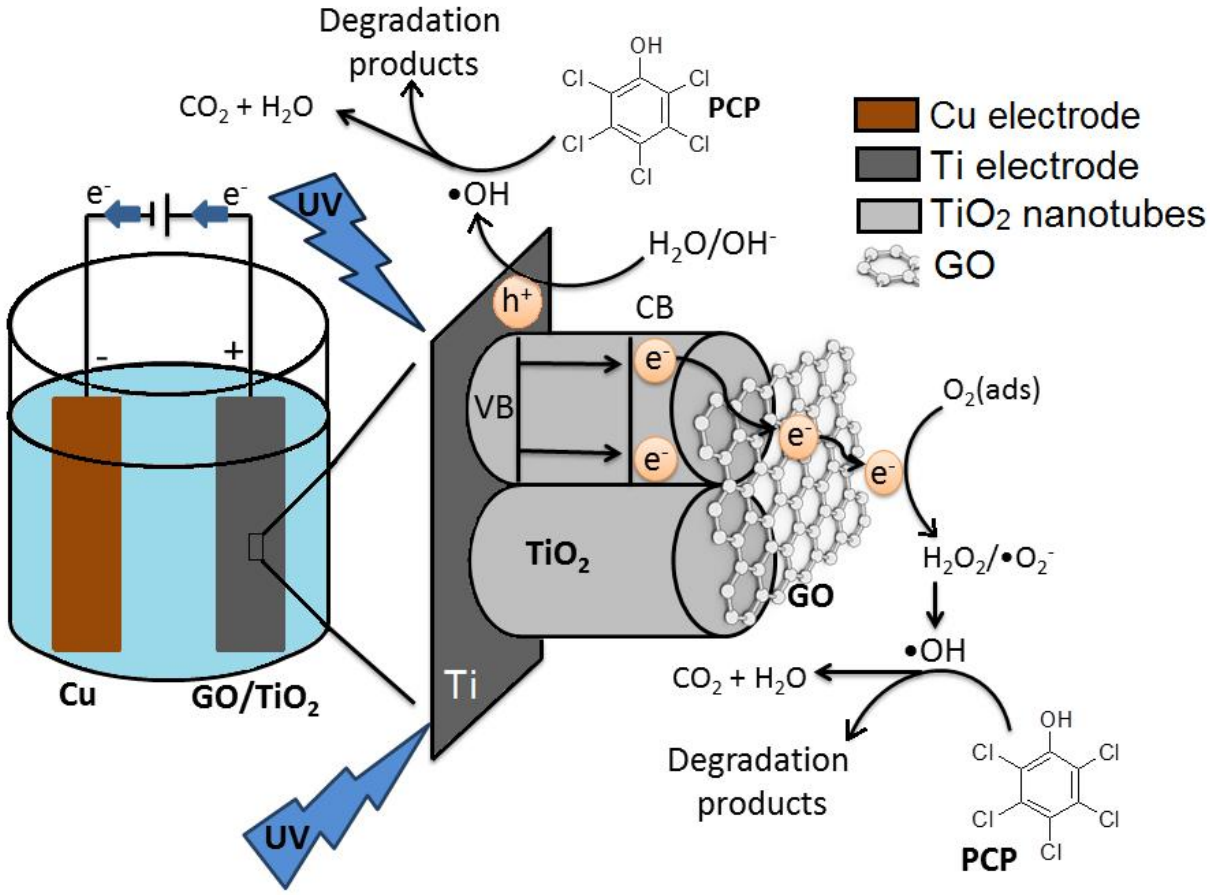

Fig. 4.38 PEC degradation of PCP using GO/TiO_2 nanotube electrodes

4.4 PEC degradation of PCP using Ag loaded GO/TiO_2 nanotube electrode

The considerable degradation of PCP was observed when GO/TiO_2 electrode was used. Afterwards, Ag loaded GO/TiO_2 nanotube photoelectrode was fabricated through anodization method for the PEC treatment of PCP. The synthesized electrode has been characterized for its physicochemical properties and compared with TiO_2 and GO/TiO_2 nanotube elctrodes. The PEC performance of Ag loaded GO/TiO_2 nanotube photoelectrode has been evaluated for the degradation of PCP. The influence of reactive species on the PEC process has been examined. Moreover, degradation intermediates have also been identified and reported.

4.4.1. Characterization of Ag-GO/TiO_2 electrodes

The laboratory synthesized electrodes have been characterized for their physical and chemical characteristics using various physicochemical analysis techniques.

4.4.1.1 FE-SEM and EDS analysis

In order to examine the structural characteristics of TiO_2, GO/TiO_2 and Ag-GO/TiO_2 nanotube electrodes, samples have been subjected to FE-SEM and their surface properties were investigated. As shown in the Figure 4.39, well aligned porous TiO_2 nanotubes have been formed over Ti substrate with open top end. Figure 4.39(b) shows that GO nanoparticles are attached to the TiO_2 top layer and coexist with rest of the uncovered region. Further, electrodeposited Ag nanoparticles can be seen as dark colour stably seated particles over TiO_2 nanotube (Figure 4.39c). The results indicated scattered presence of GO and Ag nanoparticle clusters over TiO_2 electrode. The presence of TiO_2, GO and Ag on the electrode surface can be confirmed with EDS as presented in Table 4.12.

Table 4.12 EDS analysis of Ag-GO/TiO_2, GO/TiO_2 and TiO_2 nanotube electrodes

Element	**C**	**O**	**Ti**	**Ag**	**Totals**
Weight (%)					
Ag-GO/TiO_2	4.49	26.30	66.94	2.27	100.00
GO/TiO_2	10.45	32.62	56.93	0.00	100.00
TiO_2	0.00	29.74	70.26	0.00	100.00

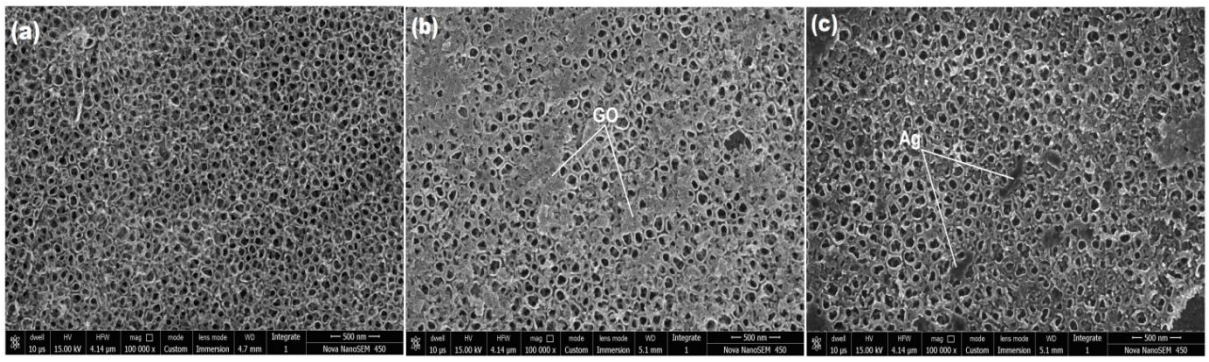

Fig. 4.39 FE-SEM image of (a) TiO_2, (b) GO/TiO_2 and (c) Ag-GO/TiO_2 nanotube electrodes

4.4.1.2 X-ray diffraction study

The XRD patterns of TiO_2, GO/TiO_2 and $Ag\text{-}GO/TiO_2$ nanotube electrodes have been shown in Figure 4.40. All synthesized nanotube electrode showed the TiO_2 anatase diffraction peaks at 25.6° (101), 38.6° (111), 48.2° (200), 63.2° (204), 72.1° (220) and 76.4° (215) (JCPDS No. 21-1272) planes which favoured better photocatalytic oxidation than rutile phase. In GO/TiO_2 and $Ag\text{-}GO/TiO_2$ nanotube electrodes a peak at 41.3° (002) of graphene oxide has been observed indicating the successful loading of GO. When compared to TiO_2 and GO/TiO_2 electrodes, the XRD pattern of $Ag\text{-}GO/TiO_2$ nanotube electrode exhibits two additional peaks at 44.3° and 77.4° corresponding to (200) and (311) reflections (JCPDS No. 65-2871) which can be indexed to cubic structure of Ag. Overlapping of few peaks has also been observed. The results confirmed that the Ag nanoparticles have been successfully anchored to the GO/TiO_2 nanotube electrode.

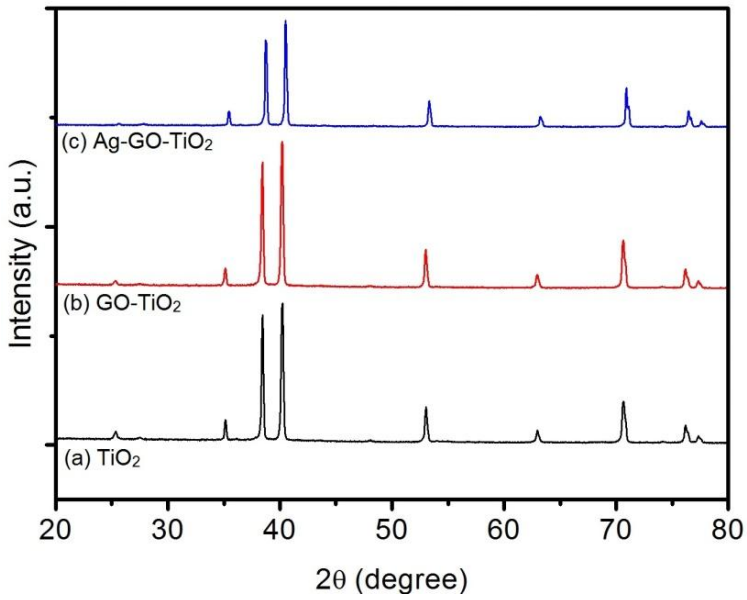

Fig. 4.40 XRD pattern of (a) TiO_2, (b) GO/TiO_2 and (c) $Ag\text{-}GO/TiO_2$ nanotube electrodes

4.4.1.3 UV-vis diffuse reflection spectroscopy

To examine the optical response of $Ag\text{-}GO/TiO_2$ nanotube electrodes UV-vis spectroscopy has been carried out and shown in Figure 4.41. The adsorption edge below 387 nm was due to the wide band gap (3.2 eV) of TiO_2. The adsorption edge near ~400 nm can be ascribed to the band to band transition of TiO_2 (anatase). When loading of GO and Ag has been performed, increase in the absorption between 600- 800 nm has been observed ascribed to the interaction of TiO_2 with GO and Ag.

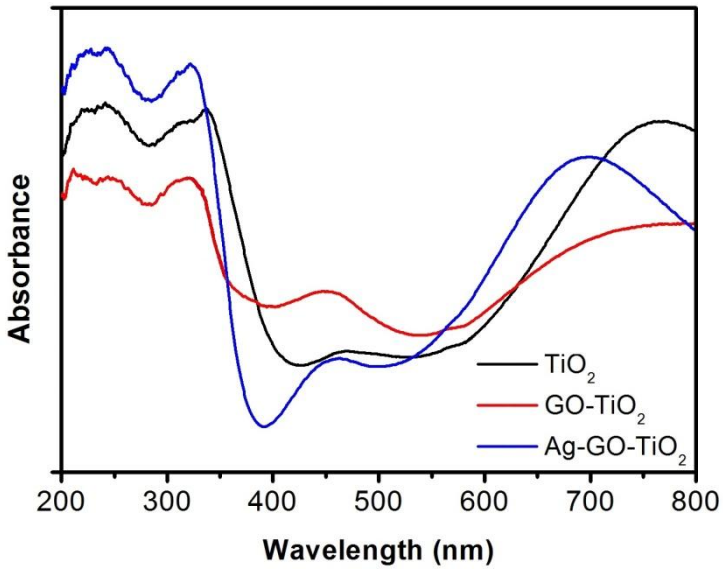

Fig. 4.41 UV-vis diffuse reflection spectrum of TiO_2, GO/TiO_2 and $Ag\text{-}GO/TiO_2$ nanotube electrodes

4.4.1.4 Raman measurements

Raman spectroscopy has been performed to further confirm the presence of Ag and GO in $Ag\text{-}GO/TiO_2$ nanotube electrodes as shown in Figure 4.42. TiO_2 nanotube electrodes exhibited four characteristic peaks at ~142 (Eg), ~396 (B_1g), 514 (A_1g) and 639 (Eg) cm^{-1}, ascribed to the existence of anatase TiO_2 in A1g + 2B1g + 3Eg modes (Cheng et al., 2014). GO/TiO_2 nanotube electrode displayed two additional peaks at ~1347 cm^{-1} (D) and ~1603 cm^{-1} (G), originated due to the presence of graphite. The D peak indicates the presence of some impurity atom or defects in the hexagonal layers of graphite, while the G peak has been related to the E_{2g} graphite mode accounted to sp^2 bonded C atoms in the two-dimensional hexagonal graphite layer (Zickler et al., 2006). After Ag loading, no distinct change in the number of peaks has been observed when compared to GO/TiO_2 nanotube electrodes. The possibility of Ag deposition on the surface of prepared GO/TiO_2 sheets increases, since Ag^+ ions might react with the oxygen containing functional groups of GO.

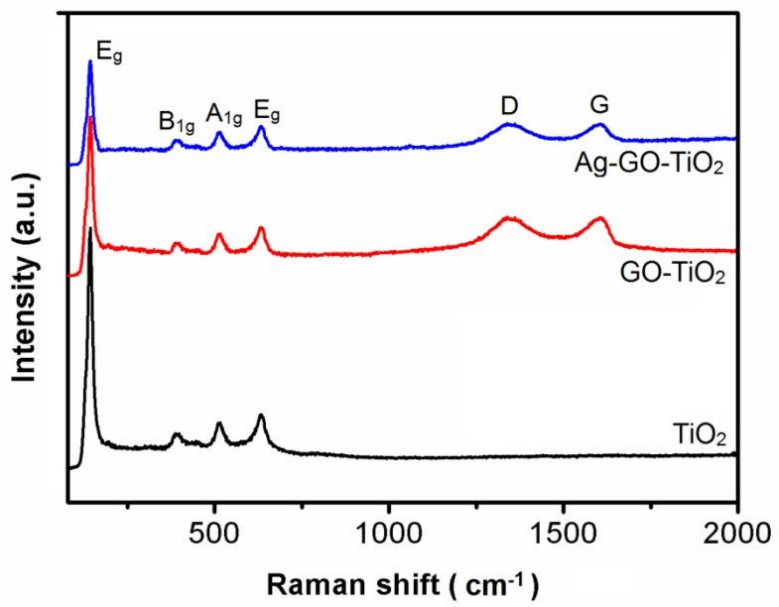

Fig. 4.42 Raman spectrum of TiO_2, GO/TiO_2 and $Ag\text{-}GO/TiO_2$ nanotube electrodes

4.4.1.5 FTIR spectrum

The FTIR spectra of TiO_2, GO/TiO_2 and $Ag\text{-}GO/TiO_2$ nanotube electrodes have been shown in Figure 4.43. The band identified near ~1216 and ~3308 cm^{-1} are superposition of O-H stretching of hydroxyl groups associated with graphene and TiO_2 (anatase) surfaces. The bands observed at 1635 cm^{-1} are designated to the C-C vibrations of GO. The peak appearing at ~591 cm^{-1} is assigned to Ti-O-Ti bond bending and stretching (McDevitt and Baun, 1964). GO exhibits a peak at ~1738 cm^{-1} for C=O groups. The XRD results clearly indicates highly crystallized TiO_2, thus, there is possibility of formation of C-O-Ti bonds in the nanotube electrode. The IR spectrum of Ag loaded GO/TiO_2 is similar to that of GO/TiO_2 nanotube electrode, suggesting that Ag loading does not change the structure of GO/TiO_2 electrode.

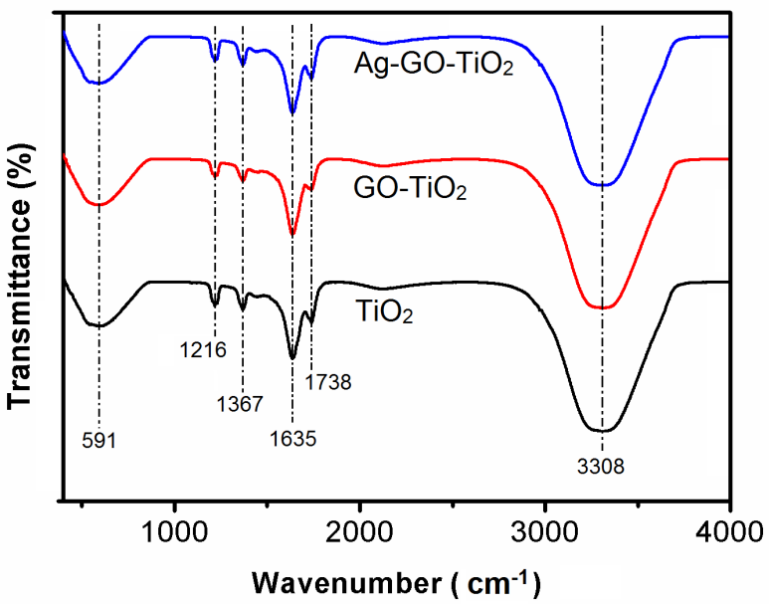

Fig. 4.43 FTIR spectrum of TiO_2, GO/TiO_2 and Ag-GO/TiO_2 nanotube electrodes

4.4.1.6 PL spectrum

The PL spectrum has been used to figure out the fate of e^--h^+ pairs in semiconductors in terms of their recombination rate (Gu et al., 2013). The intensity of spectrum gives a direct estimation of electron-hole recombination rate which means that lower intensity of PL spectrum indicates more trapping of excited electrons and their stable transfer through the interface. To study this effect of Ag loading on the electron-hole recombination rate, the PL spectra of TiO_2, GO/TiO_2 and Ag-GO/TiO_2 nanotube electrode has been determined as shown in Figure 4.44. Band at ~422 nm is due to the excitonic PL peaks trapped by surface states and defects (Liu et al., 2007). The emission signal at ~486 and ~545 nm may be attributed to the charge transfer from Ti^{3+} to oxygen vacancies present at the surface and presence of Ti site vacancies created in TiO_2, respectively (Liu et al., 2008). After the ternary composite Ag loaded GO/TiO_2 has been formed, the PL intensity reduced markedly and few of the above mentioned peaks disappeared due to the photo-excited electrons trapping by Ag and GO, which would subsequently suppress the recombination rate resulting in higher photoelectrocatalytic activity.

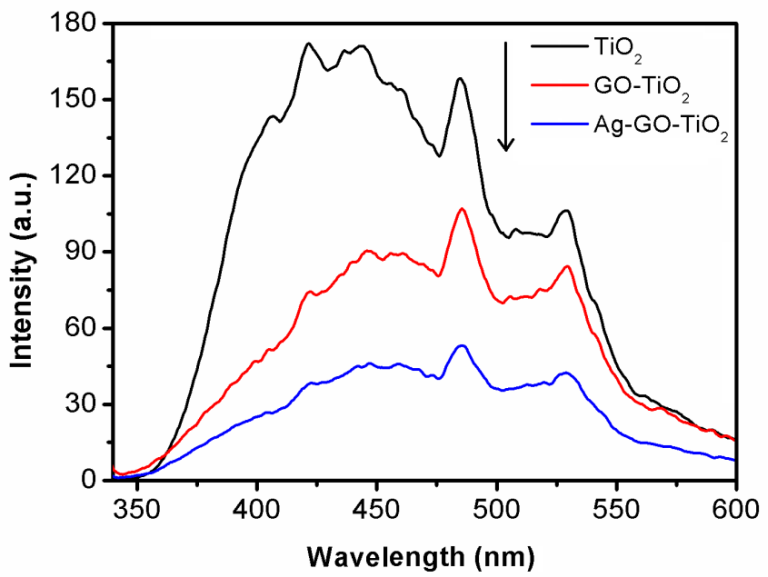

Fig. 4.44 PL spectrum of TiO_2, GO/TiO_2 and $Ag\text{-}GO/TiO_2$ nanotube electrodes

4.4.1.7 XPS analysis

Figure 4.45 represents XPS survey spectra of prepared electrodes, demonstrating the presence of Ag, Ti, C and O atoms. At intensities of 285, 368, 372, 457 and 530 eV, chemical binding energies have been represented as C 1s, Ag $3d_{5/2}$, Ag $3d_{3/2}$, Ti $2p_{3/2}$ and O 1s, respectively. The significant C 1s peak has been assigned to C-C (sp^2) graphite bond and peaks of Ti 2p and O 1s indicates the presence of titanium and O as crystal lattice oxygen confirming the formation of O-Ti-O (Yun et al., 2012). Hence, the XPS analysis also supports the successful synthesis of $Ag\text{-}GO/TiO_2$ nanotube electrodes.

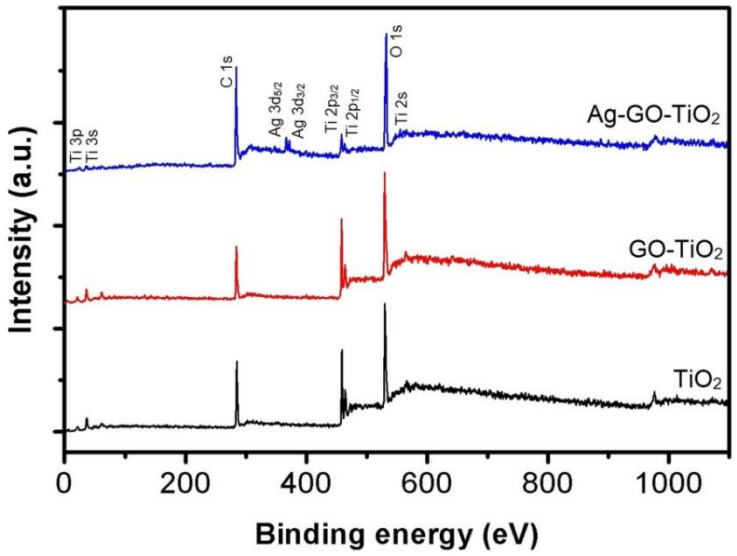

Fig. 4.45 XPS spectrum of TiO_2, GO/TiO_2 and $Ag\text{-}GO/TiO_2$ nanotube electrodes

4.4.2 PEC removal of PCP using Ag-GO/TiO_2 nanotube electrodes

Degradation study of PCP has been performed using photoelectrocatalytic treatment process under different reaction conditions and the optimized parameters were identified.

4.4.2.1 Effect of Ag loading

Generally, deposition of Ag nanoparticles on the surface of TiO_2 enhances photocatalytic activity (Sung-Suh et al., 2004) however; the activity highly depends on the amount of loaded metal. To assess this effect, Ag has been loaded onto GO/TiO_2 nanotube electrodes with varying proportion from 0.15 to 0.60 mM. As shown in Figure 4.46, photoeletrocatalytic degradation of PCP has been enhanced with the increasing concentration of Ag upto a certain extent and thereafter the degradation efficacy decreased. This effect might be due to the formation of Schottky barrier at metal and semiconductor interface indicating strong inhibition of electron and hole recombination as reported earlier for other noble metals (Subramanian et al., 2001; Bannat et al., 2009). Further, the excessive Ag loading reversed the increasing trend of PEC activity; might be due to the shielding of activation sites by superfluous Ag and perhaps also due to the reduced penetration of photons inside the porous layer.

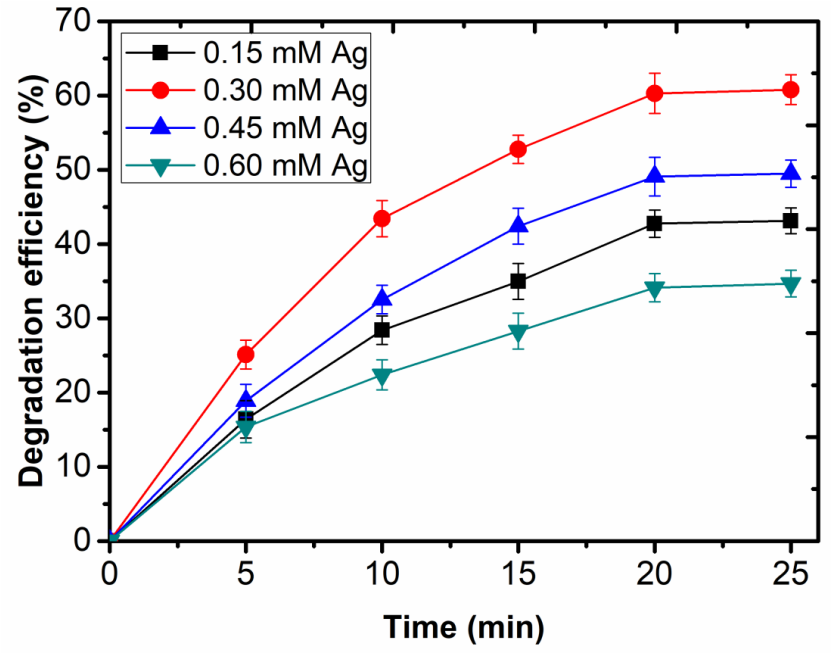

Fig. 4.46 Effect of Ag concentration on PEC degradation of PCP

4.4.2.2 Effect of pH

The influence of initial pH value on the PCP degradation rate has been shown in Figure 4.47. The degradation efficiency has been found to be highest at pH 3, and decreased both in neutral as well as alkaline conditions. The formation of active hydrogen is pH dependent and lower pH values can expedite their generation by electroreduction of the hydrogen ions (H^+), which further can efficaciously degrade PCP. In alkaline or neutral environment, enough active hydrogen could not be generated by H_2O electrolysis resulting in unsatisfactory PEC activity (Cui et al., 2008). PCP in the alkaline solution can dissociate to form phenoxide ion by donating a proton to H_2O or OH^- which can compete with $^{\bullet}OH$ active sites on anode surface resulting in a low degradation rate (Yu et al., 2014).

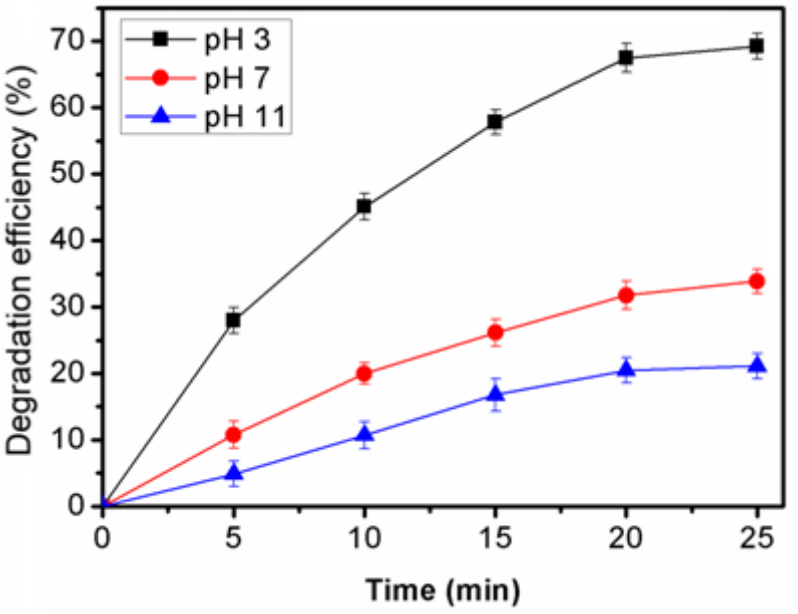

Fig. 4.47 Effect of pH on PEC degradation of PCP

4.4.2.3 Effect of conductivity

The effect of electrolyte concentration (Na_2SO_4) on the PCP degradation efficacy has been evaluated and shown in Figure 4.48. The conductivity of reaction mixture and PCP degradation rate increased with increasing concentration of supporting electrolyte. At lower sulphate concentration, smaller pollutant degradation has been observed because low electrolyte concentration leads to higher solution resistance (Hu et al., 2016). Increase in the electrolyte concentration beyond a limit did not favour increased removal rate, which may be attributed to the fact that, at higher electrolyte concentration oxygen evolution potential is decreased hence, side reactions for O_2 evolution are favoured instead of oxidation of organic

pollutant (Tiwana et al., 2011). The optimum electrolyte concentration was found to be 0.1 g L^{-1}.

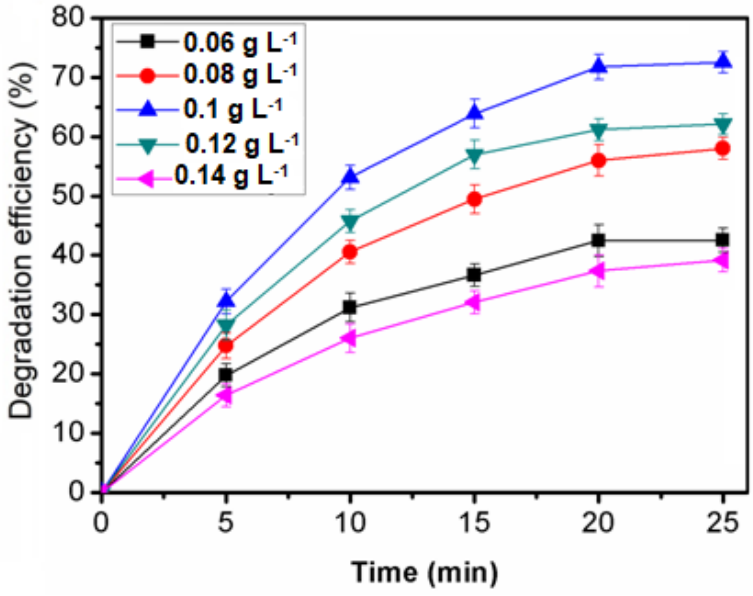

Fig. 4.48 Effect of conductivity on PEC degradation of PCP

4.4.2.4 Effect of applied current

The importance of choosing the befitting applied current for the PCP degradation has been scrutinized by the application of diverse electrode potential ranging from 0.01 to 0.04 A as shown in Figure 4.49. PCP degradation efficiency increased from 72 to 87%, when the applied current was increased from 0.01 to 0.02 A, but further increase in current did not raise the removal rate. In general, with increasing value of applied current, the separation of electron-hole pairs increased, thus, resulting in higher degradation efficiency. However, after reaching an optimum value, further increase in the current value would not achieve increase in degradation rate. The probable reason might be the separation of photogenerated electrons and holes reached saturation (Zhang et al., 2012).

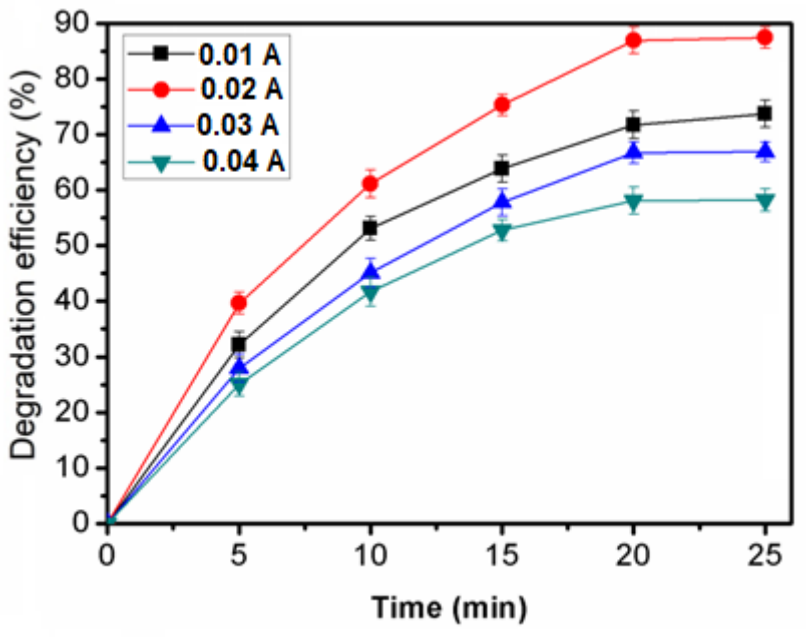

Fig. 4.49 Effect of applied current on PEC degradation of PCP

4.4.3 Comparison of PC, EC and PEC processes

The degradation of PCP has been assessed using TiO_2, GO/TiO_2 and $Ag\text{-}GO/TiO_2$ nanotube photoelectrodes by simultaneous PC, EC and PEC processes. It can be observed in Figure 4.50 that greater PCP removal has been obtained with $Ag\text{-}GO/TiO_2$ photoelectrode in all the three treatment processes after 25 min of irradiation, when compared to TiO_2 and GO/TiO_2 nanotube photoelectrodes. The pattern of TOC reduction has also been observed to be $Ag\text{-}GO/TiO_2$> GO/TiO_2> TiO_2 with corresponding TOC reduction of 78, 65, 54%, respectively. Moreover, chloride concentration in aqueous phase has been determined as an indication of fragmentation of PCP into simpler low molecular weight compounds. Chloride concentration has been observed to be 53, 38 and 32 mg L^{-1} Cl^- after 25 min of photoelectrocatalytic process with $Ag\text{-}GO/TiO_2$, GO/TiO_2 and TiO_2 photoelectrodes, respectively. The improved performance of PEC process has been attributed to the synergistic effect of PC and EC processes.

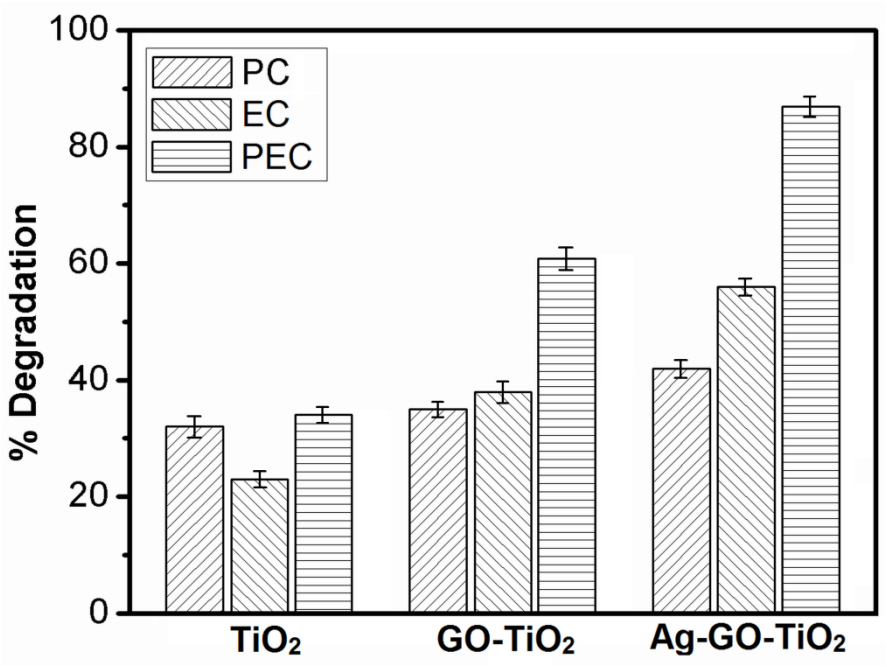

Fig. 4.50 PC, EC and PEC performance of synthesized electrodes

4.4.4 Hydroxyl radical generation

To study the contribution of $^{\bullet}OH$ in the degradation system, the fluorescent peak of 2-hydroxyterephthalic acid at 425 nm has been monitored. It is a well known fact that the $^{\bullet}OH$ produced as major species are responsible for the oxidative degradation of pollutants (Li et al., 2012). As can be seen in Figure 4.51, the PL intensity at around 425 nm of Ag loaded GO/TiO_2 electrode was much higher than GO/TiO_2 and TiO_2 nanotube electrodes indicating the higher contribution of Ag-GO/TiO_2 anode (152 mM) in $^{\bullet}OH$ production. It can also be established from the results that the exposure to UV irradiation increases the generation of hydroxyl radicals, which further improve the degradation efficacy.

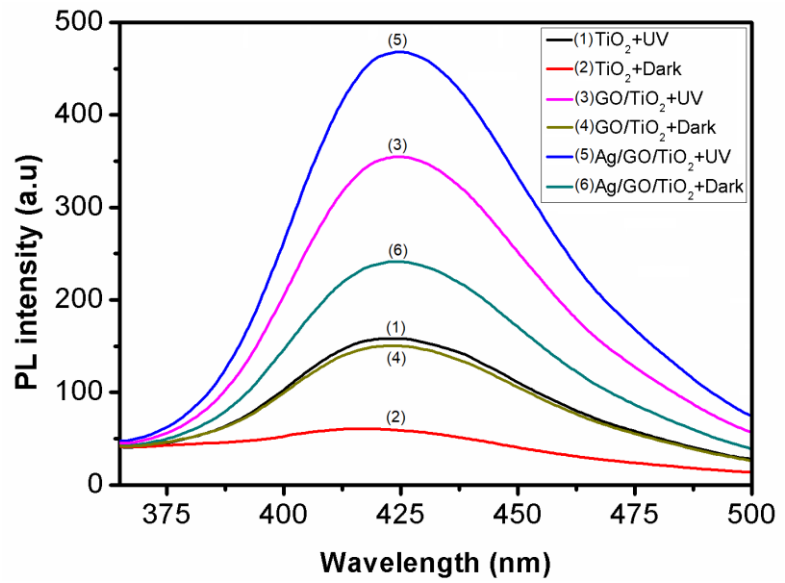

Fig. 4.51 Fluorescence spectra of hydroxyl radical production by synthesized electrodes

4.4.5 Effect of additives

In order to assess the role of active species like $^{\bullet}OH$ (hydroxyl radical), $^{\bullet}O_2^-$ (superoxide ions) and h^+ (holes), a series of scavengers have been used in the reaction system. Figure 4.52 showed the PEC activity of Ag loaded GO/TiO_2 photoelectrode towards PCP degradation under the influence of different scavengers. In this study, iso-propyl alcohol (IPA) has been added as a $^{\bullet}OH$ scavenger (Li et al., 2009), disodium ethylenediaminetetraacetate (EDTA) has been used as h^+ scavenger (Cui et al., 2014) and $_L$-ascorbic acid as scavenger of $^{\bullet}O_2^-$ (Xu et al., 2016). In the absence of scavengers, PEC degradation rate of PCP has been observed to be 87% in 25 min irradiation. When IPA was added to reaction system as a hydroxyl radical scavenger, the degradation efficiency of PCP was significantly suppressed to 43.7%. Furthermore, when EDTA and L-ascorbic acid were added, the degradation rate was moderately decreased to 49 and 56%, respectively. Through the observation, it can be concluded that each reactive species performed significant role in regulating the degradation efficiency of PEC treatment, and the involvement of $^{\bullet}OH$ was primarily responsible for the PCP removal.

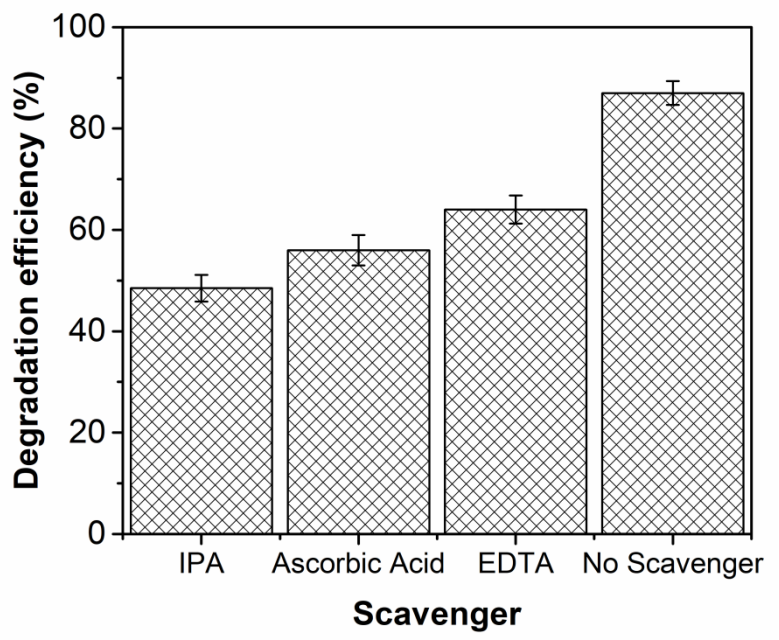

Fig. 4.52 Effect of different scavengers on PCP degradation

4.4.6 Reusability of synthesized electrode

For practical applications, reusability of the nanotube electrode is of vital concern. The reusability of Ag-GO/TiO_2 photoelectrode has been evaluated by repeating the use of synthesized electrode in the PEC degradation of PCP under optimized conditions (0.30 mM Ag, pH 3, 0.02 A applied current, 0.1 g L^{-1} Na_2SO_4 and 250 mL PCP) for 15 cycles. After each cycle, the electrode has been washed by deionized water and dried before using in the next experiment with fresh PCP (20 mg L^{-1}) solution. The PEC activity of synthesized electrodes decreased marginally from 87 to 83.6% after six repeated cycles and furthers decreased to 67% by the end of fifteenth cycle as shown in Figure 4.53, highlighting the reusability potential of Ag-GO/TiO_2 nanotube photoelectrode. The slight loss in the PEC activity after repeated usage may be ascribed to the reduction of active sites due to the adsorption of contaminants. Moreover, synthesized Ag-GO/TiO_2 nanotube electrode has been observed to be stable after repeated usage in PEC degradation process since no corrosion effects were visible even after 15 cycles.

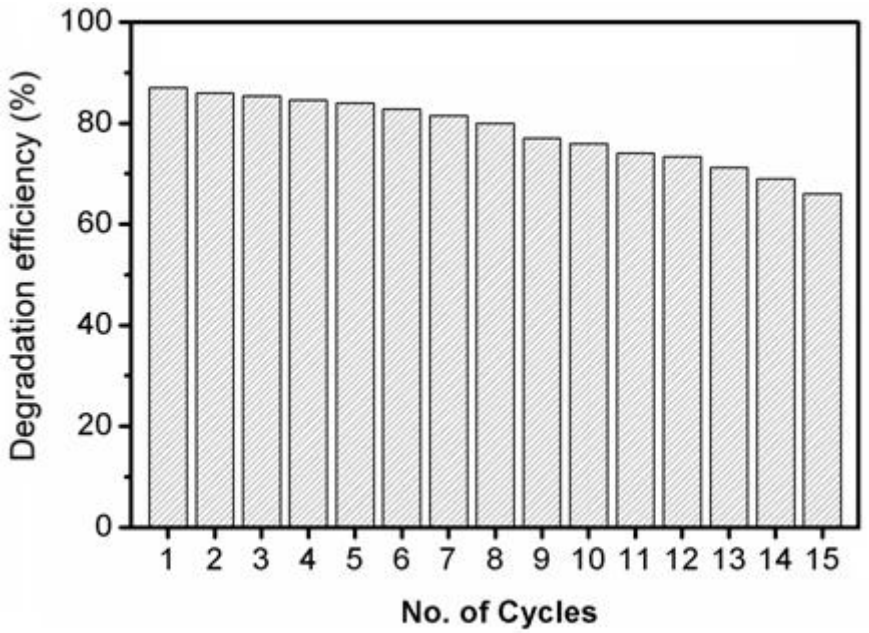

Fig. 4.53 Reusability study of Ag-GO/TiO_2 nanotube electrode

4.4.7 Identification of Intermediates formed during PCP degradation

Intermediates formed during the PEC degradation process has been identified by LC/MS analysis. Figure 4.54 shows the TIC chromatograms and Fig. 4.55 depicts the ESI mass spectra recorded with positive mode for PEC treated solution of 20 mg L^{-1} PCP (where about degradation of PCP occurs). Ten major degradation by-products have been identified, and their molecular formula as well as molecular structure is listed in Table 4.13. Identification of primary degradation intermediates allowed the prediction of tentative interlinking pathway for PCP degradation. The pathway initiates with the oxidative dechlorination of PCP (*m/z* 263, C_6HCl_5O) at para position and the mass pattern has been observed to be matching with tetrachlorohydroquinone (A) having *m/z* 245 and empirical formula $C_6H_2Cl_4O_2$. Formation of (A) has been reported previously in PC degradation of PCP (Mill et al., 1993; Silva et al., 2012). As the degradation reaction goes on, the isomers of dichlorohydroquinone (*m/z* 177) (B), (C) and (D) have been formed, which on further degradation furnished H (*m/z* 94). 2,6-dichlorohydroquinone (D) formed by the reductive dechlorination at ortho position, while 2,5-dichlorohydroquinone (B) came from substitution of chlorine by hydrogen atom at ortho and meta positions. The presence of hydroquinones can be observed when $^{\bullet}OH$ exists in the PCP reaction solution (Jardim et al., 1997) and the presence of reactive species like $^{\bullet}OH$ is already established. The free radical mediated redox reactions of (A) leads to the formation of (G, *m/z* 165, $C_4Cl_2O_3$) and (E, *m/z* 149, $C_4H_3ClO_4$).

Chlorohydroquinone (F, *m/z* 144, $C_6H_5ClO_2$) was by the reductive dechlorination of (C). C_6H_6O (H, m/z 94) was formed by further elimination of Cl from the parent compound. Furthermore, the degradation reaction of (F) leads to the formation of (I) (*m/z* 174, $C_6H_3ClO_4^{\bullet-}$) and (J) (*m/z* 83, $C_5H_7O^{\bullet}$). The identified intermediates clearly demonstrate the breakdown of PCP, which is otherwise considered as recalcitrant contaminant.

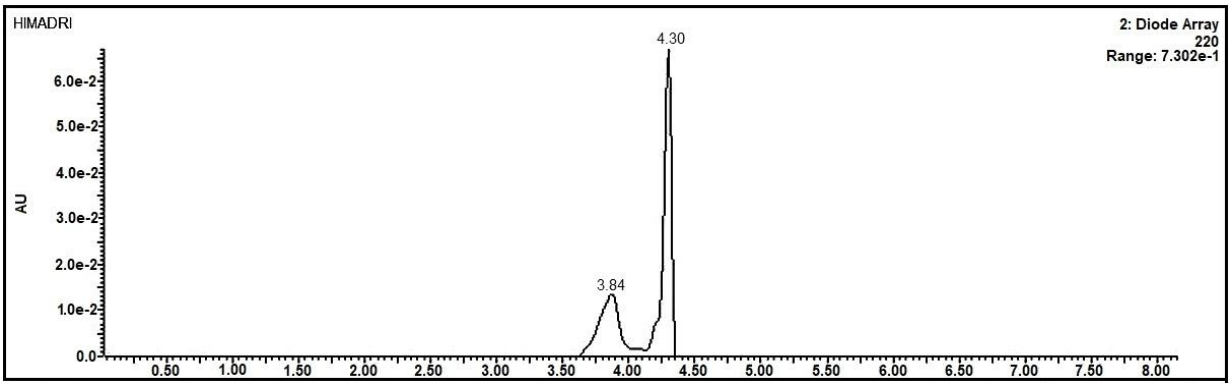

Fig. 4.54 Total ion current chromatogram recorded for aqueous solution of PCP treated with PEC

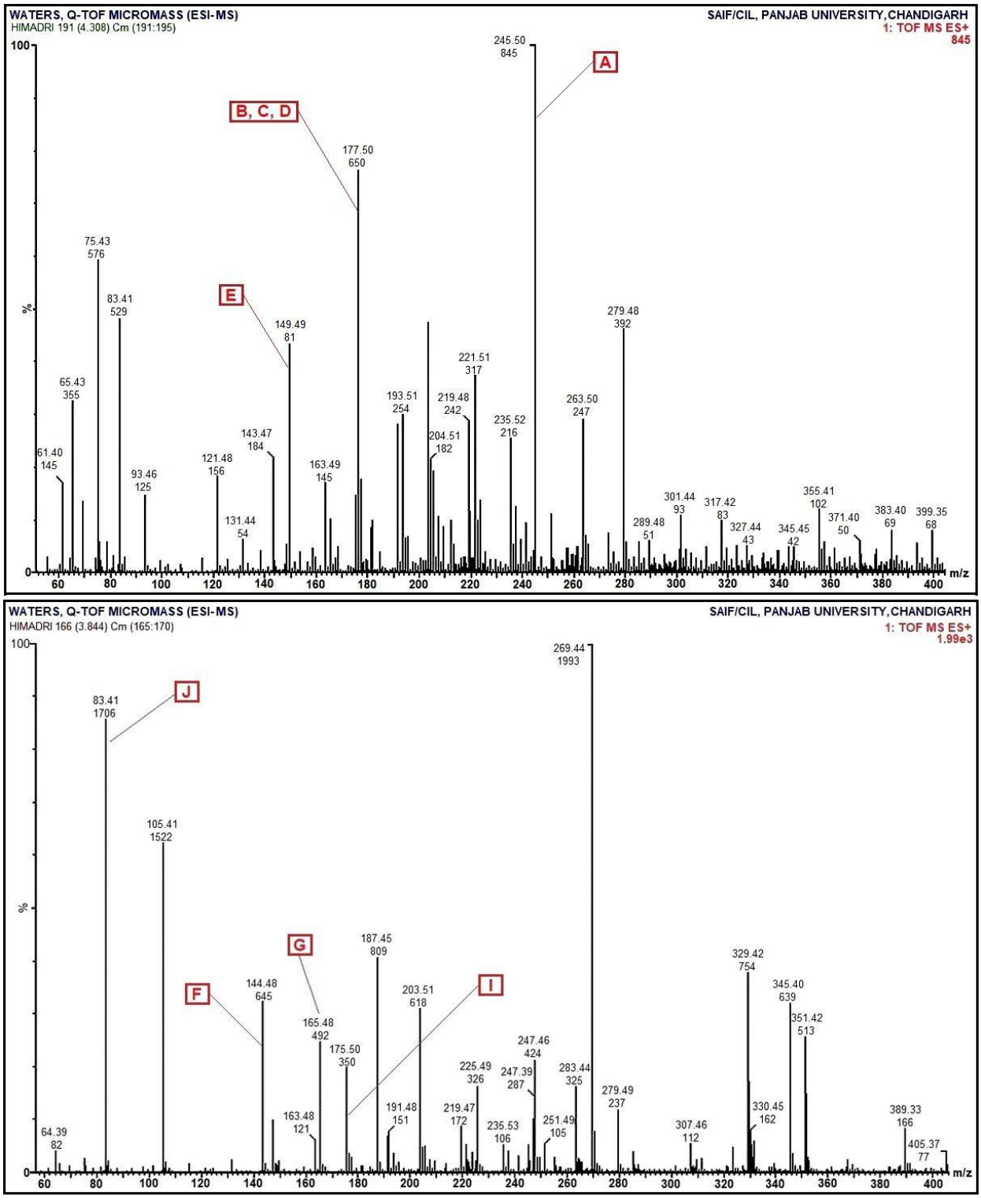

Fig. 4.55 ESI mass spectra for treatment of PCP using PEC process

Table 4.13 Identified intermediate compounds for PCP photoelectrocatalytic degradation under optimized conditions for 25 min

Compound	Main Fragment (m/z)	Molecular formula	Molecular structure
PCP	263	C_6HCl_5O	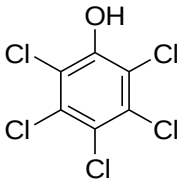
A	245	$C_6H_2Cl_4O_2$	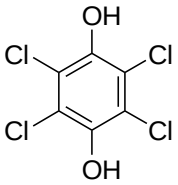
B	177	$C_6H_4Cl_2O_2$	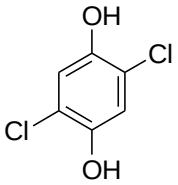
C	177	$C_6H_4Cl_2O_2$	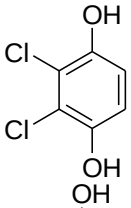
D	177	$C_6H_4Cl_2O_2$	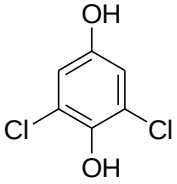
E	149	$C_4H_3ClO_4$	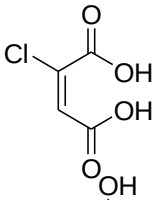
F	144	$C_6H_5ClO_2$	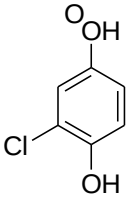
G	165	$C_4Cl_2O_3$	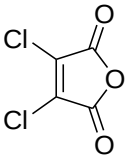

H	94	C_6H_6O	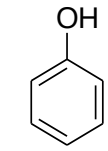
I	174	$C_6H_3ClO_4^{\bullet-}$	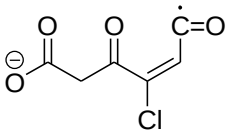
J	83	$C_5H_7O^{\bullet}$	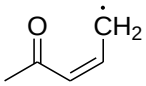

On the basis of detailed study as described above, photoelectrocatalytic degradation of PCP using Ag loaded GO/TiO_2 nanotube electrode can be summarized as shown in Figure 4.56.

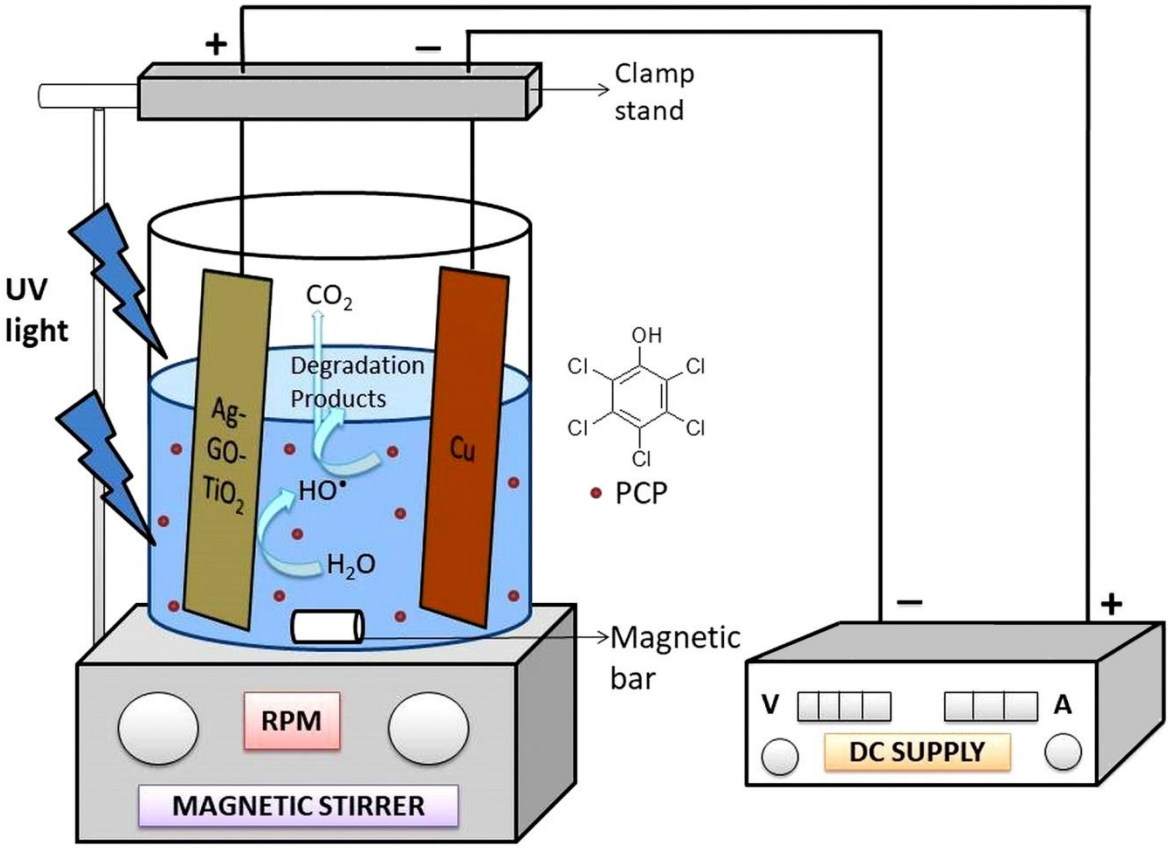

Fig. 4.56 PEC degradation of PCP using Ag-GO/TiO_2 nanotube electrode

The Ag-GO/TiO_2 nanotube electrodes exhibited significant degradation efficiency against the degradation of PCP within 25 min treatment time under UV irradiations when compared to 150 and 93 min using TiO_2 and GO/TiO_2 nanotube electrode, respectively. The probable reason might be that the yield of $^{\bullet}OH$ radical concentration was higher in the case of Ag-GO/TiO_2 nanotube electrodes (152 mM), when compared to GO/TiO_2 (135 mM) and TiO_2 (32.46 mM) nanotube electrodes. A comparative assessment of TiO_2, GO/TiO_2 and Ag-GO/TiO_2 electodes have been shown in Table 4.14.

Table 4.14 Comparative assessment of synthesized electrodes in terms of PCP degradation and $^{\bullet}OH$ radical generation

Type of electrode	**Degradation efficiency (%)**	**Average treatment time (min)**	**Light source**	**$^{\bullet}OH$ radical concentration (mM)**
TiO_2	58	150	UV	32.46
GO/TiO_2	91	93	UV	135
Ag-GO/TiO_2	87	25	UV	152

4.5 Photoelectrocatalytic degradation of simulated effluent using synthesized electrodes

The simulated effluent has been prepared by diluting the real effluent collected from the bleaching section of P & P mill located in Punjab province of India as described in section 3. The initial characterization of simulated effluent has been carried out and shown in Table 4.15. The pH and conductivity of prepared simulated effluent has not been altered and the treatment experiments were performed for 6h in case of all the electrodes under the influence of solar irradiations. External current has been selected as 0.05 A, on the basis of experiments conducted on different current values as shown in Figure 4.57. The COD reduction was observed to be highest when 0.05 A current was employed, hence for further experiments the current was kept at 0.05 A.

Table 4.15 Characterization of simulated effluent before treatment

Parameters	COD	TOC	Chloride	Sulphate	Nitrate	Nitrite	Phosphate	Total solid
Concentration (mg L^{-1})	925 ± 126	212.5 ± 91	640 ± 127	583 ± 90	2.157 ± 0.4	1.166 ± 0.2	0.816 ± 0.06	2750 ± 138

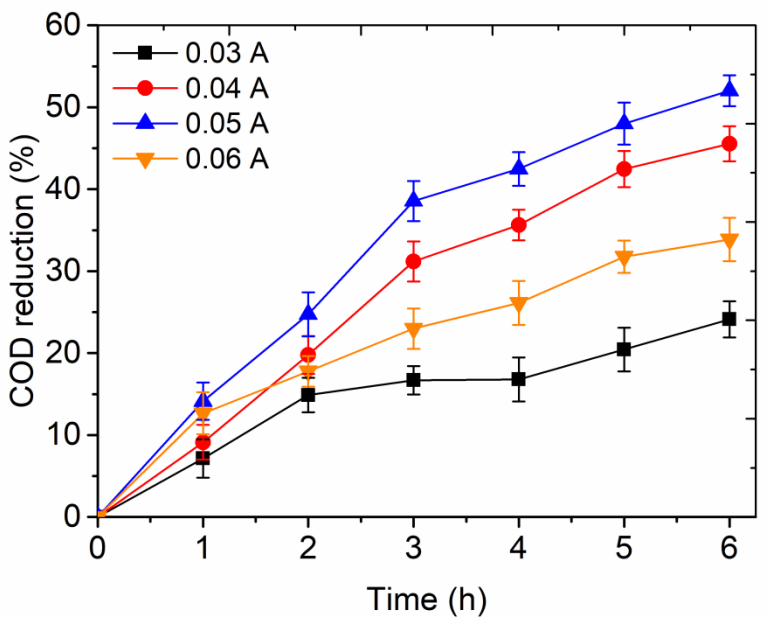

Fig. 4.57 Effect of applied current on the PEC degradation of simulated effluent

The experiments were conducted for the PEC treatment of simulated effluent using all the synthesized electrodes separately. After the treatment time of 6 h, the simulated effluent has been analyzed by measuring its COD, TOC, chloride, sulphate, nitrate, nitrite, phosphate and total solids concentration and the finding are presented in Table 4.16.

4.5.1 COD reduction

The P & P mill wastewater contains a significant amount of contaminants characterized by their high COD values mostly contributed by lignin and polysaccharide residues (Costa et al., 2017). The COD of effluent is an important factor which determines the suitability of effluent to be discharged in the natural environments. The high COD value indicates the presence of wide range of organic chemicals and low biodegradability of effluent. The reduction in COD values of simulated effluent after 6h treatment time using different type of electrodes has been evaluated. The COD of raw simulated effluent has been measured to be 925 mg L^{-1}. After 6h treatment time, TiO_2, GO/TiO_2, Cs/TiO_2, Au/TiO_2 and $Ag\text{-}GO/TiO_2$ electrodes lead to 51.7, 58.9, 71.6, 54, and 66 % COD reduction with COD value of 446, 380, 262, 423 and 310 mg L^{-1} at an external current of 0.05 A as shown in Table 4.16. The appreciable decrease in the COD value of simulated effluent after PEC treatment indicates the reduction in the concentration of organic matter.

4.5.2 TOC reduction

It has been reported that P & P mill effluent has been characterized by its high TOC values and the constituent, lignin, contributes towards 30-45 % of total organics in the wastewater (Alekhina et al., 2015). The TOC before and after the PEC treatment using synthesized electrodes has been measured to estimate the overall organic carbon removal. TOC value of raw simulated effluent has been observed to be 212.5 mg L^{-1}. After 6h treatment time, TiO_2, GO/TiO_2, Cs/TiO_2, Au/TiO_2 and $Ag\text{-}GO/TiO_2$ electrodes lead to 39, 46, 58, 40, and 53 % TOC reduction at an external current of 0.05 A as shown in Table 4.16. The obtained results signify the effective mineralization of simulated effluent after the PEC treatment as significant reduction in the TOC value has been observed.

4.5.3 Chloride ion estimation

It has been earlier reported that chlorinated compounds present in P & P mill effluent reacts with hydroxyl radicals and gets converted into aliphatic chlorinated compounds and afterwards to CO_2 and chloride ions (Tang and Huang, 1996). Hence, the partial mineralization of organic matter present in the simulated effluent has been assessed by measuring the concentration of chloride ions formed in the reaction mixture. The chloride concentration of raw simulated effluent has been calculated to be 640 mg L^{-1}. After 6h treatment time using TiO_2, GO/TiO_2, Cs/TiO_2, Au/TiO_2 and $Ag\text{-}GO/TiO_2$ electrodes, the concentration of chloride ions have been observed to be 767, 793, 998, 782 and 864 mg L^{-1} at an external current of 0.05 A as shown in Table 4.16. The increasing concentration values of chloride ions using synthesized electrodes after the PEC treatment indicates the breakdown of parent chlorinated compounds into simpler organic products. However, due to high chloride content secondary treatment for the simulated effluent is recommended for the complete removal of chlorinated ions.

4.5.4 Sulphate estimation

Sulphate has been one of the major anion present in the effluent contributed by Kraft process involved in paper production (Rodrigues et al., 2008). Special attention is required to P & P mill effluent as it contains high sulphur content which has potential to convert in very toxic hydrogen sulphide (H_2S) (Lettinga et al., 1991). However, some researchers suggested that high concentration of Ca^{2+} and SO_4^{2-} have been more important factors related to environment concern than the toxicity associated with H_2S. The concentration of sulphate ion before and after the treatment of simulated effluent has been determined. The sulphate

concentration of raw simulated effluent has been calculated to be 583 mg L^{-1}. After 6h treatment time using TiO_2, GO/TiO_2, Cs/TiO_2, Au/TiO_2 and $Ag\text{-}GO/TiO_2$ electrodes, the concentration of sulphate ions was observed to be 144, 187, 239, 161 and 200 mg L^{-1} at an external current of 0.05 A as shown in Table 4.16. The removal of sulphate ions from the effluent after PEC treatment suggested the degradation of sulphated organic molecules and mineralization of simulated effluent.

4.5.5 Nitrate estimation

The presence of nitrate contamination in wastewater is of serious concern and requires special remediation measures as it can cause several health hazards if comes in contact with drinking water as such. The widely exploited technology for nitrate removal is biological treatment, whereas it also faces limitation of requirement of secondary treatment technique for the removal of bacterial biomass from the treated water (Ayyasamy et al., 2007). The nitrate ion concentration of simulated effluent before and after the PEC treatment using various electrodes has been determined. The nitrate concentration of raw simulated effluent has been calculated to be 2.157 mg L^{-1}. After 6h treatment time using TiO_2, GO/TiO_2, Cs/TiO_2, Au/TiO_2 and $Ag\text{-}GO/TiO_2$ electrodes, the concentration of nitrate ions was observed to be 1.624, 0.806, 0.961, 0.822 and 0.784 mg L^{-1} at an external current of 0.05 A as shown in Table 4.16. The reduced values of nitrate concentration after the treatment show the successful reduction of nitrate to ammonia and breakdown of complex molecules into simpler compounds.

4.5.6 Nitrite estimation

Nitrite ion causes inhibitory effects to various bioprocesses occurring at wastewater treatment plants hence, nitrite ions needs prior removal. The free nitrous acid, protonated form of nitrite, also causes inhibitions in the functioning of WWTPs. It has been reported that high concentrations of nitrite have severe inhibitory effects on various microorganisms and could lead to reconfiguration of the structure of microbial community (Zhou et al., 2011). The nitrite ion concentration of simulated effluent before and after the PEC treatment using various electrodes has been determined. The nitrite concentration of raw simulated effluent has been calculated to be 1.166 mg L^{-1}. After 6h treatment time using TiO_2, GO/TiO_2, Cs/TiO_2, Au/TiO_2 and $Ag\text{-}GO/TiO_2$ electrodes, the concentration of nitrate ions have been observed to be 0.473, 0.391, 0.262, 0.368 and 0.24 mg L^{-1} at an external current of 0.05 A as shown in Table 4.16. The results suggest that, there is considerable possibility of conversion

of nitrite into molecular nitrogen as the decreasing pattern of nitrite concentration was observed in all the experiments.

4.5.7 Phosphate estimation

The removal of biological nutrients like phosphorus from the wastewater is a critical step as these excessive nutrients interfere in the natural environments as well as in the processes of treatment plants. High concentrations of phosphate could suppress nitrite reduction and can cause its accumulation (Zhou et al., 2011). Also, presence of phosphorus in large quantities poses the risk of overgrowth of microorganisms and is the main cause of eutrophication phenomenon that adversely influences water reservoirs (De-Bashan and Bashan, 2004). Hence, it is desirable to remove phosphorus from wastewater by utilizing treatment facilities before its returning to the environment. The phosphate concentration of simulated effluent before and after the PEC treatment using various electrodes has been determined. The phosphate concentration of raw simulated effluent has been calculated to be 0.816 mg L^{-1}. After 6h treatment time using TiO_2, GO/TiO_2, Cs/TiO_2, Au/TiO_2 and $Ag\text{-}GO/TiO_2$ electrodes, the phosphate concentration have been observed to be 0.237, 0.196, 0.129, 0.163 and 0.142 mg L^{-1} at an external current of 0.05 A as shown in Table 4.16. The outcomes illustrate the removal of phosphate after PEC treatment.

4.5.8 Estimation of total solids (TS)

The total solids present in P & P mill effluent are mainly comprised of bark/raw material particles, fibre debris, filler, coating materials, nitrate, phosphate, sulphate, lignin, polysaccharides etc. (Pokhrel and Viraraghavan et al., 2004). The P & P mill effluent faces a unique challenge of solid/liquid separation due to the presence of high quantities of fibres. The high load of total solids should be reduced or removed, as it can hinder the functioning of WWTPs resulting in the inefficient treatment efficiency of the treatment plant. The TS concentration of simulated effluent before and after the PEC treatment using various electrodes has been determined. The concentration of TS of raw simulated effluent was observed to be 2750 mg L^{-1}. After 6h treatment time using TiO_2, GO/TiO_2, Cs/TiO_2, Au/TiO_2 and $Ag\text{-}GO/TiO_2$ electrodes, the TS concentration was observed to be 997, 967, 970, 944 and 814 mg L^{-1} at an external current of 0.05 A as shown in Table 4.16. The significantly decreasing trend in the TS concentration depicts the efficiency of process and indicates high organic contents of solids particle present in wastewater.

The PEC treatment of simulated P & P mill effluent using various synthesized electrodes has been summarized as in Table 4.16.

Table 4.16 PEC treatment of simulated effluent using various synthesized electrodes

Parameters	Before Treatment	TiO_2 electrodes	GO/TiO_2 electrodes	Cs/TiO_2 electrodes	Au/TiO_2 electrodes	$Ag\text{-}GO/TiO_2$ electrodes
COD ($mg\ L^{-1}$)	925 ± 125	446 ± 95	380 ± 80	262 ± 95	423 ± 105	310 ± 75
TOC ($mg\ L^{-1}$)	212.5 ± 91	130 ± 82	113 ± 74	88 ± 59	126 ± 76	98 ± 63
Chloride ($mg\ L^{-1}$)	640 ± 127	767 ± 148	793 ± 150	998 ± 198	782 ± 155	864 ± 170
Sulphate ($mg\ L^{-1}$)	583 ± 90	144 ± 67	187 ± 85	239 ± 89	161 ± 52	200 ± 63
Nitrate ($mg\ L^{-1}$)	2.157 ± 0.4	1.624 ± 0.2	0.806 ± 0.08	0.961 ± 0.1	0.822 ± 0.07	0.784 ± 0.5
Nitrite ($mg\ L^{-1}$)	1.166 ± 0.2	0.473 ± 0.06	0.391 ± 0.04	0.262 ± 0.03	0.368 ± 0.04	0.247 ± 0.01
Phosphate ($mg\ L^{-1}$)	0.816 ± 0.06	0.237 ± 0.01	0.196 ± 0.02	0.129 ± 0.01	0.163 ± 0.01	0.142 ± 0.01
Total solid ($mg\ L^{-1}$)	2750 ± 138	997 ± 120	967 ± 165	970 ± 150	944 ± 172	814 ± 138

The performance of all the electrodes for the PEC treatment of P & P mill simulated effluent has been reported in Table 4.16. Significant reduction in the COD and TOC values have been noticed when the synthesized electrodes have been used. Doping of TiO_2 electrode exhibited improvement in the PEC performance. Co-doping of TiO_2 electrode with AG and GO has been observed to be most effective for the PEC treatment of recalcitrant compounds.

Chapter 5

Conclusions

The present study has been focused on the photoelectrocatalytic degradation of biorecalcitrant pollutants commonly found in P & P mill effluents such as pentachlorophenol and 4-chloroguaiacol and simulated effluent using laboratory synthesized electrodes under the influence of UV/solar irradiations. The PEC degradation of target compounds and simulated effluent has been performed using laboratory synthesized photoelectrodes. The titania based electrodes have been fabricated by doping with various materials such as Cs, Au, GO, Ag-GO using anodization technique and the synthesized electrodes were characterized by various physicochemical methods. Cs/TiO_2 and Au/TiO_2 nanotube electrodes were used for the PEC degradation of 4-CG, while, GO/TiO_2 and $Ag\text{-}GO/TiO_2$ nanotube electrodes were utilized for the PEC degradation of PCP. Simulated effluent was subjected to the PEC treatment by using all types of synthesized electrodes. Based on the experimental investigations, the following conclusions have been drawn from the present study:

- Cs/TiO_2NTs electrode exhibited 92% PEC degradation efficiency of 4-CG at optimized condition: 2.5 mM Cs, 160 mg L^{-1}, Na_2SO_4, 0.03 A current at pH 3 under solar irradiations and the TOC removal efficiency reached 70.2, 42.3 and 12% for PEC, PC and EC process when Cs/TiO_2NTs electrode was employed. The significant activity under solr irradiations were due to the significant influence of Cs on coordination framework of TiO_2 crystalline structure, resulting in the red shifts of the absorption band.

- In comparison to Cs/TiO_2 electrode, $Au\text{-}TiO_2$ nanotube electrodes showed 84% 4-CG degradation efficiency under optimized conditions: 0.15 mM Au, 0.08 g L^{-1} Na_2SO_4, 0.03 A current and pH 3 under UV irradiations and yielded 105 mM of $^{\bullet}OH$ radical however, merely 30.84 mM $^{\bullet}OH$ radical were obtaines with bare TiO_2 nanotube electrode.

- As compared to TiO_2 and Au/TiO_2, Cs/TiO_2 nanotube electrodes exhibited higher 4-CG degradation efficiency (92%) under solar irradiations due the yield of $^{\bullet}OH$ radical was higher in the case of Cs/TiO_2 (118.7 mM), when compared to Au/TiO_2 (105 mM) and TiO_2 (30.84 mM) nanotube electrodes.

- The degradation intermediates formed during 4-CG degradation by using Cs/TiO_2 and Au/TiO_2 NTs electrodes have been identified through GC-MS analysis and tentative degradation pathway have been proposed.

- GO/TiO_2 electrode was used for the PEC based degradation of PCP and BBD was usd for the optimization of process parameters. The ANOVA results suggested that applied current, degradation time and GO concentration were the significant variables and interaction between applied current and degradation time was significant interaction with P-value <0.0001.

- The optimized conditions were found to be: applied current 20.68 mA; pH 3.14; GO concentration 15 mg L^{-1} and treatment time 93 min, with PCP degradation and mineralization efficiency of 91 and 85%, respectively.

- Further, $Ag\text{-}GO/TiO_2$ nanotube electrode was used and under optimized conditions (0.30 mM Ag, pH 3, 0.02 A applied current, 0.1 g L^{-1} Na_2SO_4), 87% PCP removal and 152 mM $^{\bullet}OH$ production was observed.

- In order to access the recyclability, $Ag\text{-}GO/TiO_2$ electrode was reused and PEC activity decreased marginally from 87 to 83.6% after six repeated cycles and furthers decreased to 67% by the end of fifteenth cycle.

- The $^{\bullet}OH$ radical concentration was higher in the case of $Ag\text{-}GO/TiO_2$ nanotube electrodes (152 mM), when compared to GO/TiO_2 (135 mM) and TiO_2 (32.46 mM) nanotube electrodes.

- The satisfactory PEC treatment of simulated effluent was observed with all the different type of synthesized electrodes and significant reduction in the COD and TOC was observed.

- Doping of TiO_2 electrode resulted in the improvement in the PEC performance and generation of $^{\bullet}OH$ radical and co-doping of TiO_2 electrode was observed to be most effective for the PEC treatment of recalcitrant compounds and simulated effluent.

Future Recommendations:

The laboratory synthesized electrodes have exhibited their significant potential in the photoelectrocatalytic degradation of biorecalcitrant compounds and simulated effluent of P & P industry. The doping of TiO_2 nanotube electrode resulted in increased degradation efficiency towards the stable model compounds and elevated generation of $^{\bullet}OH$ radicals.

- Further research is needed in synthesizing titania based electrodes doped with different type of metals and non-metals as there are numerous doping materials which can be expored.
- The applicability of synthesized electrodes can be analyzed for the PEC treatment of variety of stable and recalcitrant pollutants commonly found in environment.
- Also, the activity of synthesized electrodes in this study can be assessed for the treatment of real P & P mill and other industrial effluents.
- In order to access the feasibiity of this process, efforts are neede in the estimation of recurring and capital cost involved in PEC treatment.
- For making this process viable, research is needed for increasing the reusability potential of synthesized electrodes.

References

1. Affam, A.C., Chaudhuri, M. and Kutty, S.R.M., 2018. Comparison of Five Advanced Oxidation Processes for Degradation of Pesticide in Aqueous Solution. Bulletin of Chemical Reaction Engineering & Catalysis, 13(1), pp.179-186.
2. Agnihotri, S., Kaur, P., Sangal, V.K., Garg, A. and Verma, A., 2018. Parametric Study for the Treatment of Simulated Cetirizine Wastewater Using Electrochemical Methods: Optimization and Cost Analysis. Journal of The Electrochemical Society, 165(11), pp.E556-E562.
3. Ahmed, S.N. and Haider, W., 2018. Heterogeneous photocatalysis and its potential applications in water and wastewater treatment: a review. Nanotechnology, 29(34), p.342001.
4. Akpan, U.G. and Hameed, B.H., 2009. Parameters affecting the photocatalytic degradation of dyes using TiO_2-based photocatalysts: a review. Journal of hazardous materials, 170(2-3), pp.520-529.
5. Akpan, U.G. and Hameed, B.H., 2010. The advancements in sol–gel method of doped-TiO_2 photocatalysts. Applied Catalysis A: General, 375(1), pp.1-11.
6. Alekhina, M., Ershova, O., Ebert, A., Heikkinen, S. and Sixta, H., 2015. Softwood kraft lignin for value-added applications: Fractionation and structural characterization. Industrial Crops and Products, 66, pp.220-228.
7. Ali, M. and Sreekrishnan, T.R., 2001. Aquatic toxicity from pulp and paper mill effluents: a review. Advances in environmental research, 5(2), pp.175-196.
8. Almeida, B.M., Melo Jr, M.A., Bettini, J., Benedetti, J.E. and Nogueira, A.F., 2015. A novel nanocomposite based on TiO_2/Cu_2O/reduced graphene oxide with enhanced solar-light-driven photocatalytic activity. Applied Surface Science, 324, pp.419-431.
9. Amat, A.M., Arques, A., López, F. and Miranda, M.A., 2005. Solar photo-catalysis to remove paper mill wastewater pollutants. Solar energy, 79(4), pp.393-401.
10. Amor, C., De Torres-Socías, E., Peres, J.A., Maldonado, M.I., Oller, I., Malato, S., Lucas, M.S., 2015. Mature landfill leachate treatment by coagulation/flocculation combined with Fenton and solar photo-Fenton processes. J. Hazard. Mater. 286, 261-268.

11. Andreozzi, R., Caprio, V., Insola, A. and Marotta, R., 1999. Advanced oxidation processes (AOP) for water purification and recovery. Catalysis today, 53(1), pp.51-59.
12. Anglada, A., Urtiaga, A. and Ortiz, I., 2009. Contributions of electrochemical oxidation to waste- water treatment: fundamentals and review of applications. Journal of Chemical Technology & Biotechnology, 84(12), pp.1747-1755.
13. Antony, S.P. and Natesan, B., 2012. Optimization of integrated electro-bio process for bleaching effluent treatment. Industrial & Engineering Chemistry Research, 51(24), pp.8211-8221.
14. Archibald, F., 2000. The presence of coliform bacteria in Canadian pulp and paper mill water systems—a cause for concern?. Water Quality Research Journal, 35(1), pp.1-22.
15. Arora, I., Ratan, J.K. and Bansal, A., 2018. TiO_2 Photocatalysis in Cementitious Systems. International Journal of Engineering Technology Science and Research, 5(3), pp.340-342.
16. Audenaert, W.T., Vermeersch, Y., Van Hulle, S.W., Dejans, P., Dumoulin, A. and Nopens, I., 2011. Application of a mechanistic UV/hydrogen peroxide model at full-scale: sensitivity analysis, calibration and performance evaluation. Chemical Engineering Journal, 171(1), pp.113-126.
17. Ayekoe, C.Y.P., Robert, D. and Lanciné, D.G., 2017. Combination of coagulation-flocculation and heterogeneous photocatalysis for improving the removal of humic substances in real treated water from Agbô River (Ivory-Coast). Catalysis Today, 281, pp.2-13.
18. Ayyasamy, P.M., Shanthi, K., Lakshmanaperumalsamy, P., Lee, S.J., Choi, N.C. and Kim, D.J., 2007. Two-stage removal of nitrate from groundwater using biological and chemical treatments. Journal of bioscience and bioengineering, 104(2), pp.129-134.
19. Bagotskii, V.S., Nekrasov, L.N. and Shumilova, N.A., 1965. Electrochemical reduction of oxygen. Russian Chemical Reviews, 34(10), pp.717-730.
20. Bajpai, P., 2000. Treatment of pulp and paper mill effluents with anaerobic technology. Pira International.

21. Balcioğlu, I.A. and Cecen, F., 1999. Treatability of kraft pulp bleaching wastewater by biochemical and photocatalytic oxidation. Water science and technology, 40(1), pp.281-288.
22. Bannat, I., Wessels, K., Oekermann, T., Rathousky, J., Bahnemann, D. and Wark, M., 2009. Improving the photocatalytic performance of mesoporous titania films by modification with gold nanostructures. Chemistry of Materials, 21(8), pp.1645-1653.
23. Baruah, B.K. and Das, M., 1997. Effect of paper mill effluent on plankton population of wetland. Environment and Ecology, 15(4), pp.770-777.
24. Berger, T., Monllor-Satoca, D., Jankulovska, M., Lana-Villarreal, T. and Gómez, R., 2012. The electrochemistry of nanostructured titanium dioxide electrodes. ChemPhysChem, 13(12), pp.2824-2875.
25. Bhatia, V., Dhir, A. and Ray, A.K., 2018. Integration of Photocatalytic and Biological Processes for Treatment of Pharmaceutical Effluent. Journal of Photochemistry and Photobiology A: Chemistry.
26. Bhatta, D., Sahoo, M.K. and Mishra, M.S.S., 1991. Role of semiconductive oxides in the thermal decomposition of barium oxalate. Thermochimica acta, 180, pp.155-158.
27. Boroski, M., Rodrigues, A.C., Garcia, J.C., Gerola, A.P., Nozaki, J. and Hioka, N., 2008. The effect of operational parameters on electrocoagulation–flotation process followed by photocatalysis applied to the decontamination of water effluents from cellulose and paper factories. Journal of Hazardous Materials, 160(1), pp.135-141.
28. Brillas, E., Mur, E., Sauleda, R., Sanchez, L., Peral, J., Domènech, X. and Casado, J., 1998. Aniline mineralization by AOP's: anodic oxidation, photocatalysis, electro-Fenton and photoelectro-Fenton processes. Applied Catalysis B: Environmental, 16(1), pp.31-42.
29. Buftia, G., Rosales, E., Pazos, M., Lazar, G. and Sanromán, M.A., 2018. Electro-Fenton process for implementation of acid black liquor waste treatment. Science of The Total Environment, 635, pp.397-404.
30. Buzzini, A.P., Miwa, D.W., Motheo, A.J. and Pires, E.C., 2006. Use of electrochemical oxidation process as post-treatment for the effluents of a UASB reactor treating cellulose pulp mill wastewater. Water science and technology, 54(2), pp.207-213.

31. Cai, Q. and Hu, J., 2018. Effect of UVA/LED/TiO_2 photocatalysis treated sulfamethoxazole and trimethoprim containing wastewater on antibiotic resistance development in sequencing batch reactors. Water research, 140, pp.251-260.
32. Carey, J.H., 1992. An introduction to advanced oxidation processes (AOP) for destruction of organics in wastewater. Water Quality Research Journal, 27(1), pp.1-22.
33. Catalkaya, E.C. and Kargi, F., 2008. Advanced oxidation treatment of pulp mill effluent for TOC and toxicity removals. Journal of environmental management, 87(3), pp.396-404.
34. Central Pollution Control Board (CPCB). Rule 2 (i) of the Environment (Protection) Third Amendments Rules, 2005 notified vide Notification G.S.R.546(E), dated 30.8.2005
35. Černigoj, U., Štangar, U.L. and Trebše, P., 2007. Degradation of neonicotinoid insecticides by different advanced oxidation processes and studying the effect of ozone on TiO_2 photocatalysis. Applied catalysis B: environmental, 75(3-4), pp.229-238.
36. Chai, S., Zhao, G., Li, P., Lei, Y., Zhang, Y.N. and Li, D., 2011. Novel sieve-like SnO_2/TiO_2 nanotubes with integrated photoelectrocatalysis: fabrication and application for efficient toxicity elimination of nitrophenol wastewater. The Journal of Physical Chemistry C, 115(37), pp.18261-18269.
37. Chang, C.N., Ma, Y.S., Fang, G.C., Chao, A.C., Tsai, M.C. and Sung, H.F., 2004. Decolorizing of lignin wastewater using the photochemical UV/TiO_2 process. Chemosphere, 56(10), pp.1011-1017.
38. Changotra, R., Guin, J.P., Dhir, A. and Varshney, L., 2018. Decomposition of antibiotic ornidazole by gamma irradiation in aqueous solution: kinetics and its removal mechanism. Environmental Science and Pollution Research, *25*(32), pp.32591-32602.
39. Changotra, R., Guin, J.P., Khader, S.A., Varshney, L. and Dhir, A., 2019. Electron beam induced degradation of ofloxacin in aqueous solution: kinetics, removal mechanism and cytotoxicity assessment. Chemical Engineering Journal, 356, pp.973-984.

40. Changotra, R., Rajput, H. and Dhir, A., 2017. Natural soil mediated photo Fenton-like processes in treatment of pharmaceuticals: Batch and continuous approach. Chemosphere, 188, pp.345-353.
41. Changotra, R., Varshney, L., Guin, J.P. and Dhir, A., 2018a. Performance of hematite particles as an Iron source for the degradation of ornidazole in photo-fenton process. Journal of Sol-Gel Science and Technology, 85(1), pp.203-212.
42. Chatterjee, A., Niwa, S. and Mizukami, F., 2005. Structure and property correlation for Ag deposition on α-Al_2O_3-a first principle study. Journal of Molecular Graphics and Modelling, 23(5), pp.447-456.
43. Chen, S., Brown, L., Levendorf, M., Cai, W., Ju, S.Y., Edgeworth, J., Li, X., Magnuson, C.W., Velamakanni, A., Piner, R.D. and Kang, J., 2011a. Oxidation resistance of graphene-coated Cu and Cu/Ni alloy. ACS nano, 5(2), pp.1321-1327.
44. Chen, X., Liu, L., Peter, Y.Y. and Mao, S.S., 2011. Increasing solar absorption for photocatalysis with black hydrogenated titanium dioxide nanocrystals. Science, p.1200448.
45. Cheng, X., Cheng, Q., Deng, X., Wang, P. and Liu, H., 2016. A facile and novel strategy to synthesize reduced TiO_2 nanotubes photoelectrode for photoelectrocatalytic degradation of diclofenac. Chemosphere, 144, pp.888-894.
46. Cheng, X., Liu, H., Chen, Q., Li, J. and Wang, P., 2014. Preparation of graphene film decorated TiO_2 nano-tube array photoelectrode and its enhanced visible light photocatalytic mechanism. Carbon, 66, pp.450-458.
47. Chiang, L.C., Chang, J.E. and Wen, T.C., 1995. Indirect oxidation effect in electrochemical oxidation treatment of landfill leachate. Water research, 29(2), pp.671-678.
48. Choi, J., Park, H. and Hoffmann, M.R., 2009. Effects of single metal-ion doping on the visible-light photoreactivity of TiO_2. The Journal of Physical Chemistry C, 114(2), pp.783-792.
49. Chong, M.N., Jin, B., Chow, C.W. and Saint, C., 2010. Recent developments in photocatalytic water treatment technology: a review. Water research, 44(10), pp.2997-3027.
50. Chu, H., Wang, Z. and Liu, Y., 2016. Application of modified bentonite granulated electrodes for advanced treatment of pulp and paper mill wastewater in three-

dimensional electrode system. Journal of environmental chemical engineering, 4(2), pp.1810-1817.

51. Chung, C.J., Lin, H.I., Tsou, H.K., Shi, Z.Y. and He, J.L., 2008. An antimicrobial TiO_2 coating for reducing hospital- acquired infection. Journal of Biomedical Materials Research Part B: Applied Biomaterials: An Official Journal of The Society for Biomaterials, The Japanese Society for Biomaterials, and The Australian Society for Biomaterials and the Korean Society for Biomaterials, 85(1), pp.220-224.
52. Codognoto, L., Machado, S.A.S. and Avaca, L.A., 2003. Selective oxidation of pentachlorophenol on diamond electrodes. Journal of applied electrochemistry, 33(10), pp.951-957.
53. Costa, S., Dedola, D.G., Pellizzari, S., Blo, R., Rugiero, I., Pedrini, P. and Tamburini, E., 2017. Lignin Biodegradation in Pulp-and-Paper Mill Wastewater by Selected White Rot Fungi. Water, 9(12), p.935.
54. Costi, R., Saunders, A.E., Elmalem, E., Salant, A. and Banin, U., 2008. Visible light-induced charge retention and photocatalysis with hybrid CdSe−Au nanodumbbells. Nano Letters, 8(2), pp.637-641.
55. Cui, C., Quan, X., Yu, H. and Han, Y., 2008. Electrocatalytic hydrodehalogenation of pentachlorophenol at palladized multiwalled carbon nanotubes electrode. Applied Catalysis B: Environmental, 80(1-2), pp.122-128.
56. Cui, C., Wang, Y., Liang, D., Cui, W., Hu, H., Lu, B., Xu, S., Li, X., Wang, C. and Yang, Y., 2014. Photo-assisted synthesis of Ag_3PO_4/reduced graphene oxide/Ag heterostructure photocatalyst with enhanced photocatalytic activity and stability under visible light. Applied Catalysis B: Environmental, 158, pp.150-160.
57. Daghrir, R., Drogui, P. and Robert, D., 2012a. Photoelectrocatalytic technologies for environmental applications. Journal of Photochemistry and Photobiology A: Chemistry, 238, pp.41-52.
58. Daghrir, R., Drogui, P. and Robert, D., 2013. Modified TiO_2 for environmental photocatalytic applications: a review. Industrial & Engineering Chemistry Research, 52(10), pp.3581-3599.
59. Daghrir, R., Drogui, P., Ka, I. and El Khakani, M.A., 2012b. Photoelectrocatalytic degradation of chlortetracycline using Ti/TiO_2 nanostructured electrodes deposited by means of a pulsed laser deposition process. Journal of hazardous materials, 199, pp.15-24.

60. De Aragao Umbuzeiro, G., Freeman, H.S., Warren, S.H., De Oliveira, D.P., Terao, Y., Watanabe, T. and Claxton, L.D., 2005. The contribution of azo dyes to the mutagenic activity of the Cristais River. Chemosphere, 60(1), pp.55-64.
61. De-Bashan, L.E. and Bashan, Y., 2004. Recent advances in removing phosphorus from wastewater and its future use as fertilizer (1997–2003). Water research, 38(19), pp.4222-4246.
62. De-Bashan, L.E. and Bashan, Y., 2004. Recent advances in removing phosphorus from wastewater and its future use as fertilizer (1997–2003). Water research, 38(19), pp.4222-4246.
63. Dhir, A., Prakash, N.T. and Sud, D., 2011. Studies on coupled biological and photochemical treatment of soda pulp bleaching effluents from agro residue based pulp and paper mill. Journal of Chemical Technology & Biotechnology, 86(12), pp.1508-1513.
64. Dhir, A., Prakash, N.T. and Sud, D., 2012. Comparative studies on TiO_2/ZnO photocatalyzed degradation of 4-chlorocatechol and bleach mill effluents. Desalination and Water Treatment, 46(1-3), pp.196-204.
65. Dhir, A., Prakash, N.T. and Sud, D., 2012a. Coupling of solar-assisted advanced oxidative and biological treatment for degradation of agro-residue-based soda bleaching effluent. Environmental Science and Pollution Research, 19(9), pp.3906-3913.
66. Di, X., Kansal, S.K. and Deng, W., 2009. Preparation, characterization and photocatalytic activity of flowerlike cadmium sulfide nanostructure. Separation and Purification Technology, 68(1), pp.61-64.
67. Ding, J., Xu, W., Wan, H., Yuan, D., Chen, C., Wang, L., Guan, G. and Dai, W.L., 2018. Nitrogen vacancy engineered graphitic C_3N_4-based polymers for photocatalytic oxidation of aromatic alcohols to aldehydes. Applied Catalysis B: Environmental, 221, pp.626-634.
68. Divyapriya, G., Nambi, I.M. and Senthilnathan, J., 2016. Nanocatalysts in fenton based advanced oxidation process for water and wastewater treatment. Journal of Bionanoscience, 10(5), pp.356-368.
69. Dixit, A., Mishra, P.K. and Alam, M.S., 2017. Titania Nanofibers: A Potential Adsorbent for Mercury and Lead Uptake. International Journal of Chemical Engineering and Applications, 8(1), pp.75.

70. Dominguez-Ramos, A., Aldaco, R. and Irabien, A., 2008. Electrochemical oxidation of lignosulfonate: total organic carbon oxidation kinetics. Industrial & Engineering Chemistry Research, 47(24), pp.9848-9853.
71. Dong, G., Chen, D., Luo, J., Zhu, Y., Zeng, Y. and Wang, C., 2017. Voids padding induced further enhancement in photocatalytic performance of porous graphene-like carbon nitride. Journal of hazardous materials, 335, pp.66-74.
72. Dos Santos, E.V., Sáez, C., Martínez-Huitle, C.A., Cañizares, P. and Rodrigo, M.A., 2015. The role of particle size on the conductive diamond electrochemical oxidation of soil-washing effluent polluted with atrazine. Electrochemistry Communications, 55, pp.26-29.
73. Dube, M., McLean, R., MacLatchy, D. and Savage, P., 2000. Reverse osmosis treatment: effects on effluent quality. Pulp & Paper Canada.
74. Dufresne, R., Caouette, L., Norval, G.W. and Kanters, C.J., 2000. Treatment of clean condensate using catalytically enhanced oxidation. In Annual Meeting-Pulp And Paper Technical Association Of Canada (Vol. 86, No. A, pp. A257-A266). Pulp and Paper Technical Association of Canada; 1999.
75. Dutta, S.K., 1999. Study of the physico-chemical properties of effluent of the paper mill that affected the paddy plants. Journal of Environment and Pollution, 6(2), pp.181-188.
76. Ericson, G. and Larsson, A., 2000. DNA Adducts in Perch (*Perca fluviatilis*) Living in Coastal Water Polluted with Bleached Pulp Mill Effluents. Ecotoxicology and Environmental Safety, 46(2), pp.167-173.
77. Esquivel, K., Rodríguez, F.J., González, M.V., Escobar-Alarcón, L., Ortiz-Frade, L. and Godínez, L.A., 2011. Titanium dioxide doped with transition metals ($MxTi_{1-x}O_2$, M: Ni, Co): synthesis and characterization for its potential application as photoanode. Journal of Nanoparticle Research, 13(8), pp.3313-3325.
78. Etacheri, V., Di Valentin, C., Schneider, J., Bahnemann, D. and Pillai, S.C., 2015. Visible-light activation of TiO_2 photocatalysts: Advances in theory and experiments. Journal of Photochemistry and Photobiology C: Photochemistry Reviews, 25, pp.1-29.
79. Fang, H.H.P., Liang, D.W., Zhang, T. and Liu, Y., 2006. Anaerobic treatment of phenol in wastewater under thermophilic condition. Water Research, 40(3), pp.427-434.

80. Florenza, X., Solano, A.M.S., Centellas, F., Martínez-Huitle, C.A., Brillas, E. and Garcia-Segura, S., 2014. Degradation of the azo dye Acid Red 1 by anodic oxidation and indirect electrochemical processes based on Fenton's reaction chemistry. Relationship between decolorization, mineralization and products. Electrochimica Acta, 142, pp.276-288.
81. Fryda, M., Matthée, T., Mulcahy, S., Hofer, M., Schafer, L. and Troster, I., 2003. Applications of DIACHEM electrodes in electrolytic water treatment. Interface, 12(1), pp.40-44.
82. Fujishima, A., Zhang, X. and Tryk, D.A., 2008. TiO_2 photocatalysis and related surface phenomena. Surface Science Reports, 63(12), pp.515-582.
83. Gan, S. and Ng, H.K., 2012. Current status and prospects of Fenton oxidation for the decontamination of persistent organic pollutants (POPs) in soils. Chemical Engineering Journal, 213, pp.295-317.
84. Ganzenko, O., Oturan, N., Sirés, I., Huguenot, D., Van Hullebusch, E.D., Esposito, G. and Oturan, M.A., 2018. Fast and complete removal of the 5-fluorouracil drug from water by electro-Fenton oxidation. Environmental Chemistry Letters, 16(1), pp.281-286.
85. Gao, F., Yang, Y. and Wang, T., 2015. Preparation of porous TiO_2/Ag heterostructure films with enhanced photocatalytic activity. Chemical Engineering Journal, 270, pp.418-427.
86. Garcia-Segura, S., Ocon, J.D. and Chong, M.N., 2018. Electrochemical oxidation remediation of real wastewater effluents—a review. Process Safety and Environmental Protection, 113, pp.48-67.
87. Gautam, S.B., Alam, M.S. and Kamsonlian, S., 2017. Adsorptive Removal of As (III) from Aqueous Solution by Raw Coconut Husk and Iron Impregnated Coconut Husk: Kinetics and Equilibrium Analyses. International Journal of Chemical Reactor Engineering, 15(2).
88. Gerischer, H., 1990. The impact of semiconductors on the concepts of electrochemistry. Electrochimica Acta, 35(11-12), pp.1677-1699.
89. Ghanem, M.A., Arunachalam, P., Amer, M.S. and Al-Mayouf, A.M., 2018. Mesoporous titanium dioxide photoanodes decorated with gold nanoparticles for boosting the photoelectrochemical alkali water oxidation. Materials Chemistry and Physics, 213, pp.56-66.

90. Ghodrati, M.S., Haghighi, M., Soltan Mohamdzadeh, J.S., Pourabas, B. and Pipelzadeh, E., 2011. Phenol decomposition under sunlight using a sonochemically synthesized CdSe/TiO_2 nanocatalyst. Reaction Kinetics, Mechanisms and Catalysis, 104(1), pp.49-60.
91. Glaze, W.H., Kang, J.W. and Chapin, D.H., 1987. The chemistry of water treatment processes involving ozone, hydrogen peroxide and ultraviolet radiation.
92. Golbaz, S., Jafari, A.J., Rafiee, M. and Kalantary, R.R., 2014. Separate and simultaneous removal of phenol, chromium, and cyanide from aqueous solution by coagulation/precipitation: Mechanisms and theory. Chemical Engineering Journal, 253, pp.251-257.
93. Gómez-Avilés, A., Peñas-Garzón, M., Bedia, J., Rodriguez, J.J. and Belver, C., 2019. C-modified TiO_2 using lignin as carbon precursor for the solar photocatalytic degradation of acetaminophen. Chemical Engineering Journal, 358, pp.1574-1582.
94. Govindan, K., Raja, M., Noel, M. and James, E.J., 2014. Degradation of pentachlorophenol by hydroxyl radicals and sulfate radicals using electrochemical activation of peroxomonosulfate, peroxodisulfate and hydrogen peroxide. Journal of hazardous materials, 272, pp.42-51.
95. Gu, L., Wang, J., Cheng, H., Zhao, Y., Liu, L. and Han, X., 2013. One-step preparation of graphene-supported anatase TiO_2 with exposed {001} facets and mechanism of enhanced photocatalytic properties. ACS applied materials & interfaces, 5(8), pp.3085-3093.
96. Haghighi, M., Rahmani, F., Kariminejad, F. and Sene, R.A., 2018. Photodegradation of lignin from pulp and paper mill effluent using TiO_2/PS composite under UV-LED radiation: Optimization, toxicity assessment and reusability study. Process Safety and Environmental Protection.
97. Hamoudi, S., Belkacemi, K., Sayari, A. and Larachi, F., 2001. Catalytic oxidation of 4-chloroguaiacol reaction kinetics and catalytic studies. Chemical engineering science, 56(4), pp.1275-1283.
98. Hanna, K., Chiron, S. and Oturan, M.A., 2005. Coupling enhanced water solubilization with cyclodextrin to indirect electrochemical treatment for pentachlorophenol contaminated soil remediation. Water Research, 39(12), pp.2763-2773.

99. Haq, I., Kumar, S., Raj, A., Lohani, M. and Satyanarayana, G.N.V., 2017. Genotoxicity assessment of pulp and paper mill effluent before and after bacterial degradation using Allium cepa test. Chemosphere, 169, pp.642-650.
100. He, C., Shu, D., Su, M., Xia, D., Asi, M.A., Lin, L. and Xiong, Y., 2010. Photocatalytic activity of metal (Pt, Ag, and Cu)-deposited TiO_2 photoelectrodes for degradation of organic pollutants in aqueous solution. Desalination, 253(1-3), pp.88-93.
101. He, C., Xiong, Y., Chen, J., Zha, C. and Zhu, X., 2003. Photoelectrochemical performance of Ag–TiO_2/ITO film and photoelectrocatalytic activity towards the oxidation of organic pollutants. Journal of Photochemistry and Photobiology A: Chemistry, 157(1), pp.71-79.
102. He, Z., Phan, H., Liu, J., Nguyen, T.Q. and Tan, T.T.Y., 2013. Understanding TiO_2 Size- Dependent Electron Transport Properties of a Graphene- TiO_2 Photoanode in Dye- Sensitized Solar Cells Using Conducting Atomic Force Microscopy. Advanced Materials, 25(47), pp.6900-6904.
103. Herrmann, J.M., Guillard, C., Arguello, M., Agüera, A., Tejedor, A., Piedra, L. and Fernandez-Alba, A., 1999. Photocatalytic degradation of pesticide pirimiphos-methyl: Determination of the reaction pathway and identification of intermediate products by various analytical methods. Catalysis Today, 54(2-3), pp.353-367.
104. Hiwarkar, A.D., Singh, S., Srivastava, V.C. and Mall, I.D., 2017. Mineralization of pyrrole, a recalcitrant heterocyclic compound, by electrochemical method: Multi-response optimization and degradation mechanism. Journal of environmental management, 198, pp.144-152.
105. Hoffmann, M.R., Martin, S.T., Choi, W. and Bahnemann, D.W., 1995. Environmental applications of semiconductor photocatalysis. Chemical reviews, 95(1), pp.69-96.
106. Holmbom, B., Harju, L., Lindholm, J. and Groening, A., 1994. Effect of a pulp and paper mill on metal concentrations in the receiving lake system. Aqua Fennica, 24(1), pp.93-110.
107. Hong, P.A. and Zeng, Y., 2002. Degradation of pentachlorophenol by ozonation and biodegradability of intermediates. Water Research, 36(17), pp.4243-4254.

108. Hossain, K. and Ismail, N., 2015. Bioremediation and detoxification of pulp and paper mill effluent: A review. Research Journal of Environmental Toxicology, 9(3), p.113.
109. Howe, J. and Wagner, M.R., 1999. Effects of pulpmill effluent irrigation on the distribution of elements in the profile of an arid region soil. Environmental Pollution, 105(1), pp.129-135.
110. Hu, B., Wang, Y., Hu, C. and Zhou, X., 2016. Design, fabrication and high efficient visible-light assisted photoelectric-synergistic performance of 3-D mesoporous DSA electrodes. Materials & Design, 91, pp.201-210.
111. Hubbe, M.A., Metts, J.R., Hermosilla, D., Blanco, M., Yerushalmi, L., Haghighat, F., Lindholm-Lehto, P., Khodaparast, Z., Kamali, M. and Elliott, A., 2016. Wastewater treatment and reclamation: A review of pulp and paper industry practices and opportunities. BioResources, 11.
112. Hwangbo, M., Claycomb, E.C., Liu, Y., Alivio, T.E., Banerjee, S. and Chu, K.H., 2019. Effectiveness of zinc oxide-assisted photocatalysis for concerned constituents in reclaimed wastewater: 1, 4-Dioxane, trihalomethanes, antibiotics, antibiotic resistant bacteria (ARB), and antibiotic resistance genes (ARGs). Science of The Total Environment, 649, pp.1189-1197.
113. Ishibashi, K.I., Fujishima, A., Watanabe, T. and Hashimoto, K., 2000. Detection of active oxidative species in TiO_2 photocatalysis using the fluorescence technique. Electrochemistry Communications, 2(3), pp.207-210.
114. Jardim, W.F., Moraes, S.G. and Takiyama, M.M.K., 1997. Photocatalytic degradation of aromatic chlorinated compounds using TiO_2: toxicity of intermediates. Water Research, 31(7), pp.1728-1732.
115. Joseph, A.I.J. and Thiripuranthagan, S., 2018. Non-Metal Doped Titania Photocatalysts for the Degradation of Neonicotinoid Insecticides Under Visible Light Irradiation. Journal of nanoscience and nanotechnology, 18(5), pp.3158-3164.
116. Kamali, M. and Khodaparast, Z., 2015. Review on recent developments on pulp and paper mill wastewater treatment. Ecotoxicology and Environmental Safety, 114, pp.326-342.
117. Kanakaraju, D., Glass, B.D. and Oelgemöller, M., 2014. Titanium dioxide photocatalysis for pharmaceutical wastewater treatment. Environmental Chemistry Letters, 12(1), pp.27-47.

118. Kansal, S.K., Singh, M. and Sud, D., 2008. Effluent quality at kraft/soda agro-based paper mills and its treatment using a heterogeneous photocatalytic system. Desalination, 228(1-3), pp.183-190.
119. Karrasch, B., Parra, O., Cid, H., Mehrens, M., Pacheco, P., Urrutia, R., Valdovinos, C. and Zaror, C., 2006. Effects of pulp and paper mill effluents on the microplankton and microbial self-purification capabilities of the Biobio River, Chile. Science of the Total Environment, 359(1-3), pp.194-208.
120. Kaur, P., Sangal, V.K. and Kushwaha, J.P., 2015. Modeling and evaluation of electro-oxidation of dye wastewater using artificial neural networks. RSC Advances, 5(44), pp.34663-34671.
121. Kaur, R., Kushwaha, J.P. and Singh, N., 2018. Electro-oxidation of Ofloxacin antibiotic by dimensionally stable Ti/RuO_2 anode: Evaluation and mechanistic approach. Chemosphere, 193, pp.685-694.
122. Khansorthong, S. and Hunsom, M., 2009. Remediation of wastewater from pulp and paper mill industry by the electrochemical technique. Chemical Engineering Journal, 151(1-3), pp.228-234.
123. Khatri, I., Singh, S. and Garg, A., 2018. Performance of electro-Fenton process for phenol removal using Iron electrodes and activated carbon. Journal of environmental chemical engineering, 6(6), pp.7368-7376.
124. Kim, D.H. and Anderson, M.A., 1994. Photoelectrocatalytic degradation of formic acid using a porous titanium dioxide thin-film electrode. Environmental science & technology, 28(3), pp.479-483.
125. King, H.M., Baldwin, D.S., Rees, G.N. and McDonald, S., 1999. Apparent bioaccumulation of Mn derived from paper-mill effluent by the freshwater crayfish Cherax destructor—the role of Mn oxidising bacteria. Science of the total environment, 226(2-3), pp.261-267.
126. Kringstad, K.P. and Lindström, K., 1984. Spent liquors from pulp bleaching. Environmental science & technology, 18(8), pp.236A-248A.
127. Kumar, P., Kumar, S. and Bhardwaj, N.K., 2011a. Chlorophenolics degradation from paper industry wastewater using UV/TiO_2 and UV/TiO_2/H_2O_2 processes. In Vth World Aqua Congress, New Delhi, India (Vol. 2, p. 496).

128. Kumar, P., Kumar, S., Bhardwaj, N.K. and Choudhary, A.K., 2011. Optimization of process parameters for the photocatalytic treatment of paper mill wastewater. Environmental Engineering & Management Journal (EEMJ), 10(5).
129. Kumar, V. and Chopra, A.K., 2012. Effects of paper mill effluent irrigation on agronomical characteristics of Vigna radiata (L.) in two different seasons. Communications in soil science and plant analysis, 43(16), pp.2142-2166.
130. Kusumawati, Y., Martoprawiro, M.A. and Pauporté, T.H., 2014. Effects of graphene in graphene/TiO_2 composite films applied to solar cell photoelectrode. The Journal of Physical Chemistry C, 118(19), pp.9974-9981.
131. Labiadh, L., Barbucci, A., Cerisola, G., Gadri, A., Ammar, S. and Panizza, M., 2015. Role of anode material on the electrochemical oxidation of methyl orange. Journal of Solid State Electrochemistry, 19(10), pp.3177-3183.
132. Laine, D.F. and Cheng, I.F., 2007. The destruction of organic pollutants under mild reaction conditions: A review. Microchemical journal, 85(2), pp.183-193.
133. Lanao, M., Ormad, M.P., Goñi, P., Miguel, N., Mosteo, R. and Ovelleiro, J.L., 2010. Inactivation of Clostridium perfringens spores and vegetative cells by photolysis and TiO_2 photocatalysis with H_2O_2. Solar energy, 84(4), pp.703-709.
134. Landeros, C.R., Díaz, C.E.B., Cháves, A.A. and Morales, G.R., 2017. Evaluation of a coupled system of electro-oxidation and ozonation to remove the pesticide Thiodan® 35 CE (endosulfan) in aqueous solution. Fuel, 198, pp.91-98.
135. Lara, M.A., Rodríguez-Malaver, A.J., Rojas, O.J., Holmquist, O., González, A.M., Bullón, J., Peñaloza, N. and Araujo, E., 2003. Black liquor lignin biodegradation by Trametes elegans. International biodeterioration & biodegradation, 52(3), pp.167-173.
136. Lee, L.S., Rao, P.S.C. and Brusseau, M.L., 1991. Nonequilibrium sorption and transport of neutral and ionized chlorophenols. Environmental science & technology, 25(4), pp.722-729.
137. Legrini, O., Oliveros, E. and Braun, A.M., 1993. Photochemical processes for water treatment. Chemical reviews, 93(2), pp.671-698.
138. Leng, W.H., Zhu, W.C., Ni, J., Zhang, Z., Zhang, J.Q. and Cao, C.N., 2006. Photoelectrocatalytic destruction of organics using TiO_2 as photoanode with simultaneous production of H_2O_2 at the cathode. Applied Catalysis A: General, 300(1), pp.24-35.

139. Lettinga, G., Field, J.A., Sierra-Alvarez, R., Van Lier, J.B. and Rintala, J., 1991. Future perspectives for the anaerobic treatment of forest industry wastewaters. Water Science and Technology, 24(3-4), p.91.
140. Levchuk, I., Rueda-Márquez, J.J., Suihkonen, S., Manzano, M.A. and Sillanpää, M., 2015. Application of UVA-LED based photocatalysis for plywood mill wastewater treatment. Separation and Purification Technology, 143, pp.1-5.
141. Lewandowski, G.A. and de Filippi, L.J., 1998. Biological treatment of hazardous waste.
142. Lewis, R.J. and Irving, N., 2003. Sax's dangerous properties of industrial materials (Vol. 3). Van Nostrand Reinhold.
143. Li, D., Jia, J., Zhang, Y., Wang, N., Guo, X. and Yu, X., 2016. Preparation and characterization of Nano-graphite/TiO_2 composite photoelectrode for photoelectrocatalytic degradation of hazardous pollutant. Journal of hazardous materials, 315, pp.1-10.
144. Li, E., Bolser, D.G., Kroll, K.J., Brockmeier, E.K., Falciani, F. and Denslow, N.D., 2018. Comparative toxicity of three phenolic compounds on the embryo of fathead minnow, Pimephales promelas. Aquatic Toxicology.
145. Li, G., Qu, J., Zhang, X. and Ge, J., 2006a. Electrochemically assisted photocatalytic degradation of Acid Orange 7 with β-PbO_2 electrodes modified by TiO_2. Water research, 40(2), pp.213-220.
146. Li, G., Wong, K.H., Zhang, X., Hu, C., Jimmy, C.Y., Chan, R.C.Y. and Wong, P.K., 2009. Degradation of acid orange 7 using magnetic AgBr under visible light: the roles of oxidizing species. Chemosphere, 76(9), pp.1185-1191.
147. Li, H., Zhang, X., Huo, Y. and Zhu, J., 2007. Supercritical preparation of a highly active S-doped TiO_2 photocatalyst for methylene blue mineralization. Environmental science & technology, 41(12), pp.4410-4414.
148. Li, J., Zheng, L., Li, L., Xian, Y. and Jin, L., 2007. Fabrication of TiO_2/Ti electrode by laser-assisted anodic oxidation and its application on photoelectrocatalytic degradation of methylene blue. Journal of Hazardous Materials, 139(1), pp.72-78.
149. Li, M.C. and Shen, J.N., 2006. Phoelectrochemical oxidation behavior of organic substance on TiO_2 thin-film electrodes. Journal of Solid State Electrochemistry, 10, pp.980-986.

150. Li, P., Zhao, G., Cui, X., Zhang, Y. and Tang, Y., 2009a. Constructing stake structured TiO_2-NTs/Sb-doped SnO2 electrode simultaneously with high electrocatalytic and photocatalytic performance for complete mineralization of refractory aromatic acid. The Journal of Physical Chemistry C, 113(6), pp.2375-2383.
151. Li, T., Zhang, Z., Li, W., Liu, C., Wang, J. and An, L., 2016. $H_4SiW_{12}O_{40}$/polymethylmethacrylate/polyvinyl alcohol sandwich nanofibrous membrane with enhanced photocatalytic activity. Colloids and Surfaces A: Physicochemical and Engineering Aspects, 489, pp.289-296.
152. Li, W., Li, D., Lin, Y., Wang, P., Chen, W., Fu, X. and Shao, Y., 2012. Evidence for the active species involved in the photodegradation process of methyl orange on TiO_2. The Journal of Physical Chemistry C, 116(5), pp.3552-3560.
153. Li, Y., Niu, J., Yin, L., Wang, W., Bao, Y., Chen, J. and Duan, Y., 2011. Photocatalytic degradation kinetics and mechanism of pentachlorophenol based on superoxide radicals. Journal of Environmental Sciences(China), 23(11), pp.1911-1918.'
154. Li, Y., Wang, H., Feng, Q., Zhou, G. and Wang, Z.S., 2013. Gold nanoparticles inlaid TiO_2 photoanodes: a superior candidate for high-efficiency dye-sensitized solar cells. Energy & Environmental Science, 6(7), pp.2156-2165.
155. Lin, H., Niu, J., Ding, S. and Zhang, L., 2012. Electrochemical degradation of perfluorooctanoic acid (PFOA) by Ti/SnO_2–Sb, Ti/SnO_2–Sb/PbO_2 and Ti/SnO_2–Sb/MnO_2 anodes. Water research, 46(7), pp.2281-2289.
156. Liu, B., Wen, L. and Zhao, X., 2007. The photoluminescence spectroscopic study of anatase TiO_2 prepared by magnetron sputtering. Materials Chemistry and Physics, 106(2-3), pp.350-353.
157. Liu, J., Li, J., Sedhain, A., Lin, J. and Jiang, H., 2008. Structure and photoluminescence study of TiO_2 nanoneedle texture along vertically aligned carbon nanofiber arrays. The Journal of Physical Chemistry C, 112(44), pp.17127-17132.
158. Liu, J., Wang, L., Tang, J. and Ma, J., 2016. Photocatalytic degradation of commercially sourced naphthenic acids by TiO_2-graphene composite nanomaterial. Chemosphere, 149, pp.328-335.

159. Liu, L., Li, R., Liu, Y. and Zhang, J., 2016. Simultaneous degradation of ofloxacin and recovery of Cu (II) by photoelectrocatalysis with highly ordered TiO_2 nanotubes. Journal of hazardous materials, 308, pp.264-275.
160. Liu, Y. and Du, H., 2011. Study on Photoelectrocatalytic Technology of Three-Dimensional Electrode. In Advances in Computer Science, Intelligent System and Environment (pp. 447-451). Springer, Berlin, Heidelberg.
161. Luo, J., Yang, X.Y. and Li, D.L., 2010. Preparation of TiO_2 nanoparticles doped with Cs^+ and Sr^{2+} and their photocatalytic activity under solar light. In Advanced Materials Research (Vol. 113, pp. 1945-1950). Trans Tech Publications.
162. Mahmoodi, N.M., Arami, M. and Zhang, J., 2011. Preparation and photocatalytic activity of immobilized composite photocatalyst (titania nanoparticle/activated carbon). Journal of Alloys and Compounds, 509(14), pp.4754-4764.
163. Makris, S.P. and Banerjee, S., 2002. Fate of resin acids in pulp mill secondary treatment systems. Water research, 36(11), pp.2878-2882.
164. Mandal, T.N., 1996. Studies in physico-chemical and biological characteristics of pulp and paper mill effluent and its impact on human beings. Journal of Freshwater Biology, 8(4), pp.191-196.
165. Mansilla, H.D., Villaseñor, J., Maturana, G., Baeza, J., Freer, J. and Durán, N., 1994. ZnO-catalysed photodegradation of kraft black liquor. Journal of Photochemistry and Photobiology A: Chemistry, 78(3), pp.267-273.
166. Marcano, D.C., Kosynkin, D.V., Berlin, J.M., Sinitskii, A., Sun, Z., Slesarev, A., Alemany, L.B., Lu, W. and Tour, J.M., 2010. Improved synthesis of graphene oxide. ACS nano, 4(8), pp.4806-4814.
167. Marinho, B.A., Djellabi, R., Cristóvão, R.O., Loureiro, J.M., Boaventura, R.A., Dias, M.M., Lopes, J.C.B. and Vilar, V.J., 2017. Intensification of heterogeneous TiO_2 photocatalysis using an innovative micro–meso-structured-reactor for Cr (VI) reduction under simulated solar light. Chemical Engineering Journal, 318, pp.76-88.
168. Matthews, R.W., 1991. Environment: photochemical and photocatalytic processes. Degradation of organic compounds. In Photochemical conversion and storage of solar energy (pp. 427-449). Springer, Dordrecht.
169. McDevitt, N.T. and Baun, W.L., 1964. Infrared absorption study of metal oxides in the low frequency region (700-240 cm^{-1}). Spectrochimica Acta, 20(5), pp.799-808.

170. McGinnis, G.D., Borazjani, H., Hannigan, M., Hendrix, F., McFarland, L., Pope, D., Strobel, D. and Wagner, J., 1991. Bioremediation studies at a northern California Superfund site. Journal of Hazardous Materials, 28(1-2), pp.145-158.
171. Meekins, B.H. and Kamat, P.V., 2011. Role of water oxidation catalyst IrO_2 in shuttling photogenerated holes across TiO_2 interface. The Journal of Physical Chemistry Letters, 2(18), pp.2304-2310.
172. Mehrjouei, M., Müller, S. and Möller, D., 2015. A review on photocatalytic ozonation used for the treatment of water and wastewater. Chemical Engineering Journal, 263, pp.209-219.
173. Mills, G. and Hoffmann, M.R., 1993. Photocatalytic degradation of pentachlorophenol on titanium dioxide particles: identification of intermediates and mechanism of reaction. Environmental science & technology, 27(8), pp.1681-1689.
174. Minu, K., Jiby, K.K. and Kishore, V.V.N., 2012. Isolation and purification of lignin and silica from the black liquor generated during the production of bioethanol from rice straw. Biomass and Bioenergy, 39, pp.210-217.
175. Mir, N.A., Khan, A., Muneer, M. and Vijayalakhsmi, S., 2013. Photocatalytic degradation of a widely used insecticide Thiamethoxam in aqueous suspension of TiO_2: adsorption, kinetics, product analysis and toxicity assessment. Science of the total environment, 458, pp.388-398.
176. Mohamed, M., Matayun, M. and Lim, T.S., 1989. Chlorinated organics in tropical hardwood kraft pulp and paper mill effluents and their elimination in an activated sludge treatment system. Pertanika, 2(3), pp.387-394.
177. Momeni, M.M. and Hosseini, M.G., 2016. Photo-electrocatalytic activity of TiO_2 nanotubes prepared with two-step anodization and treated under UV light irradiation. Nanochemistry Research, 1(1), pp.9-18.
178. Montiel, V., Valero, D., Gallud, F., García-García, V., Expósito, E. and Iniesta, J., 2018. Prospective Applications of Renewable Energy-Based Electrochemical Systems in Wastewater Treatment. In Electrochemical Water and Wastewater Treatment, pp. 513-541.
179. Moodley, B., Mulholland, D.A. and Brookes, H.C., 2011. The electro-oxidation of lignin in Sappi Saiccor dissolving pulp mill effluent. Water Sa, 37(1).
180. Mudhoo, A., Bhatnagar, A., Rantalankila, M., Srivastava, V. and Sillanpää, M., 2018. Endosulfan removal through bioremediation, photocatalytic degradation,

adsorption and membrane separation processes: A review. Chemical Engineering Journal. 360, pp.912-928.

181. Nethravathi, C. and Rajamathi, M., 2008. Chemically modified graphene sheets produced by the solvothermal reduction of colloidal dispersions of graphite oxide. Carbon, 46(14), pp.1994-1998.
182. Ni, M., Leung, M.K., Leung, D.Y. and Sumathy, K., 2007. A review and recent developments in photocatalytic water-splitting using TiO_2 for hydrogen production. Renewable and Sustainable Energy Reviews, 11(3), pp.401-425.
183. Nidheesh, P.V., Zhou, M. and Oturan, M.A., 2018. An overview on the removal of synthetic dyes from water by electrochemical advanced oxidation processes. Chemosphere, 197, pp.210-227.
184. Novotny, V., 1994. Water quality: prevention, identification and management of diffuse pollution. Van Nostrand-Reinhold Publishers.
185. Nurdin, M., 2014. Maulidiyah. Fabrication of TiO_2/Ti nanotube electrode by anodizing method and its application on photoelectrocatalytic system. International Journal of Scientific & Technology Research, 3(2), pp.122-4.
186. O'Connor, B., Kovacs, T., Gibbons, S. and Strang, A.L., 2000. Carbon dioxide in pulp and paper mill effluents from oxygen-activated sludge treatment plants as a potential source of distress and toxicity to fish. Water Quality Research Journal, 35(2), pp.189-200.
187. Olvera-Vargas, H., Rouch, J.C., Coetsier, C., Cretin, M. and Causserand, C., 2018. Dynamic cross-flow electro-Fenton process coupled to anodic oxidation for wastewater treatment: Application to the degradation of acetaminophen. Separation and Purification Technology, 203, pp.143-151.
188. Panizza, M. and Cerisola, G., 2009. Electro-Fenton degradation of synthetic dyes. Water research, 43(2), pp.339-344.
189. Parsons, S. ed., 2004. Advanced oxidation processes for water and wastewater treatment. IWA publishing.
190. Patel, U.D. and Suresh, S., 2008. Electrochemical treatment of pentachlorophenol in water and pulp bleaching effluent. Separation and Purification Technology, 61(2), pp.115-122.

191. Pathak, C., Chopra, A.K. and Srivastava, S., 2012. Enrichment of various metals in Abelmoschus esculentus grown in wastewater irrigated soil area of Dehradun city, India. Journal of Applied and Natural Science, 4(2), pp.291-296.
192. Pattanaik, P. and Sahoo, M.K., 2014. TiO_2 photocatalysis: progress from fundamentals to modification technology. Desalination and Water Treatment, 52(34-36), pp.6567-6590.
193. Paulose, M., Prakasam, H.E., Varghese, O.K., Peng, L., Popat, K.C., Mor, G.K., Desai, T.A. and Grimes, C.A., 2007. TiO2 nanotube arrays of 1000 μm length by anodization of titanium foil: phenol red diffusion. The Journal of Physical Chemistry C, 111(41), pp.14992-14997.
194. Peralta-Zamora, P., Esposito, E., Pelegrini, R., Groto, R., Reyes, J. and Durán, N., 1998. Effluent treatment of pulp and paper, and textile industries using immobilised horseradish peroxidase. Environmental technology, 19(1), pp.55-63.
195. Perez, M., Torrades, F., Domenech, X. and Peral, J., 2002. Treatment of bleaching Kraft mill effluents and polychlorinated phenolic compounds with ozonation. Journal of Chemical Technology & Biotechnology: International Research in Process, Environmental & Clean Technology, 77(8), pp.891-897.
196. Perng, Y.S., Wang, I.C., Yu, S.T. and Lin, Y.F., 2008. Application of an electro-oxidation treatment method to industrial paper mill effluents in the lab. Taiwan Journal for Sciences, 23(2), pp.111-123.
197. Pichat, P., Disdier, J., Hoang-Van, C., Mas, D., Goutailler, G. and Gaysse, C., 2000. Purification/deodorization of indoor air and gaseous effluents by TiO_2 photocatalysis. Catalysis today, 63(2-4), pp.363-369.
198. Pokhrel, D. and Viraraghavan, T., 2004. Treatment of pulp and paper mill wastewater—a review. Science of the total environment, 333(1-3), pp.37-58.
199. Pokhrel, D. and Viraraghavan, T., 2004. Treatment of pulp and paper mill wastewater—a review. Science of the total environment, 333(1-3), pp.37-58.
200. Priya, S.S., Deshpande, A. and Dwarakanath, R., 2015. Visible light solar photocatalytic degradation of pulp and paper wastewater using dye-sensitised TiO_2. Int J Res Eng Technol, 4, pp.200-204.
201. Quan, X., Ruan, X., Zhao, H., Chen, S. and Zhao, Y., 2007. Photoelectrocatalytic degradation of pentachlorophenol in aqueous solution using a TiO_2 nanotube film electrode. Environmental Pollution, 147(2), pp.409-414.

202. Radjenovic, J. and Sedlak, D.L., 2015. Challenges and opportunities for electrochemical processes as next-generation technologies for the treatment of contaminated water. Environmental Science & Technology, 49(19), pp.11292-11302.
203. Raghuveer, S. and Sastry, C.A. 1991. Biological treatment of pulp mill wastewater and study of biokinetic constants. Indian Journal of Environmental Protection, 11(8), pp.614-21.
204. Ramírez, R.J., Arellano, C.A.P., Gallegos, A.A.Á., González, A.E.J. and Martínez, S.S., 2015. H_2O_2-assisted TiO_2 generation during the photoelectrocatalytic process to decompose the acid green textile dye by Fenton reaction. Journal of Photochemistry and Photobiology A: Chemistry, 305, pp.51-59.
205. Rao, K. ed., 2013. Pentachlorophenol: chemistry, pharmacology, and environmental toxicology (Vol. 12). Springer Science & Business Media.
206. Repetto, G., Jos, A., Hazen, M.J., Molero, M.L., Del Peso, A., Salguero, M., Del Castillo, P., Rodrıguez-Vicente, M.C. and Repetto, M., 2001. A test battery for the ecotoxicological evaluation of pentachlorophenol. Toxicology in Vitro, 15(4-5), pp.503-509.
207. Report on the Paper Industry Development Council for Pulp, Paper and Allied Industries, Government of India, New Delhi, 1995.
208. Requejo, A., Rodríguez, A., Colodette, J.L., Gomide, J.L. and Jiménez, L., 2012. TCF bleaching sequence in kraft pulping of olive tree pruning residues. Bioresource technology, 117, pp.117-123.
209. Rezaei, E., Soltan, J. and Chen, N., 2013. Catalytic oxidation of toluene by ozone over alumina supported manganese oxides: effect of catalyst loading. Applied Catalysis B: Environmental, 136, pp.239-247.
210. Rocha, J.H.B., Gomes, M.M.S., Fernandes, N.S., da Silva, D.R. and Martínez-Huitle, C.A., 2012. Application of electrochemical oxidation as alternative treatment of produced water generated by Brazilian petrochemical industry. Fuel Processing Technology, 96, pp.80-87.
211. Rodrigues, A.C., Boroski, M., Shimada, N.S., Garcia, J.C., Nozaki, J. and Hioka, N., 2008. Treatment of paper pulp and paper mill wastewater by coagulation–flocculation followed by heterogeneous photocatalysis. Journal of Photochemistry and Photobiology A: Chemistry, 194(1), pp.1-10.

212. Rodriguez, J., Fuentes, S., Freer, J., Mansilla, H.D., Ferraz, A. and Baeza, J., 1998. Response to ozonation of different cellulose pulp bleaching effluents. Environmental technology, 19(1), pp.75-81.
213. Rodríguez-Chueca, J., Polo-López, M.I., Mosteo, R., Ormad, M.P. and Fernández-Ibáñez, P., 2014. Disinfection of real and simulated urban wastewater effluents using a mild solar photo-Fenton. Applied Catalysis B: Environmental, 150, pp.619-629.
214. Roshani, B., McMaster, I., Rezaei, E. and Soltan, J., 2014. Catalytic ozonation of benzotriazole over alumina supported transition metal oxide catalysts in water. Separation and Purification Technology, 135, pp.158-164.
215. Sadek, A.Z., Zheng, H., Latham, K., Wlodarski, W. and Kalantar-Zadeh, K., 2008. Anodization of Ti thin film deposited on ITO. Langmuir, 25(1), pp.509-514.
216. Saha, B., Das, S., Saikia, J. and Das, G., 2011. Preferential and enhanced adsorption of different dyes on iron oxide nanoparticles: a comparative study. The Journal of Physical Chemistry C, 115(16), pp.8024-8033.
217. Sahoo, C., Gupta, A.K. and Sasidharan Pillai, I.M., 2012. Photocatalytic degradation of methylene blue dye from aqueous solution using silver ion-doped TiO_2 and its application to the degradation of real textile wastewater. Journal of Environmental Science and Health, Part A, 47(10), pp.1428-1438.
218. Sahoo, M.K., Sayoo, L., Naik, D.B. and Sharan, R.N., 2013. Improving the operational parameters with high electrical energy efficiency for UVC induced advanced oxidation and mineralization of Acid blue 29: Generation of eco-friendly effluent. Separation and Purification Technology, 106, pp.110-116.
219. Samsudin, E.M., Goh, S.N., Wu, T.Y., Ling, T.T., Abd, S. and Juan, J., 2015. Evaluation on the photocatalytic degradation activity of reactive blue 4 using pure anatase nano-TiO_2. Sains Malays, 44(7), pp.1011-1019.
220. Santos, A., Yustos, P., Gomis, S., Ruiz, G. and Garcia-Ochoa, F., 2006. Reaction network and kinetic modeling of wet oxidation of phenol catalyzed by activated carbon. Chemical engineering science, 61(8), pp.2457-2467.
221. Särkkä, H., Bhatnagar, A. and Sillanpää, M., 2015. Recent developments of electro-oxidation in water treatment—a review. Journal of Electroanalytical Chemistry, 754, pp.46-56.

222. Sasaki, T. and Watanabe, M., 1997. Semiconductor nanosheet crystallites of quasi-TiO_2 and their optical properties. The Journal of Physical Chemistry B, 101(49), pp.10159-10161.
223. Sellappan, R., Sun, J., Galeckas, A., Lindvall, N., Yurgens, A., Kuznetsov, A.Y. and Chakarov, D., 2013. Influence of graphene synthesizing techniques on the photocatalytic performance of graphene–TiO_2 nanocomposites. Physical Chemistry Chemical Physics, 15(37), pp.15528-15537.
224. Selvabharathi, G. and Kanmani, S., 2010. Tertiary treatment of pulp and paper industrial wastewater by electro-Fenton process. Journal of environmental science & engineering, 52(2), pp.103-106.
225. Shahrezaei, F., Mansouri, Y., Zinatizadeh, A.A.L. and Akhbari, A., 2012. Process modeling and kinetic evaluation of petroleum refinery wastewater treatment in a photocatalytic reactor using TiO_2 nanoparticles. Powder Technology, 221, pp.203-212.
226. Shaogui, Y., Xie, Q., Xinyong, L., Yazi, L., Shuo, C. and Guohua, C., 2004. Preparation, characterization and photoelectrocatalytic properties of nanocrystalline Fe_2O_3/TiO_2, ZnO/TiO_2, and $Fe_2O_3/ZnO/TiO_2$ composite film electrodes towards pentachlorophenol degradation. Physical Chemistry Chemical Physics, 6(3), pp.659-664.
227. Shen, W., Li, Z., Wang, H., Liu, Y., Guo, Q. and Zhang, Y., 2008. Photocatalytic degradation for methylene blue using zinc oxide prepared by codeposition and sol–gel methods. Journal of Hazardous Materials, 152(1), pp.172-175.
228. Shet, A. and Vidya, S.K., 2016. Solar light mediated photocatalytic degradation of phenol using Ag core–TiO_2 shell (Ag@ TiO_2) nanoparticles in batch and fluidized bed reactor. Solar Energy, 127, pp.67-78.
229. Sibu, C.P., Kumar, S.R., Mukundan, P. and Warrier, K.G.K., 2002. Structural modifications and associated properties of lanthanum oxide doped sol-gel nanosized titanium oxide. Chemistry of Materials, 14(7), pp.2876-2881.
230. Silva, M., Calvete, M.J.F., Gonçalves, N.P.F., Burrows, H.D., Sarakha, M., Fernandes, A., Ribeiro, M.F., Azenha, M.E. and Pereira, M.M., 2012. Zinc (II) phthalocyanines immobilized in mesoporous silica Al-MCM-41 and their applications in photocatalytic degradation of pesticides. Journal of hazardous materials, 233, pp.79-88.

231. Singh, C., Chowdhary, P., Singh, J.S. and Chandra, R., 2016. Pulp and paper mill wastewater and coliform as health hazards: a review. Microbiol Res Int, 4(3), pp.28-39.
232. Singh, P., Dhir, A. and Sangal, V.K., 2015. Optimization of photocatalytic process parameters for the degradation of acrylonitrile using Box Behnken Design. Desalination and Water Treatment, 55(6), pp.1501-1508.
233. Singh, R.S., Marwaha, S.S. and Khanna, P.K., 1996. Characteristics of pulp and paper mill effluents. Journal of Industrial Pollution Control, 12, pp.163-172.
234. Singh, S. and Garg, A., 2019. Performance of Photo-catalytic Oxidation for Degradation of Chlorophenols: Optimization of Reaction Parameters and Quantification of Transformed Oxidized Products. Journal of Hazardous Materials, 361, pp.73-84.
235. Singh, S., Mahalingam, H. and Singh, P.K., 2013. Polymer-supported titanium dioxide photocatalysts for environmental remediation: A review. Applied Catalysis A: General, 462, pp.178-195.
236. Sirés, I. and Brillas, E., 2012. Remediation of water pollution caused by pharmaceutical residues based on electrochemical separation and degradation technologies: a review. Environment international, 40, pp.212-229.
237. Sirés, I., Brillas, E., Oturan, M.A., Rodrigo, M.A. and Panizza, M., 2014. Electrochemical advanced oxidation processes: today and tomorrow. A review. Environmental Science and Pollution Research, 21(14), pp.8336-8367.
238. Siripala, W., Ivanovskaya, A., Jaramillo, T.F., Baeck, S.H. and McFarland, E.W., 2003. A Cu_2O/TiO_2 heterojunction thin film cathode for photoelectrocatalysis. Solar Energy Materials and Solar Cells, 77(3), pp.229-237.
239. Soloman, P.A., Basha, C.A., Velan, M., Balasubramanian, N. and Marimuthu, P., 2009. Augmentation of biodegradability of pulp and paper industry wastewater by electrochemical pre-treatment and optimization by RSM. Separation and Purification Technology, 69(1), pp.109-117.
240. Solomon, R.V., Lydia, I.S., Merlin, J.P. and Venuvanalingam, P., 2012. Enhanced photocatalytic degradation of azo dyes using nano Fe_3O_4. Journal of the Iranian Chemical Society, 9(2), pp.101-109.

241. Song-Hu, Y. and Xiao-Hua, L., 2005. Comparison treatment of various chlorophenols by electro-Fenton method: relationship between chlorine content and degradation. Journal of hazardous materials, 118(1-3), pp.85-92.
242. Sopaj, F., Rodrigo, M.A., Oturan, N., Podvorica, F.I., Pinson, J. and Oturan, M.A., 2015. Influence of the anode materials on the electrochemical oxidation efficiency. Application to oxidative degradation of the pharmaceutical amoxicillin. Chemical Engineering Journal, 262, pp.286-294.
243. Su, K., Ai, Z. and Zhang, L., 2012. Efficient Visible Light-Driven Photocatalytic Degradation of Pentachlorophenol with Bi_2O_3/TiO_2–x Bx. The Journal of Physical Chemistry C, 116(32), pp.17118-17123.
244. Su, Y., Chen, S., Quan, X., Zhao, H. and Zhang, Y., 2008. A silicon-doped TiO_2 nanotube arrays electrode with enhanced photoelectrocatalytic activity. Applied Surface Science, 255(5), pp.2167-2172.
245. Subramanian, V., Wolf, E. and Kamat, P.V., 2001. Semiconductor-metal composite nanostructures. To what extent do metal nanoparticles improve the photocatalytic activity of TiO_2 films?. The Journal of Physical Chemistry B, 105(46), pp.11439-11446.
246. Subramonian, W., Wu, T.Y. and Chai, S.P., 2017. Photocatalytic degradation of industrial pulp and paper mill effluent using synthesized magnetic Fe_2O_3-TiO_2: Treatment efficiency and characterizations of reused photocatalyst. Journal of environmental management, 187, pp.298-310.
247. Sumathi, S. and Hung, Y.T., 2006. Treatment of pulp and paper mill wastes. Waste treatment in the process industries, pp.453-497.
248. Sung-Suh, H.M., Choi, J.R., Hah, H.J., Koo, S.M. and Bae, Y.C., 2004. Comparison of Ag deposition effects on the photocatalytic activity of nanoparticulate TiO_2 under visible and UV light irradiation. Journal of Photochemistry and Photobiology A: Chemistry, 163(1-2), pp.37-44.
249. Szczepanik, B., Rogala, P., Słomkiewicz, P.M., Banaś, D., Kubala-Kukuś, A. and Stabrawa, I., 2017. Synthesis, characterization and photocatalytic activity of TiO_2-halloysite and Fe_2O_3-halloysite nanocomposites for photodegradation of chloroanilines in water. Applied Clay Science, 149, pp.118-126.
250. Tam, D., Varhanickova, D., Shiu, W.Y. and Mackay, D., 1994. Aqueous solubility of chloroguaiacols. Journal of Chemical and Engineering Data, 39(1), pp.83-86.

251. Tang, W.Z. and Huang, C.P., 1996. 2, 4-dichlorophenol oxidation kinetics by Fenton's reagent. Environmental Technology, 17(12), pp.1371-1378.
252. Tang, Y., Zhang, G., Liu, C., Luo, S., Xu, X., Chen, L. and Wang, B., 2013. Magnetic TiO_2-graphene composite as a high-performance and recyclable platform for efficient photocatalytic removal of herbicides from water. Journal of hazardous materials, 252, pp.115-122.
253. Tantis, I., Antonopoulou, M., Konstantinou, I. and Lianos, P., 2016. Coupling of electrochemical and photocatalytic technologies for accelerating degradation of organic pollutants. Journal of Photochemistry and Photobiology A: Chemistry, 317, pp.100-107.
254. Tanzifi, M., Yaraki, M.T., Karami, M., Karimi, S., Kiadehi, A.D., Karimipour, K. and Wang, S., 2018. Modelling of dye adsorption from aqueous solution on polyaniline/carboxymethyl cellulose/TiO_2 nanocomposites. Journal of colloid and interface science, 519, pp.154-173.
255. Thompson, G., Swain, J., Kay, M. and Forster, C.F., 2001. The treatment of pulp and paper mill effluent: a review. Bioresource technology, 77(3), pp.275-286.
256. Tian, F., Zhang, Y., Zhang, J. and Pan, C., 2012. Raman spectroscopy: a new approach to measure the percentage of anatase TiO_2 exposed (001) facets. The Journal of Physical Chemistry C, 116(13), pp.7515-7519.
257. Tian, Y. and Tatsuma, T., 2005. Mechanisms and applications of plasmon-induced charge separation at TiO_2 films loaded with gold nanoparticles. Journal of the American Chemical Society, 127(20), pp.7632-7637.
258. Tiwana, P., Docampo, P., Johnston, M.B., Snaith, H.J. and Herz, L.M., 2011. Electron mobility and injection dynamics in mesoporous ZnO, SnO_2, and TiO_2 films used in dye-sensitized solar cells. ACS nano, 5(6), pp.5158-5166.
259. Traversa, E., Di Vona, M.L., Nunziante, P., Licoccia, S., Sasaki, T. and Koshizaki, N., 2000. Sol-gel preparation and characterization of Ag-TiO_2 nanocomposite thin films. Journal of Sol-Gel Science and Technology, 19(1-3), pp.733-736.
260. Tryba, B., Jafari, S., Sillanpää, M., Nitta, A., Ohtani, B. and Morawski, A.W., 2019. Influence of TiO_2 structure on its photocatalytic activity towards acetaldehyde decomposition. Applied Surface Science, 470, pp.376-385.
261. Tsutsui, T., Hayashi, N., Maizumi, H., Huff, J. and Barrett, J.C., 1997. Benzene-, catechol-, hydroquinone-and phenol-induced cell transformation, gene mutations,

chromosome aberrations, aneuploidy, sister chromatid exchanges and unscheduled DNA synthesis in Syrian hamster embryo cells. Mutation Research/Fundamental and Molecular Mechanisms of Mutagenesis, 373(1), pp.113-123.

262. Uğurlu, M., Gürses, A., Doğar, Ç. and Yalçın, M., 2008. The removal of lignin and phenol from paper mill effluents by electrocoagulation. Journal of environmental management, 87(3), pp.420-428.
263. Umemura, T., Kai, S., Hasegawa, R., Sai, K., Kurokawa, Y. and Williams, G.M., 1999. Pentachlorophenol (PCP) produces liver oxidative stress and promotes but does not initiate hepatocarcinogenesis in B6C3F1 mice. Carcinogenesis, 20(6), pp.1115-1120.
264. Vaiano, V., Matarangolo, M., Murcia, J.J., Rojas, H., Navío, J.A. and Hidalgo, M.C., 2018. Enhanced photocatalytic removal of phenol from aqueous solutions using ZnO modified with Ag. Applied Catalysis B: Environmental, 225, pp.197-206.
265. Vaiano, V., Matarangolo, M., Sacco, O. and Sannino, D., 2017. Photocatalytic treatment of aqueous solutions at high dye concentration using praseodymium-doped ZnO catalysts. Applied Catalysis B: Environmental, 209, pp.621-630.
266. Vashi, H., Iorhemen, O.T. and Tay, J.H., 2017. Aerobic granulation: A recent development on the biological treatment of pulp and paper wastewater. Environmental Technology & Innovation.
267. Vatankhah, H., Murray, C.C., Brannum, J.W., Vanneste, J. and Bellona, C., 2018. Effect of pre-ozonation on nanofiltration membrane fouling during water reuse applications. Separation and Purification Technology, 205, pp.203-211.
268. Velegraki, T. and Mantzavinos, D., 2015. Solar photo-Fenton treatment of winery effluents in a pilot photocatalytic reactor. Catalysis Today, 240, pp.153-159.
269. Waldner, G., Pourmodjib, M., Bauer, R. and Neumann-Spallart, M., 2003. Photoelectrocatalytic degradation of 4-chlorophenol and oxalic acid on titanium dioxide electrodes. Chemosphere, 50(8), pp.989-998.
270. Wang, J. and Zhang, W.D., 2012. Modification of TiO_2 nanorod arrays by graphite-like C_3N_4 with high visible light photoelectrochemical activity. Electrochimica Acta, 71, pp.10-16.
271. Wang, S., Guan, Y., Wang, L., Zhao, W., He, H., Xiao, J., Yang, S. and Sun, C., 2015. Fabrication of a novel bifunctional material of $BiOI/Ag_3VO_4$ with high

adsorption–photocatalysis for efficient treatment of dye wastewater. Applied Catalysis B: Environmental, 168, pp.448-457.

272. Wu, L., Li, F., Xu, Y., Zhang, J.W., Zhang, D., Li, G. and Li, H., 2015. Plasmon-induced photoelectrocatalytic activity of Au nanoparticles enhanced TiO_2 nanotube arrays electrodes for environmental remediation. Applied catalysis B: environmental, 164, pp.217-224.
273. Wu, Y.T., Yu, Y.H., Nguyen, V.H. and Wu, J.C., 2015. In-situ FTIR spectroscopic study of the mechanism of photocatalytic reduction of NO with methane over Pt/TiO_2 photocatalysts. Research on Chemical Intermediates, 41(4), pp.2153-2164.
274. Xie, J., Zhang, L., Li, M., Hao, Y., Lian, Y., Li, Z. and Wei, Y., 2015. α-Fe_2O_3 modified ZnO flower-like microstructures with enhanced photocatalytic performance for pentachlorophenol degradation. Ceramics International, 41(8), pp.9420-9425.
275. Xie, K., Sun, L., Wang, C., Lai, Y., Wang, M., Chen, H. and Lin, C., 2010. Photoelectrocatalytic properties of Ag nanoparticles loaded TiO_2 nanotube arrays prepared by pulse current deposition. Electrochimica Acta, 55(24), pp.7211-7218.
276. Xie, Y.B. and Li, X.Z., 2006. Preparation and characterization of TiO_2/Ti film electrodes by anodization at low voltage for photoelectrocatalytic application. Journal of applied electrochemistry, 36(6), pp.663-668.
277. Xiong, Z., Luo, Y., Zhao, Y., Zhang, J., Zheng, C. and Wu, J.C., 2016. Synthesis, characterization and enhanced photocatalytic CO_2 reduction activity of graphene supported TiO_2 nanocrystals with coexposed {001} and {101} facets. Physical Chemistry Chemical Physics, 18(19), pp.13186-13195.
278. Xu, D., Shi, W., Song, C., Chen, M., Yang, S., Fan, W. and Chen, B., 2016. In-situ synthesis and enhanced photocatalytic activity of visible-light-driven plasmonic $Ag/AgCl/NaTaO_3$ nanocubes photocatalysts. Applied Catalysis B: Environmental, 191, pp.228-234.
279. Yadav, B.R. and Garg, A., 2017. Performance assessment of activated carbon supported catalyst during catalytic wet oxidation of simulated pulping effluents generated from wood and bagasse based pulp and paper mills. RSC Advances, 7(16), pp.9754-9763.

280. Yadav, B.R. and Garg, A., 2018. Hetero-catalytic hydrothermal oxidation of simulated pulping effluent: Effect of operating parameters and catalyst stability. Chemosphere, 191, pp.128-135.
281. Yadav, S. and Chandra, R., 2018. Detection and assessment of the phytotoxicity of residual organic pollutants in sediment contaminated with pulp and paper mill effluent. Environmental monitoring and assessment, 190(10), p.581.
282. Yamada, K.I., Mukaihata, N., Kawahara, T. and Tada, H., 2007. Electrochemically assisted visible light photocatalysis in a heterosupramolecular system consisting of α-Fe_2O_3 and surfactant molecular assembly. Langmuir, 23(16), pp.8593-8596.
283. Yan, W.A.N.G., Fan, C.M., Bo, H.U.A., Liang, Z.H. and Sun, Y.P., 2009. Photoelectrocatalytic activity of two antimony doped SnO_2 films for oxidation of phenol pollutants. Transactions of Nonferrous Metals Society of China, 19(3), pp.778-783.
284. Yang, L., Li, Z., Jiang, H., Jiang, W., Su, R., Luo, S. and Luo, Y., 2016. Photoelectrocatalytic oxidation of bisphenol A over mesh of TiO_2/graphene/Cu_2O. Applied Catalysis B: Environmental, 183, pp.75-85.
285. Yang, S., Liu, Y. and Sun, C., 2006. Preparation of anatase TiO_2/Ti nanotube-like electrodes and their high photoelectrocatalytic activity for the degradation of PCP in aqueous solution. Applied Catalysis A: General, 301(2), pp.284-291.
286. Yang, Y., Kao, L.C., Liu, Y., Sun, K., Yu, H., Guo, J., Liou, S.Y.H. and Hoffmann, M.R., 2018. Cobalt-Doped Black TiO_2 Nanotube Array as a Stable Anode for Oxygen Evolution and Electrochemical Wastewater Treatment. ACS catalysis, 8(5), pp.4278-4287.
287. Yao, Y., Jiao, L., Yu, N., Guo, F. and Chen, X., 2016. Comparison of electrocatalytic characterization of Ti/Sb-SnO_2 and Ti/F-PbO_2 electrodes. Journal of Solid State Electrochemistry, 20(2), pp.353-359.
288. Yeber, M.C., Rodriguez, J., Baeza, J., Freer, J., Zaror, C., Duran, N. and Mansilla, H.D., 1999. Toxicity abatement and biodegradability enhancement of pulp mill bleaching effluent by advanced chemical oxidation. Water Science and Technology, 40(11-12), pp.337-342.
289. Yeber, M.C., Rodríguez, J., Freer, J., Durán, N. and Mansilla, H.D., 2000. Photocatalytic degradation of cellulose bleaching effluent by supported TiO_2 and ZnO. Chemosphere, 41(8), pp.1193-1197.

290. Yen, N.T., Oanh, N.T.K., Reutergardh, L.B., Wise, D.L. and Lan, N.T.T., 1997. An integrated waste survey and environmental effects of COGIDO, a bleached pulp and paper mill in Vietnam, on the receiving waterbody. Studies in Environmental Science, 66, pp.349-364.
291. Yin, L., Niu, J., Shen, Z. and Chen, J., 2010. Mechanism of reductive decomposition of pentachlorophenol by Ti-doped β-Bi_2O_3 under visible light irradiation. Environmental science & technology, 44(14), pp.5581-5586.
292. Yin, S., Zhang, Q., Saito, F. and Sato, T., 2003. Preparation of visible light-activated titania photocatalyst by mechanochemical method. Chemistry Letters, 32(4), pp.358-359.
293. Yu, J., Qi, L., Cheng, B. and Zhao, X., 2008a. Effect of calcination temperatures on microstructures and photocatalytic activity of tungsten trioxide hollow microspheres. Journal of Hazardous materials, 160(2-3), pp.621-628.
294. Yu, X., Guo, Y., Xu, L., Yang, X. and Guo, Y., 2008. A novel preparation of mesoporous $CsxH_3{-}xPW_{12}O_{40}/TiO_2$ nanocomposites with enhanced photocatalytic activity. Colloids and Surfaces A: Physicochemical and Engineering Aspects, 316(1-3), pp.110-118.
295. Yu, X., Li, Y., Wlodarski, W., Kandasamy, S. and Kalantar-Zadeh, K., 2008. Fabrication of nanostructured TiO_2 by anodization: A comparison between electrolytes and substrates. Sensors and Actuators B: Chemical, 130(1), pp.25-31.
296. Yun, J.H., Wong, R.J., Ng, Y.H., Du, A. and Amal, R., 2012. Combined electrophoretic deposition–anodization method to fabricate reduced graphene oxide–TiO_2 nanotube films. RSC Advances, 2(21), pp.8164-8171.
297. Zagklis, D.P., Vavouraki, A.I., Kornaros, M.E. and Paraskeva, C.A., 2015. Purification of olive mill wastewater phenols through membrane filtration and resin adsorption/desorption. Journal of hazardous materials, 285, pp.69-76.
298. Zainith, S., Chowdhary, P. and Bharagava, R.N., 2019. Recent Advances in Physico-chemical and Biological Techniques for the Management of Pulp and Paper Mill Waste. In Emerging and Eco-Friendly Approaches for Waste Management (pp. 271-297). Springer, Singapore.
299. Zaleska, A., 2008. Doped-TiO_2: a review. Recent patents on engineering, 2(3), pp.157-164.

300. Zanoni, M.V.B., Sene, J.J. and Anderson, M.A., 2003. Photoelectrocatalytic degradation of Remazol Brilliant Orange 3R on titanium dioxide thin-film electrodes. Journal of Photochemistry and Photobiology A: chemistry, 157(1), pp.55-63.
301. Zazou, H., Oturan, N., Sönmez-Çelebi, M., Hamdani, M. and Oturan, M.A., 2016. Mineralization of chlorobenzene in aqueous medium by anodic oxidation and electro-Fenton processes using Pt or BDD anode and carbon felt cathode. Journal of Electroanalytical Chemistry, 774, pp.22-30.
302. Zeghioud, H., Khellaf, N., Djelal, H., Amrane, A. and Bouhelassa, M., 2016. Photocatalytic Reactors Dedicated to the Degradation of Hazardous Organic Pollutants: Kinetics, Mechanistic Aspects, and Design–A Review. Chemical Engineering Communications, 203(11), pp.1415-1431.
303. Zha, Z., Ren, Y., Wang, S., Qian, Z., Yang, L., Cheng, P., Han, Y. and Wang, M., 2018. Phosphate adsorption onto thermally dehydrated aluminate cement granules. RSC Advances, 8(34), pp.19326-19334.
304. Zhai, C., Zhu, M., Lu, Y., Ren, F., Wang, C., Du, Y. and Yang, P., 2014. Reduced graphene oxide modified highly ordered TiO_2 nanotube arrays photoelectrode with enhanced photoelectrocatalytic performance under visible-light irradiation. Physical Chemistry Chemical Physics, 16(28), pp.14800-14807.
305. Zhang, G., Miao, H., Hu, X., Mu, J., Liu, X., Han, T., Fan, J., Liu, E., Yin, Y. and Wan, J., 2017. A facile strategy to fabricate Au/TiO_2 nanotubes photoelectrode with excellent photoelectrocatalytic properties. Applied Surface Science, 391, pp.345-352.
306. Zhang, H., Lv, X., Li, Y., Wang, Y. and Li, J., 2009. P25-graphene composite as a high performance photocatalyst. ACS nano, 4(1), pp.380-386.
307. Zhang, X., Tang, Y., Li, Y., Wang, Y., Liu, X., Liu, C. and Luo, S., 2013. Reduced graphene oxide and PbS nanoparticles co-modified TiO_2 nanotube arrays as a recyclable and stable photocatalyst for efficient degradation of pentachlorophenol. Applied Catalysis A: General, 457, pp.78-84.
308. Zhang, Y., Xiong, X., Han, Y., Zhang, X., Shen, F., Deng, S., Xiao, H., Yang, X., Yang, G. and Peng, H., 2012. Photoelectrocatalytic degradation of recalcitrant organic pollutants using TiO_2 film electrodes: an overview. Chemosphere, 88(2), pp.145-154.

309. Zhao, M., 2004. Absorption Property in Visible Region of TiO_2-xNx Films Prepared by Reactive Sputtering. Chinese Journal of Materials Research, 18(1), pp.108-112.
310. Zhao, X., Zhang, Y., Wen, P., Xu, G., Ma, D. and Qiu, P., 2018. NH_2-MIL-125 (Ti)/TiO_2 composites as superior visible-light photocatalysts for selective oxidation of cyclohexane. Molecular Catalysis, 452, pp.175-183.
311. Zheng, D., Xin, Y., Ma, D., Wang, X., Wu, J. and Gao, M., 2016. Preparation of graphene/TiO_2 nanotube array photoelectrodes and their photocatalytic activity for the degradation of alachlor. Catalysis Science & Technology, 6(6), pp.1892-1902.
312. Zhong, D., Liao, X., Liu, Y., Zhong, N. and Xu, Y., 2018. Enhanced electricity generation performance and dye wastewater degradation of microbial fuel cell by using a petaline NiO@ polyaniline-carbon felt anode. Bioresource technology, 258, pp.125-134.
313. Zhou, X., Zhang, X., Feng, X., Zhou, J. and Zhou, S., 2016. Preparation of a La/N co-doped TiO_2 film electrode with visible light response and its photoelectrocatalytic activity on a Ni substrate. Dyes and Pigments, 125, pp.375-383.
314. Zhou, Y., Oehmen, A., Lim, M., Vadivelu, V. and Ng, W.J., 2011. The role of nitrite and free nitrous acid (FNA) in wastewater treatment plants. Water research, 45(15), pp.4672-4682.
315. Zickler, G.A., Smarsly, B., Gierlinger, N., Peterlik, H. and Paris, O., 2006. A reconsideration of the relationship between the crystallite size La of carbons determined by X-ray diffraction and Raman spectroscopy. Carbon, 44(15), pp.3239-3246.

Acknowledgement

This study has been supported by Council of Scientific & Industrial Research **(CSIR),** Government of India (**09/677(0026)/2016 EMR I**).

List of contributions:

Publications:

- **Himadri Rajput**, Amit Dhir, Vikas Kumar Sangal, "GO Mediated TiO_2 Nanotube Electrode for the Photoelectrocatalytic Degradation of Pentachlorophenol", Journal of The Electrochemical Society, 165 (2018) H16-H26. **Impact Factor- 3.662**
- **Himadri Rajput**, Vikas Kumar Sangal, Amit Dhir, "Synthesis of highly stable and efficient Ag loaded GO/TiO_2 nanotube electrodes for the photoelectrocatalytic degradation of pentachlorophenol", Journal of Electroanalytical Chemistry, 814 (2018) 118-126. **Impact Factor- 3.235**
- **Himadri Rajput**, Rahil Changotra, Vikas Kumar Sangal, Sunil Kumar Mahla, Amit Dhir, "A facile synthesis of Cs nanoparticles loaded TiO_2 nanotube photoelectrode for photoelectrocatalytic degradation of 4-chloroguaiacol", Chemosphere, 218 (2019) 687-695. **Impact Factor- 4.427**

Conference and Workshop Presntations/Attended:

- Poster presentation on "Fabrication of electrodes and assessment of their activity in the photoelectrocatalytic degradation of pentachlorophenol". International conference AOP 2016, BITS-Goa, December 2016. (Won "**Best Poster Award**")
- Attended "International Conference on Harnessing Engineering Technology & Innovation for Sustainable Growth", HETIS 2016, Punjab University, Chandigarh.
- Participated in the National symposium on "Applications of Radioisotopes and Radiation Technology in industry, Healthcare and Agriculture", Thapar University, Patiala. November 28-29, 2016.
- Participated in International Workshop on "Heterogeneous Catalysis and Applications" delivered by Prof. Alex Ibhadon, The University of Hull, UK organized by Global Initiative for Academic Networks (Gian) held at Panjab University, Chandigarh. August 01-05, 2016.